PECS Radar Remote Sensing Course
ESA – University of Maribor
10th September 2015 – Maribor

SAR Interferometry

Dr. Paco López-Dekker (DLR, German Aerospace Center)

Deutsches Zentrum für Luft- und Raumfahrt e.V.
in der Helmholtz-Gemeinschaft

Outline

- SAR Interferometry
  - Introduction
  - Cross-track interferometry (InSAR)
  - Along-track interferometry (ATI)
  - Differential InSAR (DInSAR)
  - Typical processing chain
- (Advanced topics)
  - (Bistatic SAR)
  - (SAR Tomography)
  - (Circular SAR)
  - (High Resolution Wide Swath (HRWS))
  - …
- (Interferometric missions & sensors)

SAR Interferometry:

Introduction

Earthquakes

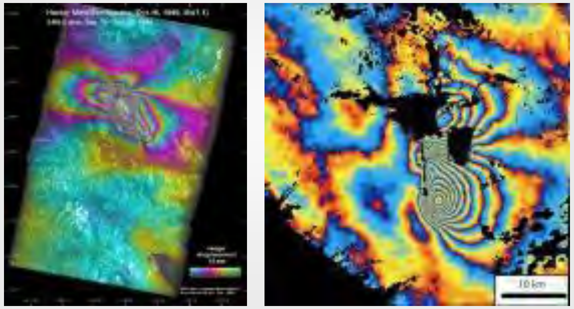

Volcanoes

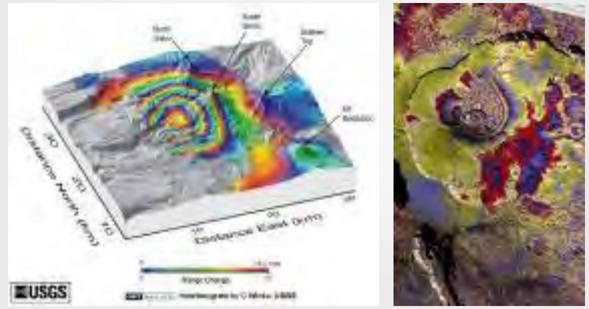

Land & Sea Ice

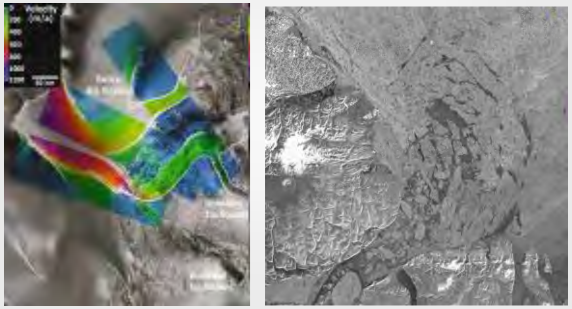

Ocean

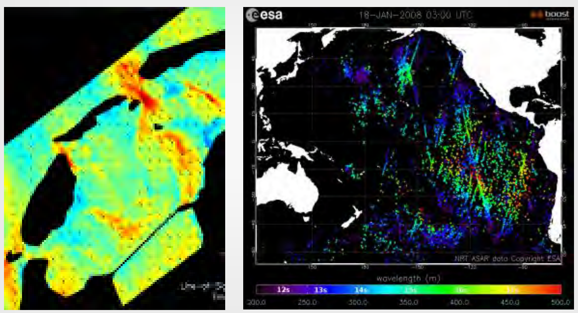

Land Environment

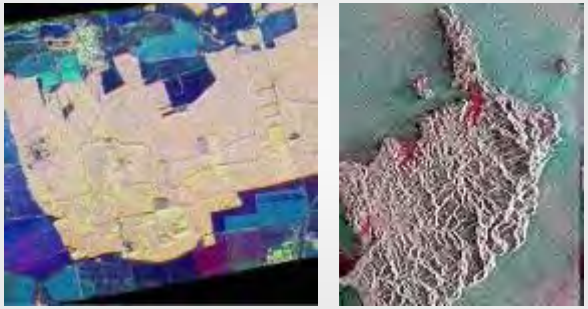

Subsidence

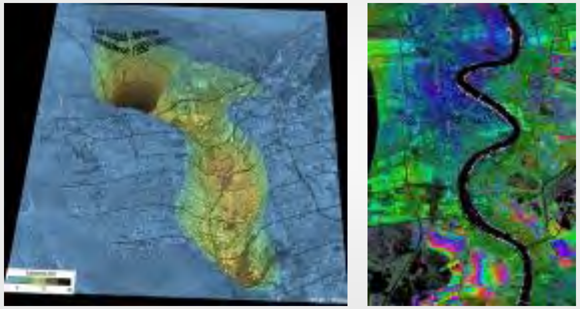

Traffic

Disaster

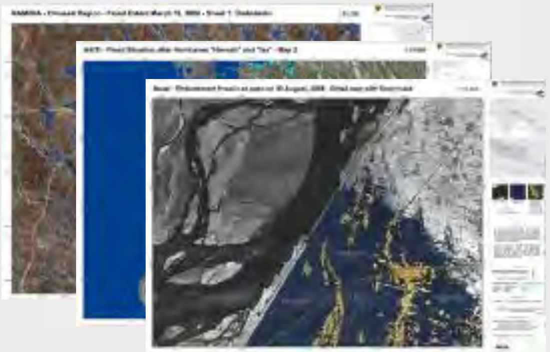

Reconnaissance

SAR Basic Principle

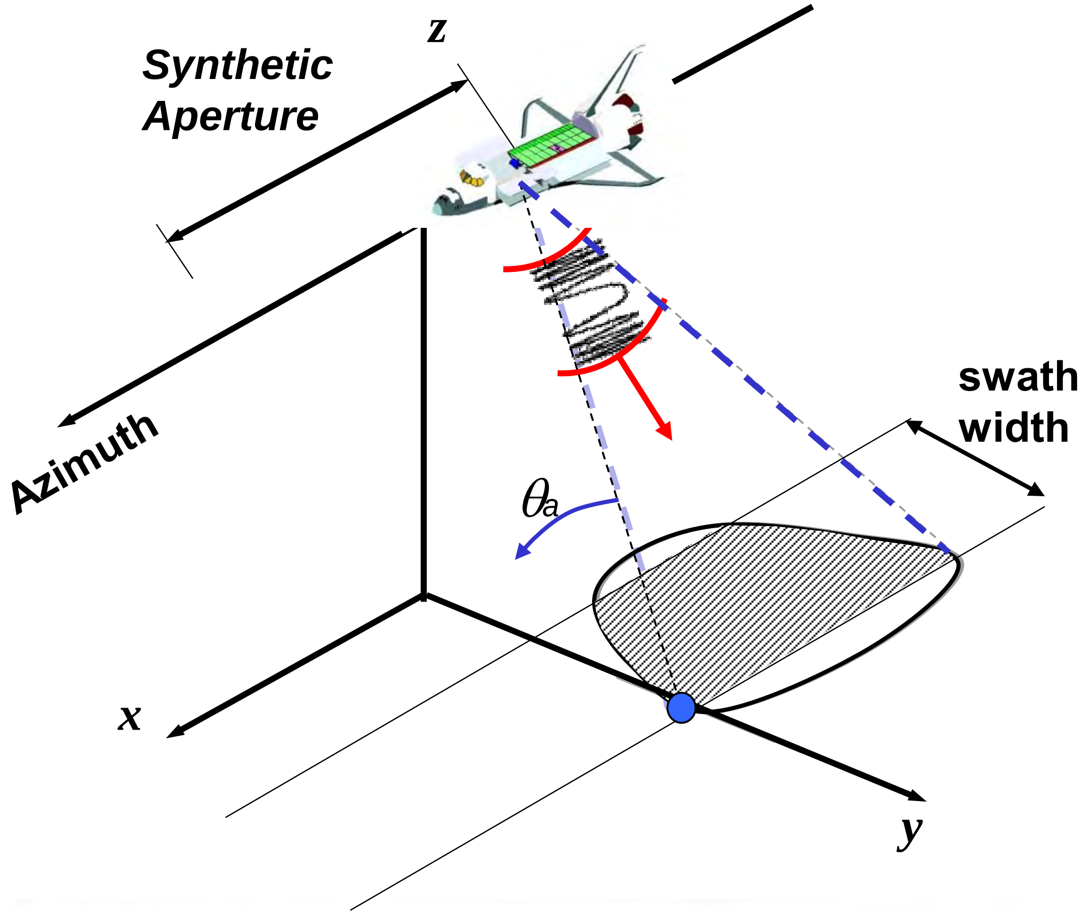

SAR Raw and Image Data

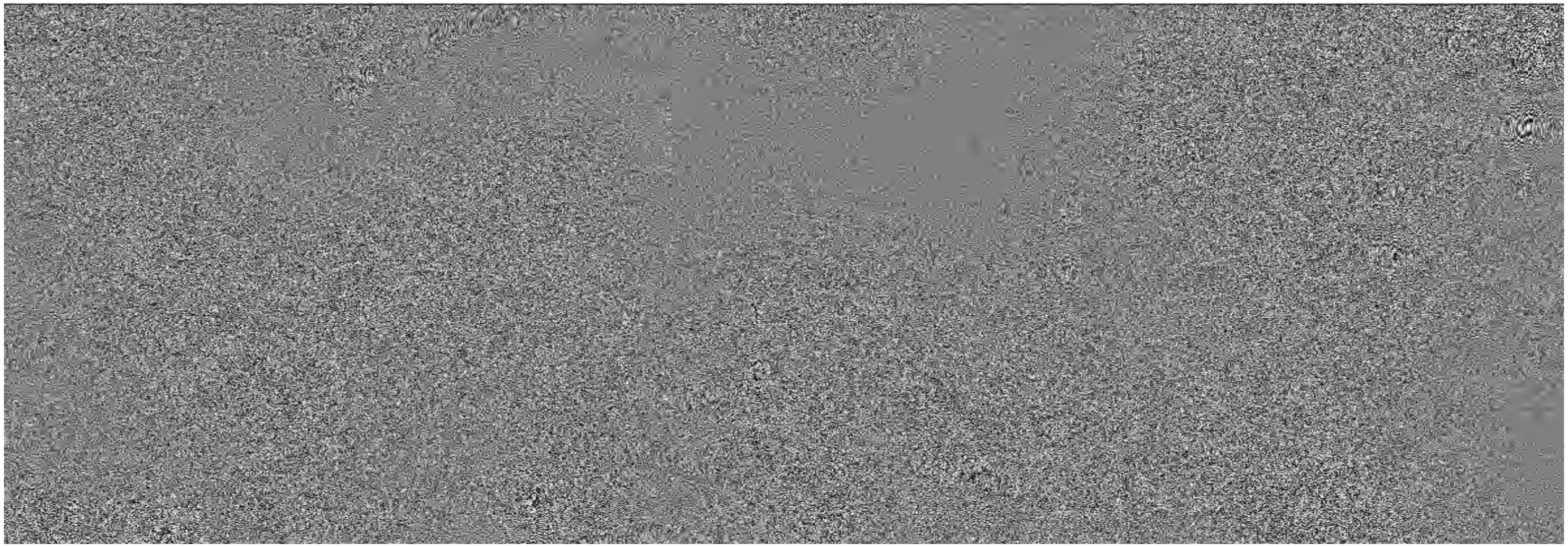

SAR
raw data

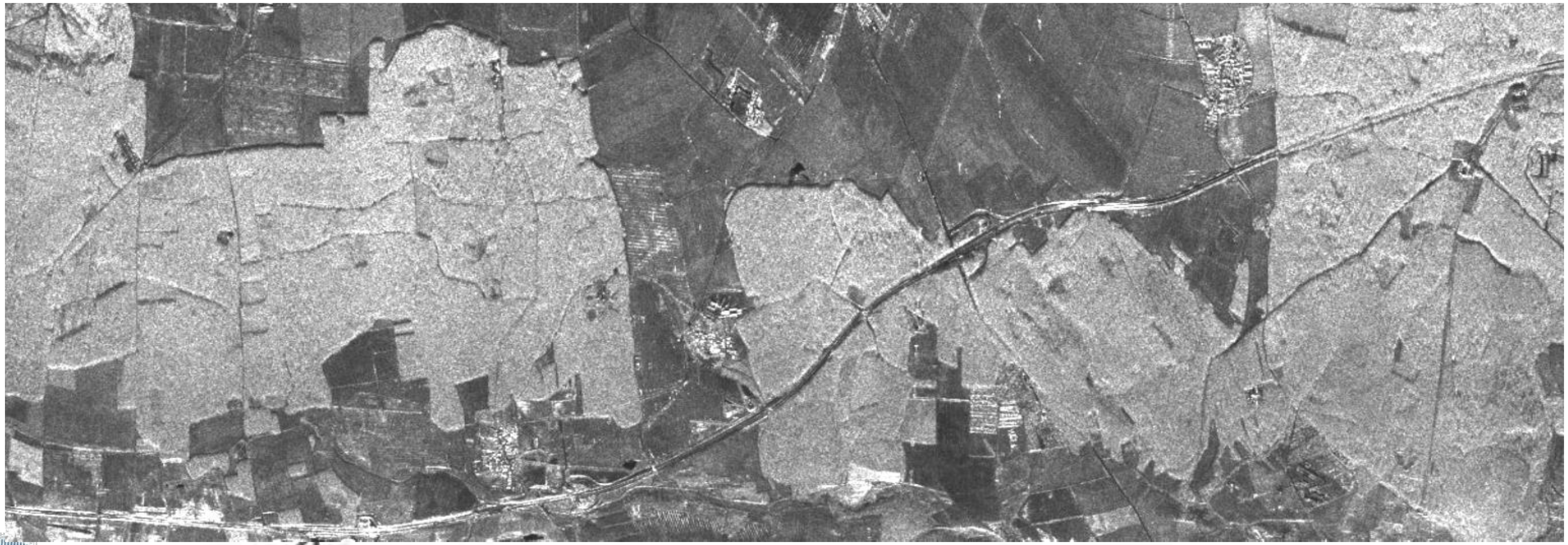

SAR
image

SAR Processing: Two-Dimensional Matched Filter

$s_o\,(x, r)$ → **range compression** $h_r\,(x, r)$ → **azimuth compression** $h_a\,(x, r)$ → **detection** $\sqrt{u_i^2 + u_q^2}$ → **2D pulse** $|u_o\,(x, r)|$

SAR Processing (simplified)

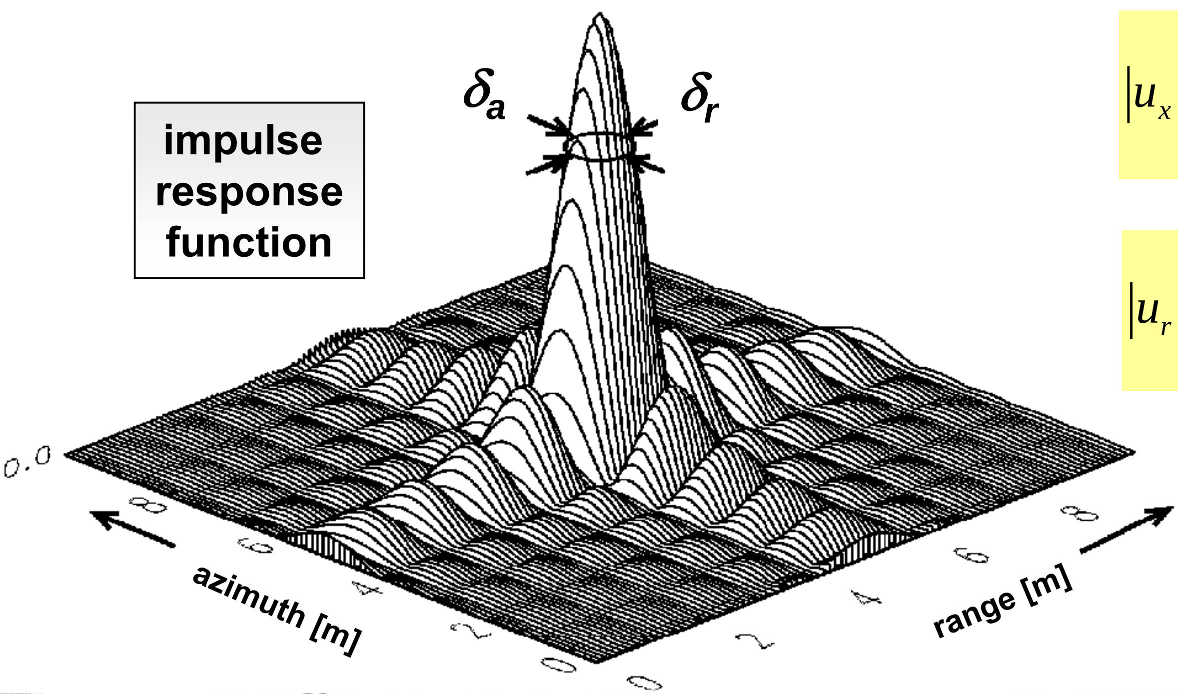

$$|u_x(x)| = \left| \sqrt{B_a T_a}\, \mathrm{sinc}\left[\pi \frac{B_a (x - x_0)}{v_p} \right] \right|$$

$$|u_r(r)| = \left| \sqrt{B_r \tau_p}\, \mathrm{sinc}\left[2\pi \frac{B_r (r - r_0)}{c} \right] \right|$$

SAR as a linear system

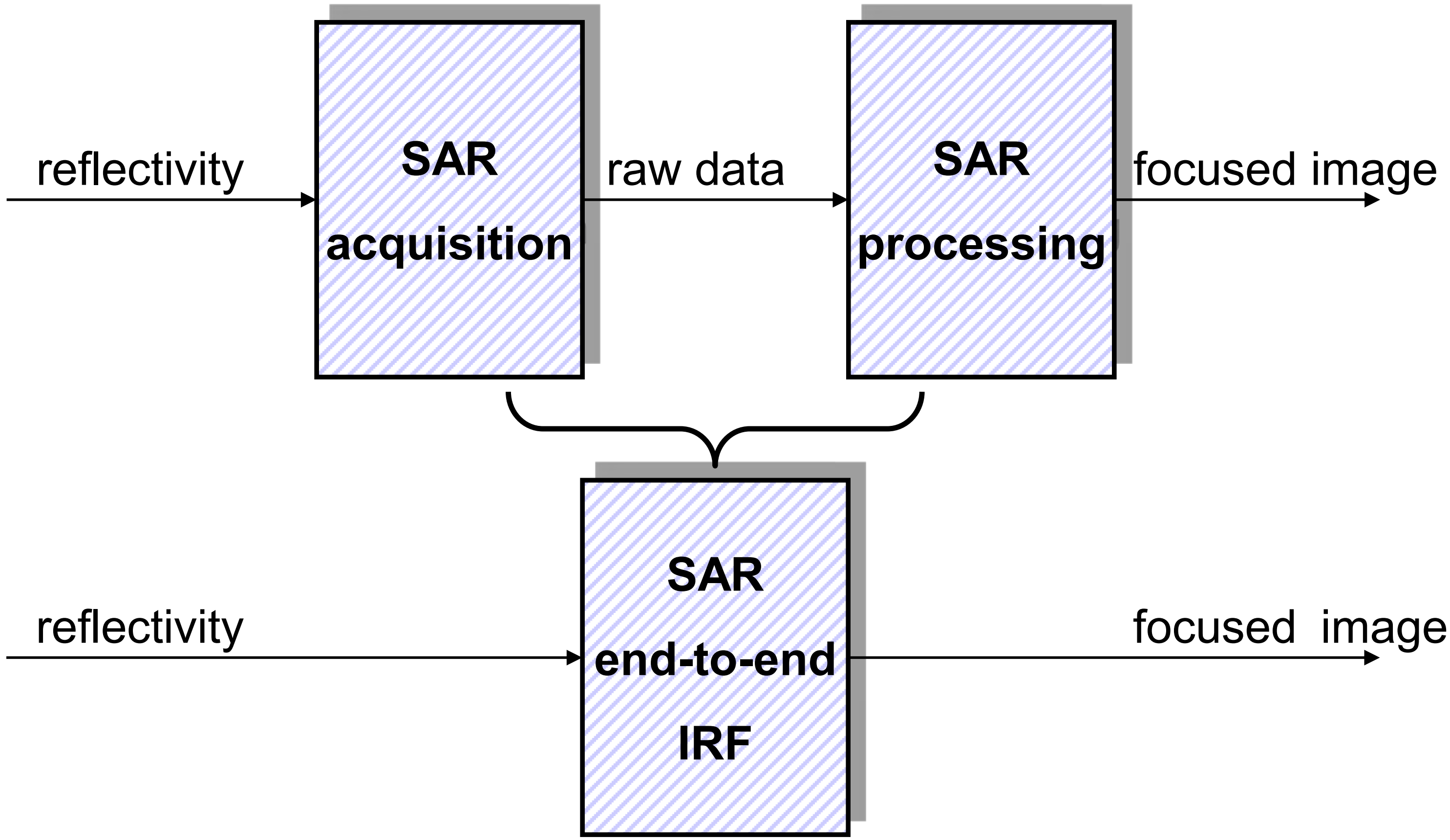

Phase and impulse response details

- Due to the band-pass characteristic of the IRF, the final signal can be thought as the convolution between the modulated reflectivity and a 2-D impulse response function

- The reflectivity itself is really the integration of the reflectivity along the elevation angle (cylindrical geometry):

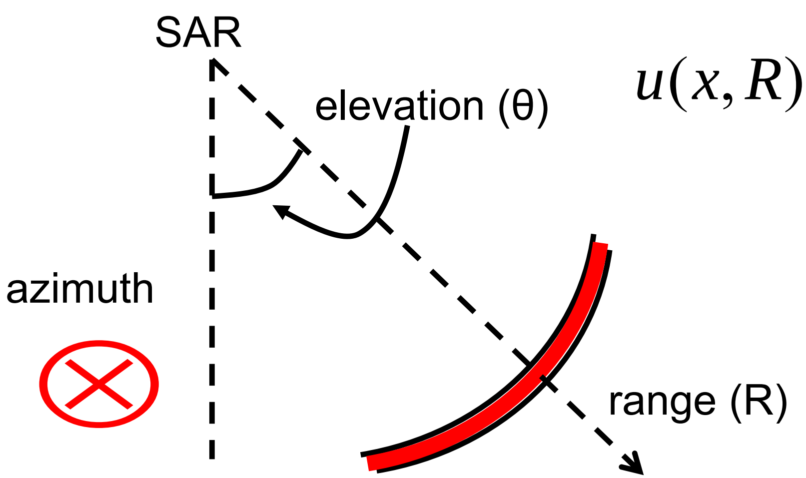

$$u(x,R) = \int a(r')\exp\{-j2kR'\}h(x-x',R-R')dV'$$

$$= \underbrace{\left(\int a(r)Rd\theta \times \exp\{-j2kR\}\right)}_{\substack{\text{modulated reflectivity} \\ \text{(cilindrically integrated)}}} ** \underbrace{h(x,R)}_{\text{2-D IRF}}$$

A SAR image has a 2-D cylindrical geometry (but the world is 3-D at least)

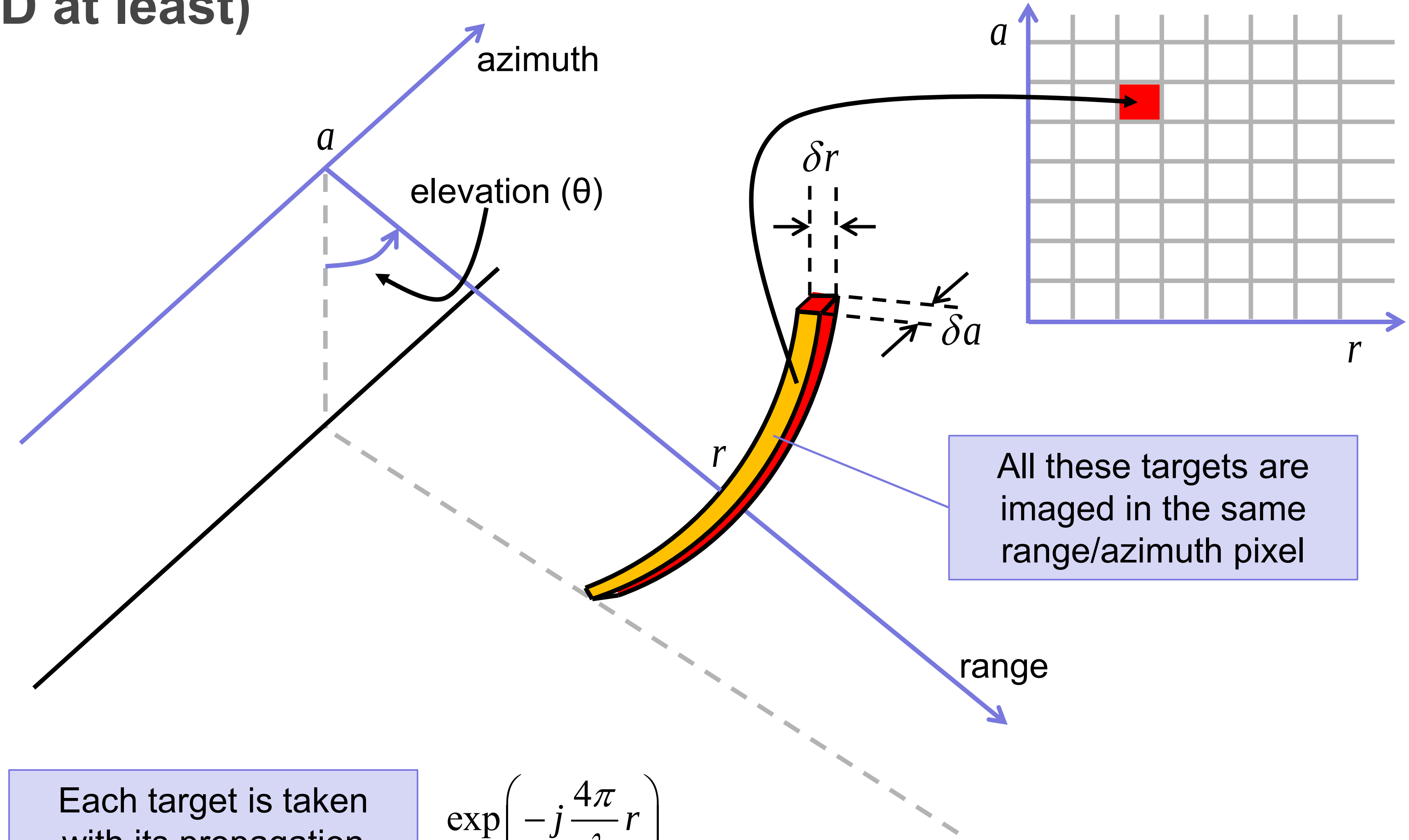

All these targets are imaged in the same range/azimuth pixel

Each target is taken with its propagation phase

$$\exp\left(-j\frac{4\pi}{\lambda}r\right)$$

Single scatterer contribution

- Every scatterer (target) contributes to the image with its complex amplitude and a propagation phase

$$s = a \exp\left(-j \frac{4\pi}{\lambda} r\right)$$

- Within one pixel (resolution cell) the phase oscillates fast (e.g. 100 times for TerraSAR-X)

- The wavelength is typically in the order of a few centimeters / decimeters

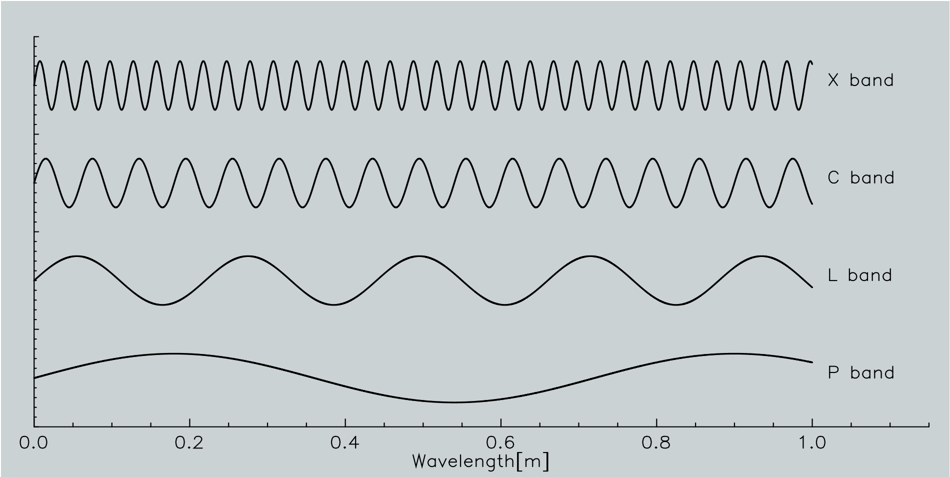

~3 cm

~6 cm

~22 cm

~76 cm

The propagation phase

$$s = a\exp\left(-j\frac{4\pi}{\lambda}r\right) = a\cos\left(\frac{4\pi}{\lambda}r\right) - a\,j\sin\left(\frac{4\pi}{\lambda}r\right)$$

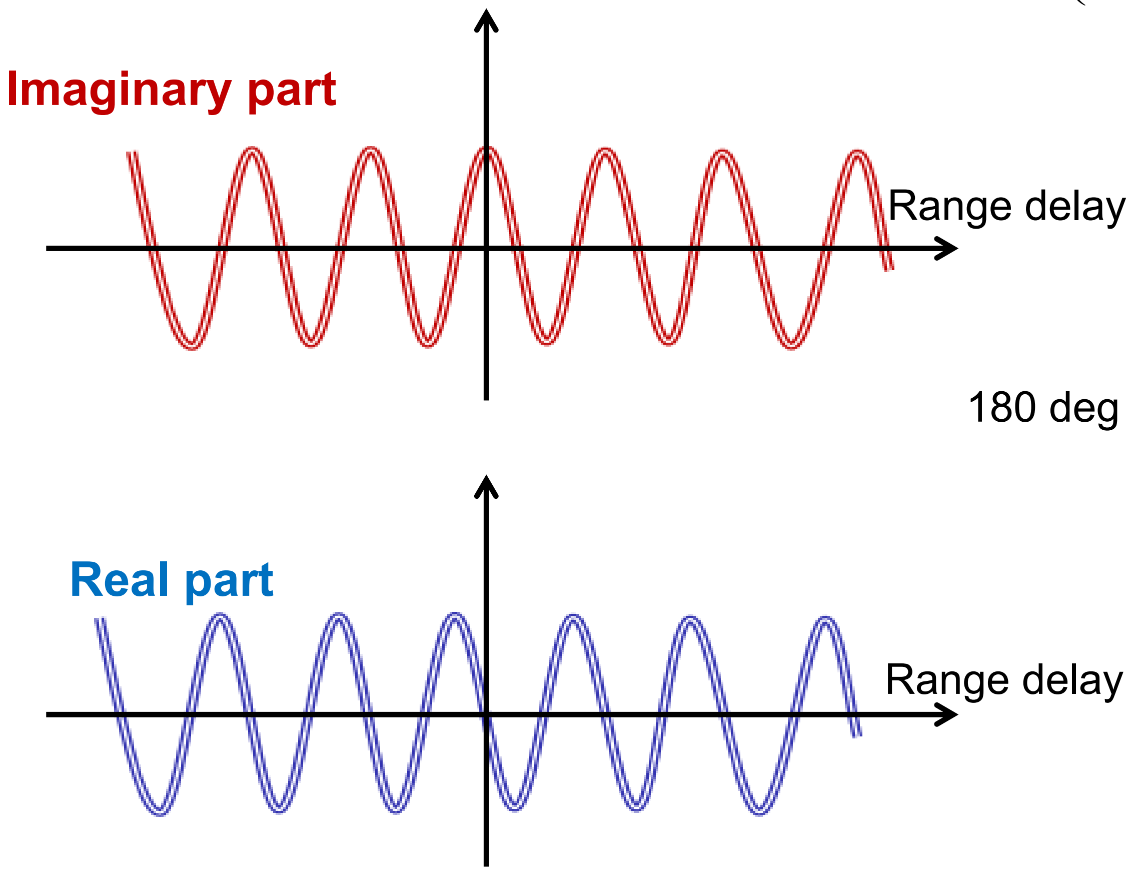

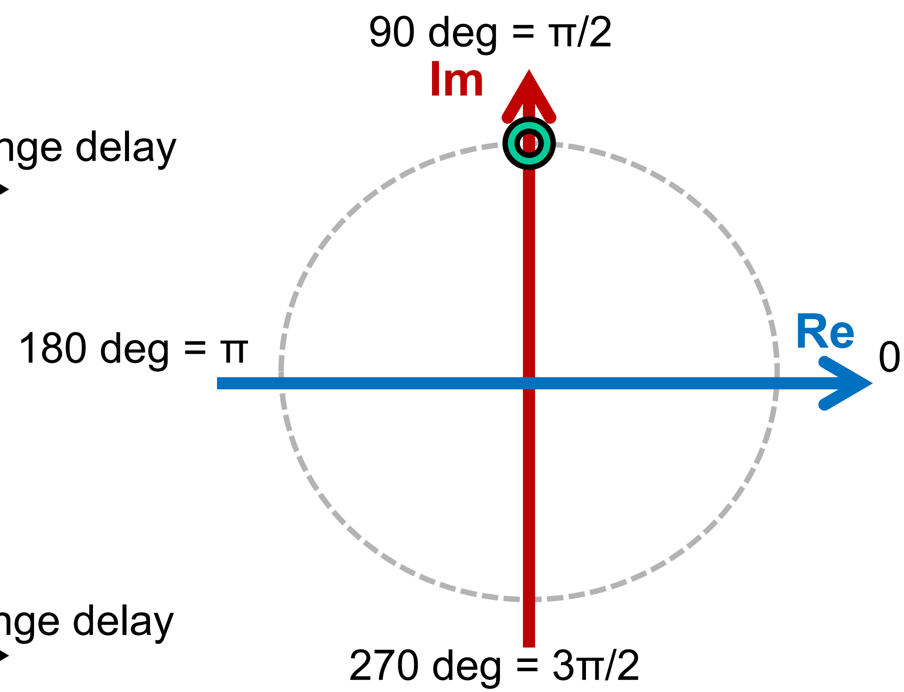

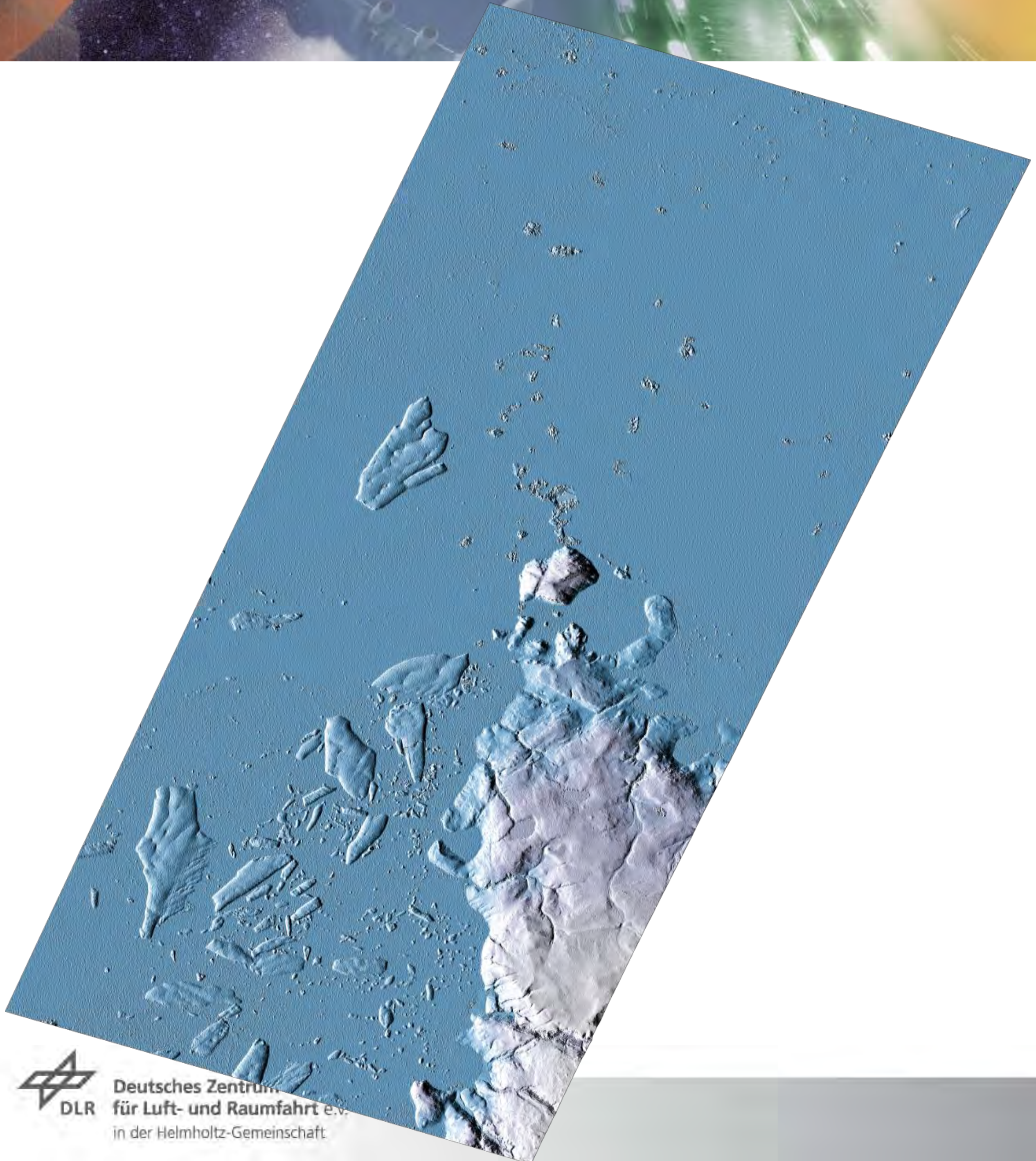

Interferometry Principle

SAR Interferometry

- Two or more complex-valued SAR images are combined
- Information about the imaged objects (compared to a single image) are derived by exploiting the **phase differences** …
- Therefore the images must differ in at least one aspect ($\Rightarrow$ "Baseline")

Baseline Type	Name	Measurements and Applications
$\Delta\phi$	Across-Track	Topography, digital elevation models (DEMs)
Δt = ms … s	Along-Track	ocean currents, moving object detection
Δt = days	Differential	glacier / ice fields, lava flows, hydrology
Δt = days … years	Differential	subsidence, seismic events, volcanic activities, crustal displacements
Δt = ms … years	Coherence Estimator	sea surface decorrelation times, land cover classification

Interferometry Principle

SAR

- Tw … SAR imag
- Inf … objects (c … re
  de … e differe
- Th … fer in at le …)

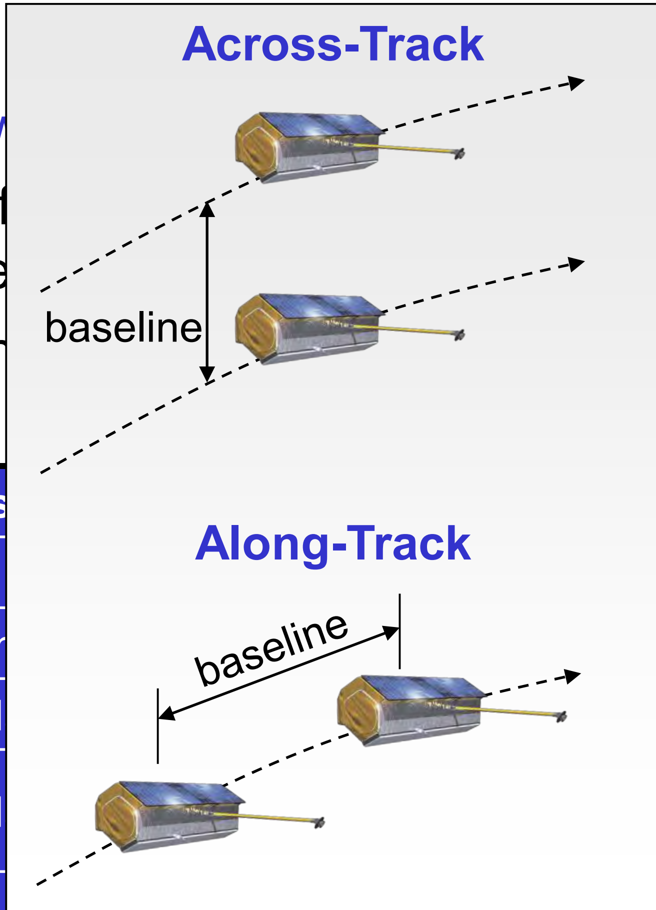

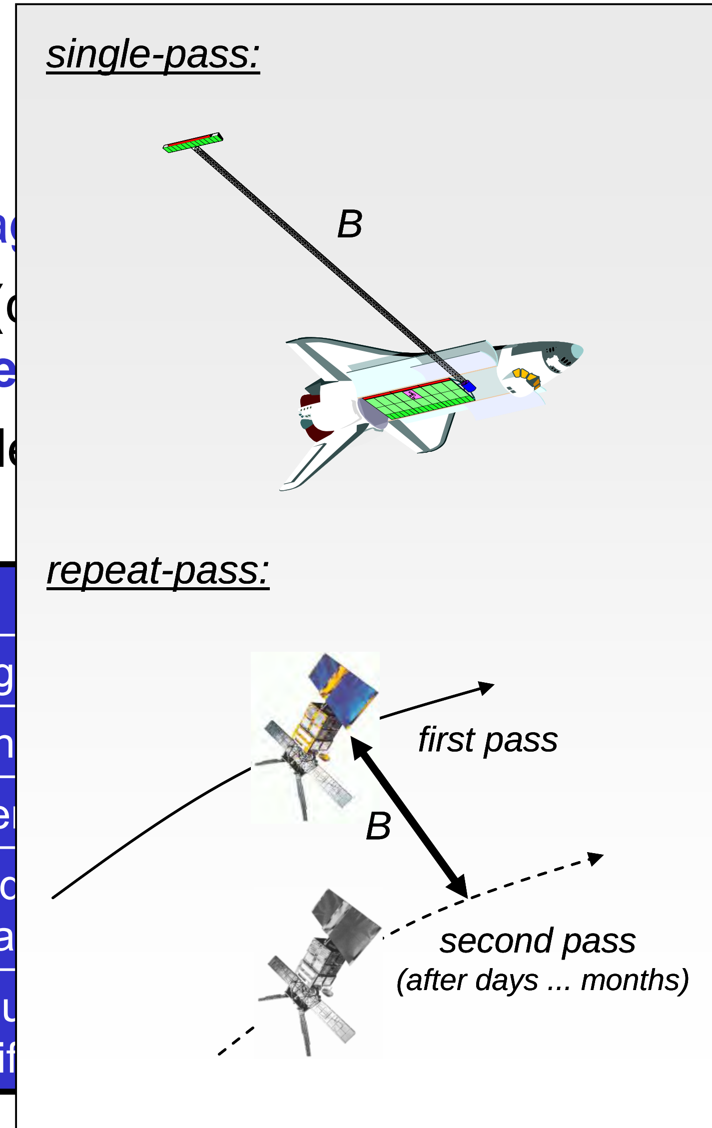

Bas			
$\Delta\phi$		Topog	)
Δt = m		ocean	
Δt = d		glacier	
Δt = d		subsic crusta	es,
Δt = ms … years	Coherence Estimator	sea su classif	

Interferometry Principle

- Phase of a complex SAR pixel

$$\varphi = -\frac{4\pi}{\lambda} \underbrace{r}_{\text{range dependent}}$$

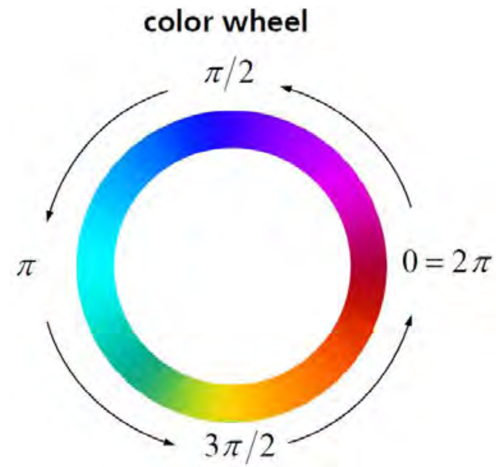

Phase is always ambiguous w.r.t. integer multiples of 2π
$\Rightarrow$ phase unwrapping required!

SAR Image 1

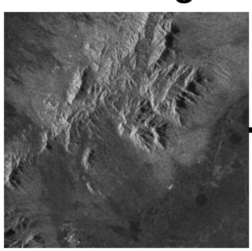

$$u_1 = |G_1| \exp\left(j\varphi_1\right)$$

SAR Image 2

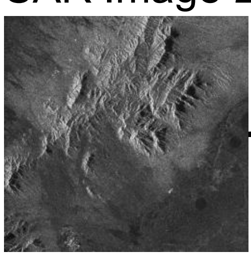

$$u_2 = |G_2| \exp\left(j\varphi_2\right)$$

$\otimes$ *

$$v = |G_1||G_2| \exp\left[j\left(\varphi_1 - \varphi_2\right)\right]$$

arg()

$$\Delta\phi = \varphi_1 - \varphi_2$$

Interferogram

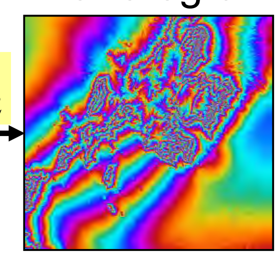

* … means complex conjugated

Deutsches Zentrum für Luft- und Raumfahrt e.V. in der Helmholtz-Gemeinschaft

Applications:
Across-Track Interferometry (XTI)

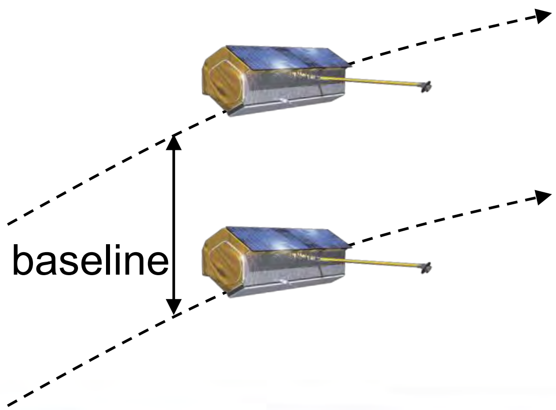

Across-Track Interferometry Principle

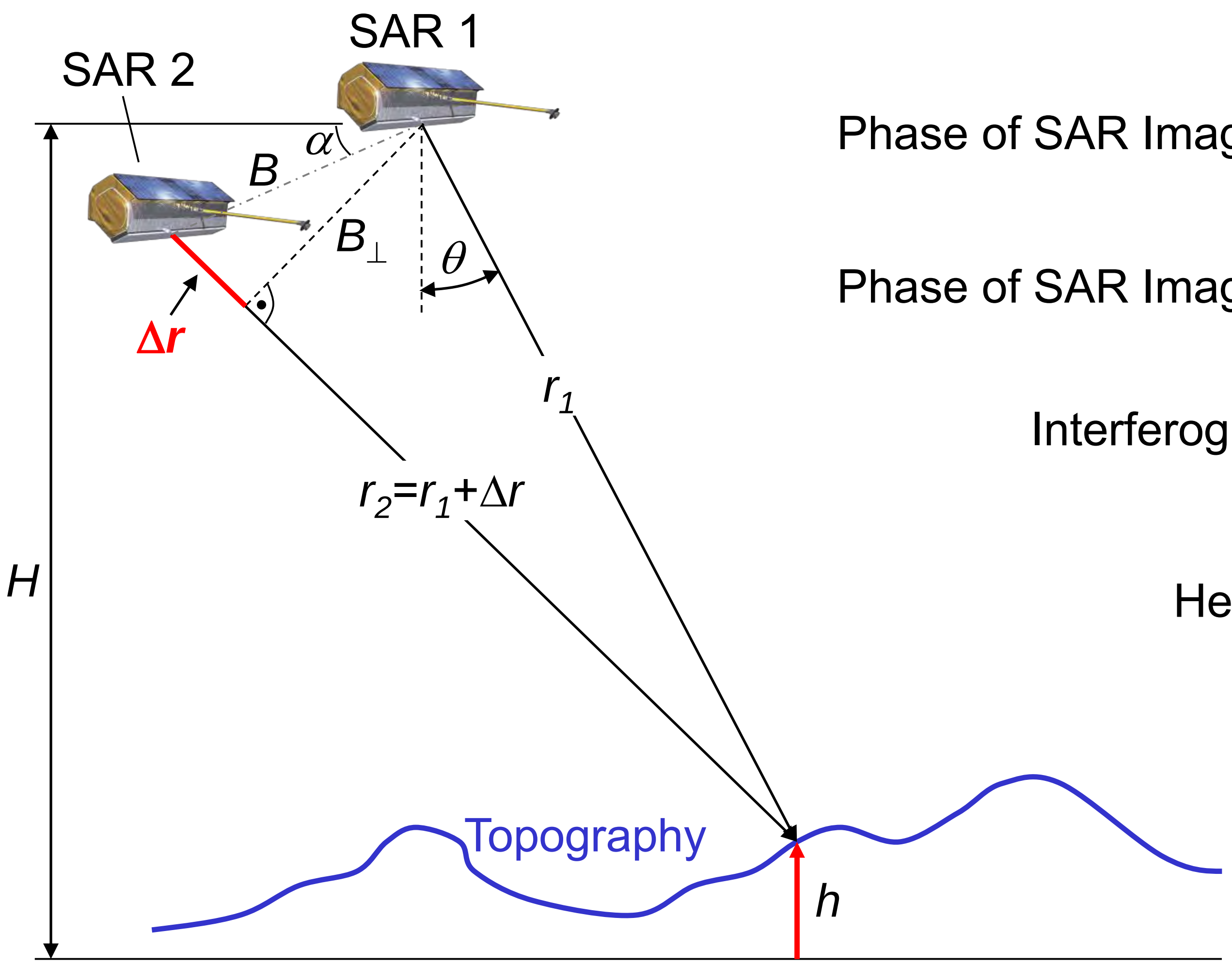

Phase of SAR Image 1: $\varphi_1 = -\frac{4\pi}{\lambda} r_1$

Phase of SAR Image 2: $\varphi_2 = -\frac{4\pi}{\lambda} (r_1 + \Delta r)$

Interferogram: $\Delta\phi = \varphi_1 - \varphi_2 = \frac{4\pi}{\lambda} \Delta r$

Height: $h = H - r_1 \cos\theta$

Needs to be estimated!

Interferometry allows to locate targets in the third dimension (elevation or cross-range)

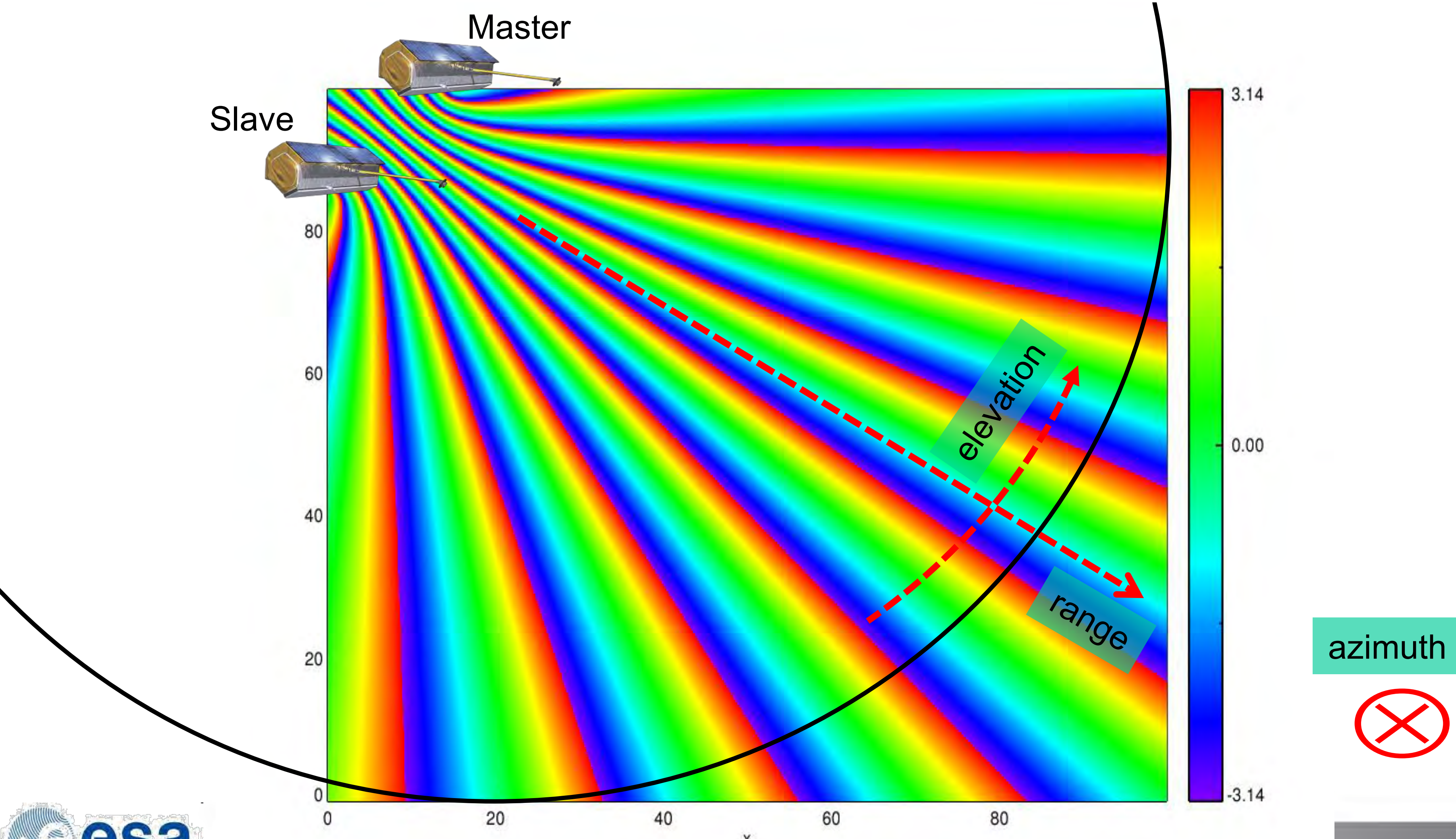

Across-Track Interferometry as a Measurement of Angle

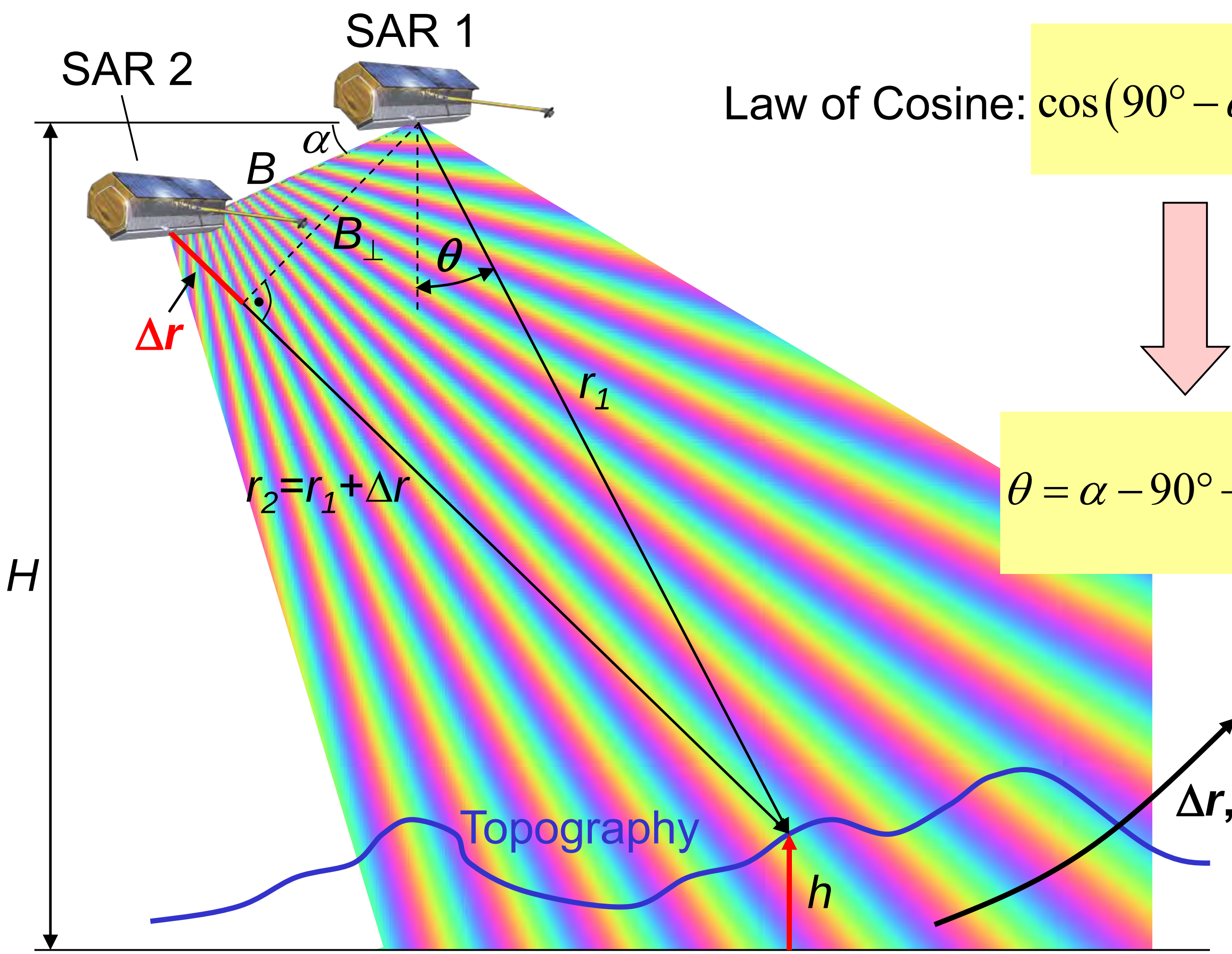

Law of Cosine: $\cos\left(90° - \alpha + \theta\right) = \dfrac{r_1^2 + B^2 - \left(r_1 + \Delta r\right)^2}{2 r_1 B}$

H, B and α are known,
r_1 and Δr ($\leftarrow \Delta\phi$)
are measured

$$\theta = \alpha - 90° + \operatorname{acos}\left(\frac{r_1^2 + B^2 - \left(r_1 + \Delta r\right)^2}{2 r_1 B}\right)$$

Height: $h = H - r_1 \cos\theta$

Deutsches Zentrum
für Luft- und Raumfahrt e.V.
in der Helmholtz-Gemeinschaft

Example: Interferogram of Cotopaxi, Acquired with SRTM

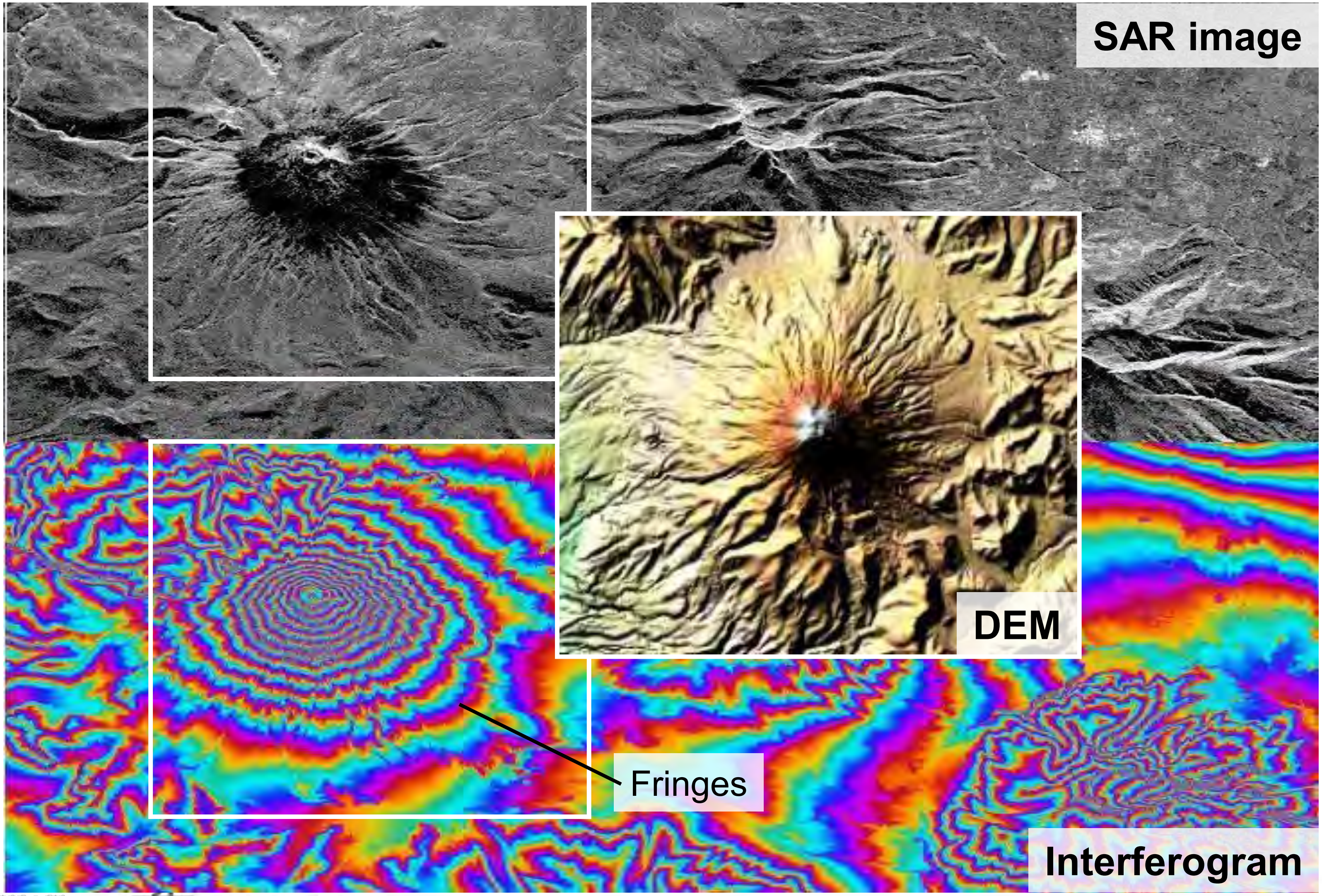

TerraSAR-X Repeat Pass Interferogram of Paris

(HS 300 MHz 16.1.-27.1.2008)

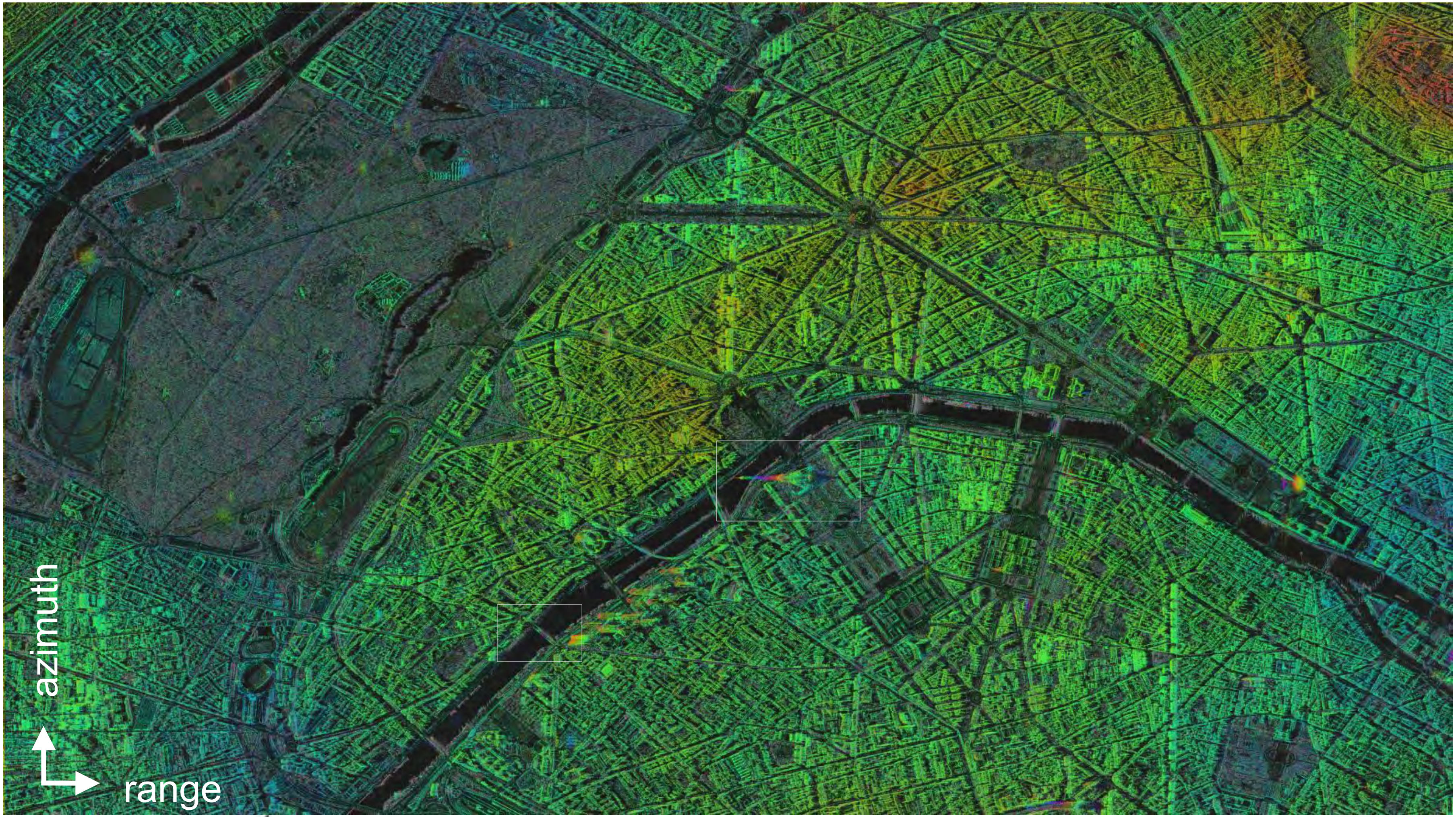

by Remote Sensing Technology Institute

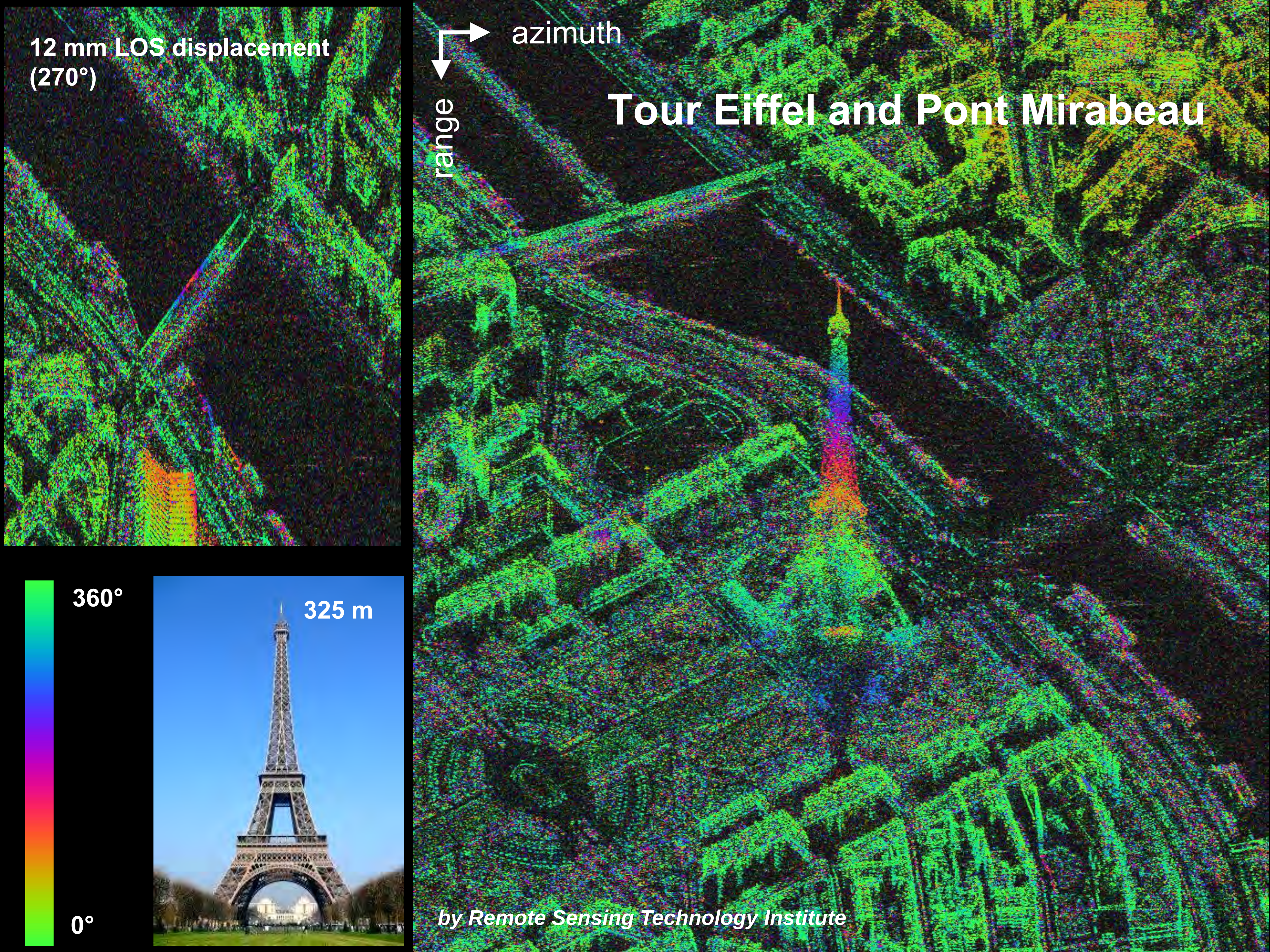
12 mm LOS displacement
(270°)
azimuth
range
Tour Eiffel and Pont Mirabeau
360°
0°
325 m
by Remote Sensing Technology Institute

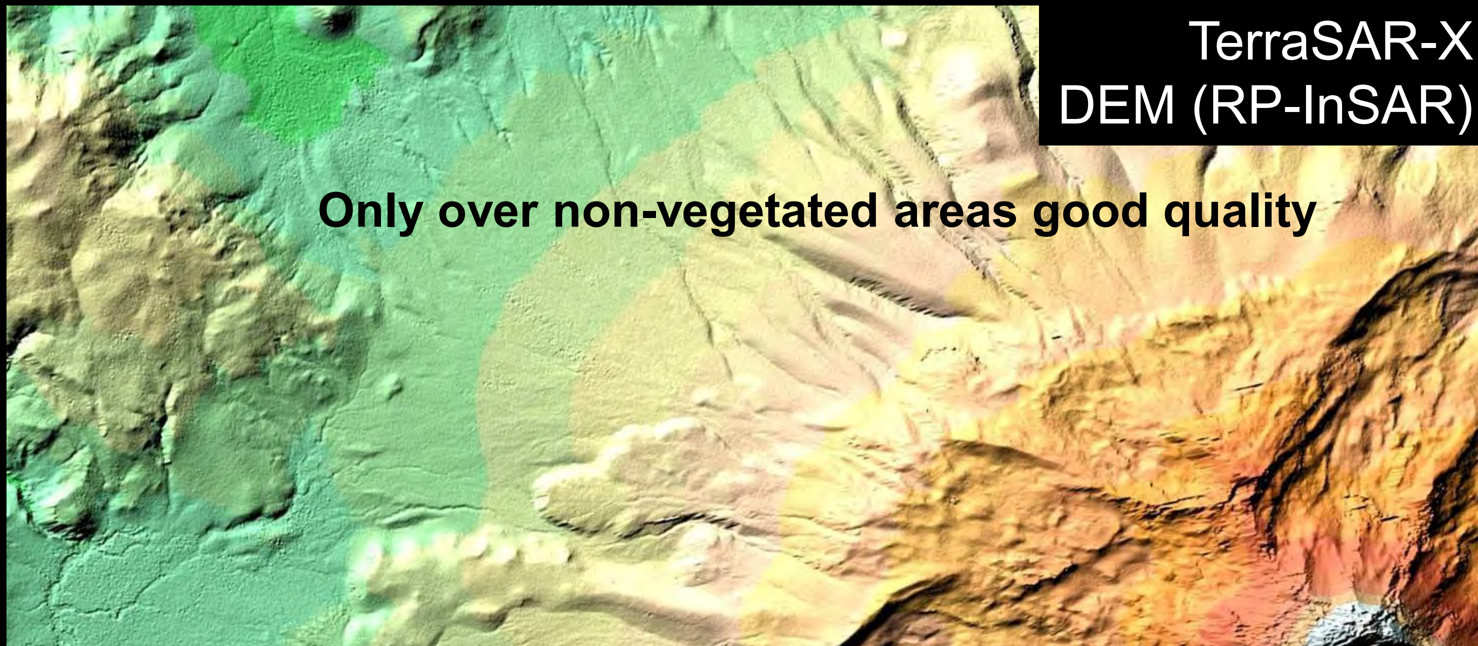
TerraSAR-X
DEM (RP-InSAR)
Only over non-vegetated areas good quality


SRTM
DEM

Coherence: measure of interferometric quality

Coherence

$$\gamma = \frac{E\left[m\, s^*\right]}{\sqrt{E\left[m\, m^*\right] E\left[s\, s^*\right]}}$$

a correlation coefficient,

sometimes just called *correlation*

$$0 \leq |\gamma| \leq 1$$

Sample coherence

$$\hat{\gamma} = \frac{\sum_k m(k) s^*(k)}{\sqrt{\sum_k m(k) m^*(k) \sum_k s(k) s^*(k)}}$$

averaged over

a small window

of N pixels

k = 1, 2,…, N

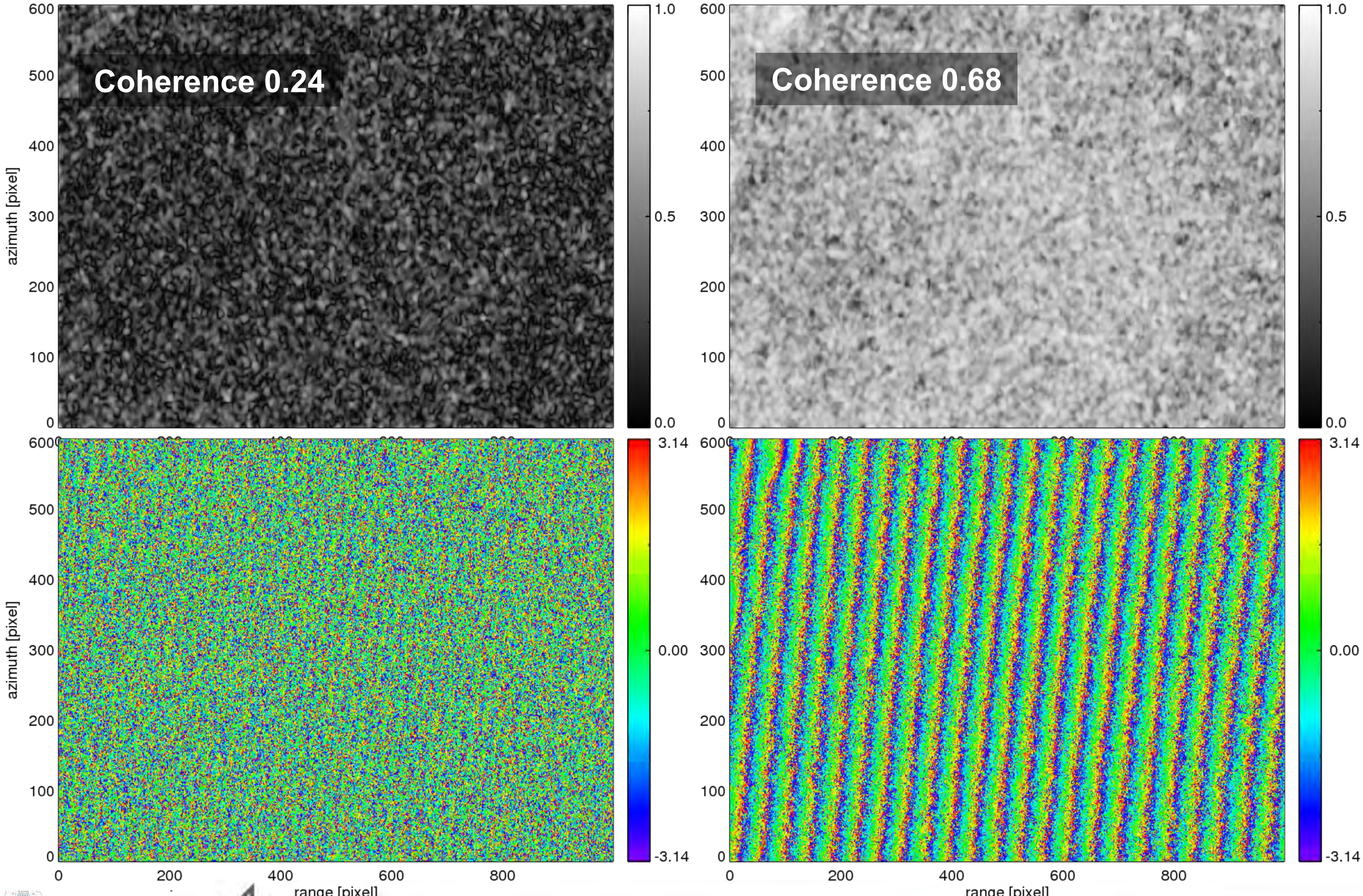

Coherence 0.24
Coherence 0.68
azimuth [pixel]
range [pixel]
1.0
0.5
0.0
3.14
0.00
-3.14
0
100
200
300
400
500
600
800

Coherence: phase variance

- Coherence is linked to phase variance in a neighborhood
  - More coherence = less phase variance
  - The absolute value of the coherence is what matters
  - Cramér-Rao Bound for phase estimates (averages)

$$\varphi = \arg\left(\sum_{k=1}^{N} m(k) s^*(k) \right)$$

$$\sigma_\varphi^2 \approx \frac{1-|\gamma|^2}{2N|\gamma|^2}$$

Summing complex numbers

Number of independent samples (looks)

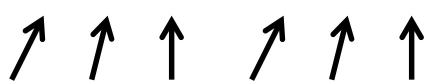

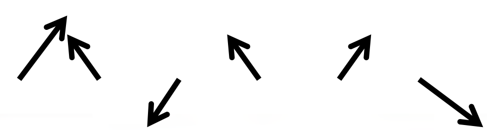

Interferometric phase quality: coherence

- Coherence is a measure of how much two “pixels” look alike. It takes values between 0 and 1.

$$\gamma_{\text{int}} = \gamma_{\text{temp}} \cdot \gamma_{\text{geo}} \cdot \gamma_{\text{vol}} \cdot \gamma_{\text{Doppler}} \cdot \gamma_{\text{cor}} \cdot \gamma_{\text{amb}} \cdot \gamma_{\text{quant}} \cdot \gamma_{\text{SNR}}$$

- Sources of decorrelation:
  - Temporal decorrelation (things change: λ, Vegetation, Water, Ice, Dry soil, Urban)
  - Geometric decorrelation: due to variations of the interferometric phase within a resolution cell
    - Causes range spectral shift
    - Increases with baseline (critical baseline causes total coherence loss)
    - Decreases if we increase the pulse bandwidth (=improve range resolution)
    - Leads to trade off between height sensitivity and interferometric quality
  - Volume decorrelation: due multiple targets with different interferometric phase at the same exact range
    - Increases with baseline, and with penetration depth

Interferometric phase quality: coherence

- Coherence is a measure of how much two “pixels” look alike. It takes values between 0 and 1.

$$\gamma_{\text{int}} = \gamma_{\text{temp}} \cdot \gamma_{\text{geo}} \cdot \gamma_{\text{vol}} \cdot \gamma_{\text{Doppler}} \cdot \gamma_{\text{cor}} \cdot \gamma_{\text{amb}} \cdot \gamma_{\text{quant}} \cdot \gamma_{\text{SNR}}$$

- Sources of decorrelation:
  - „Doppler decorrelation“: Due to acquistions under different squint/Doppler Centroid. Implies that resolution cell is being observed from a different direction.
    - Can be mitigated by „common band filtering“ at the expense of resolution.
    - Doppler Centroid difference = Doppler bandwidth

      ⬇

      Complete decorrelation
  - Co-registration errors.
  - Ambiguities, quantization and thermal/system noise.

Deutsches Zentrum für Luft- und Raumfahrt e.V. in der Helmholtz-Gemeinschaft

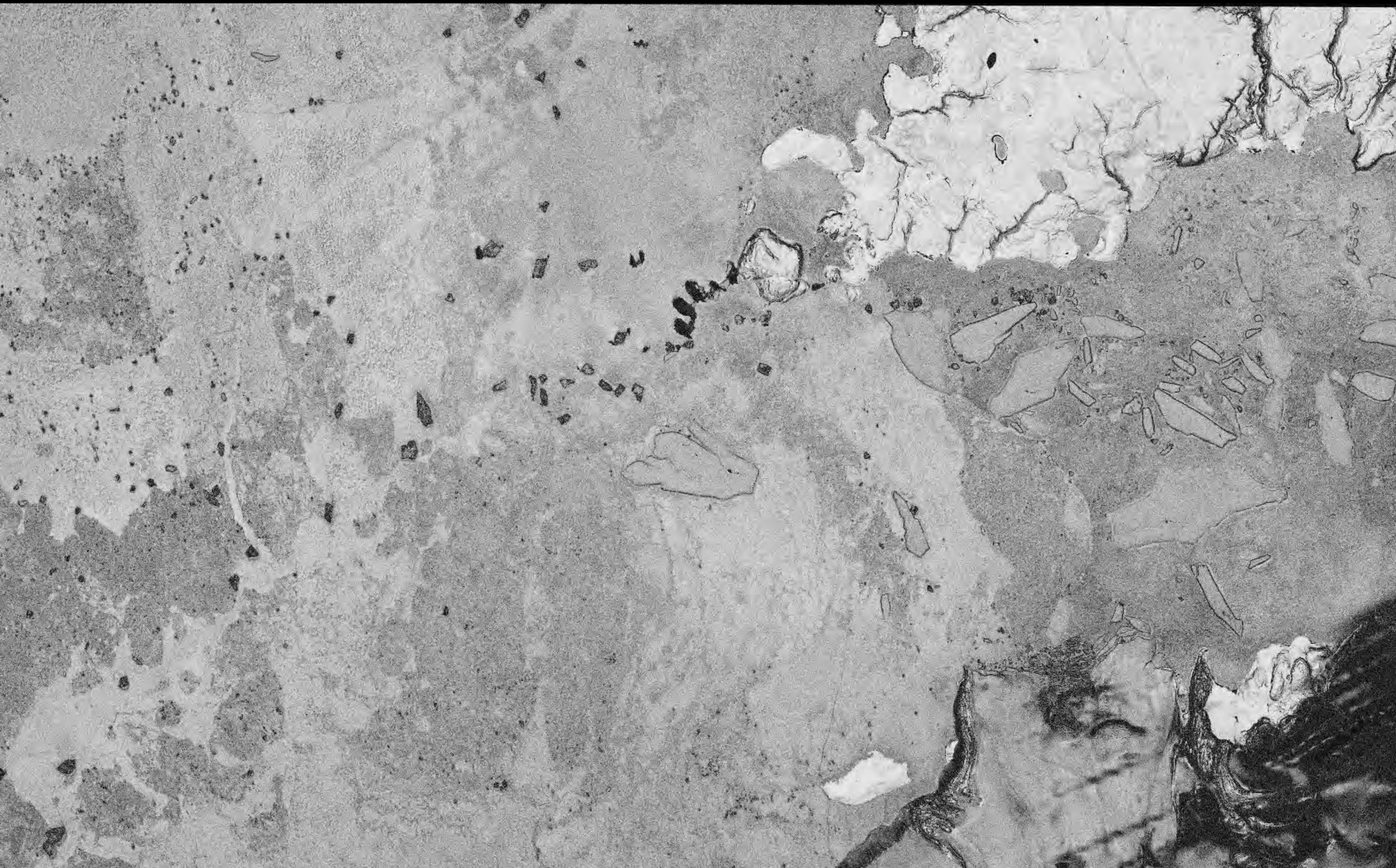


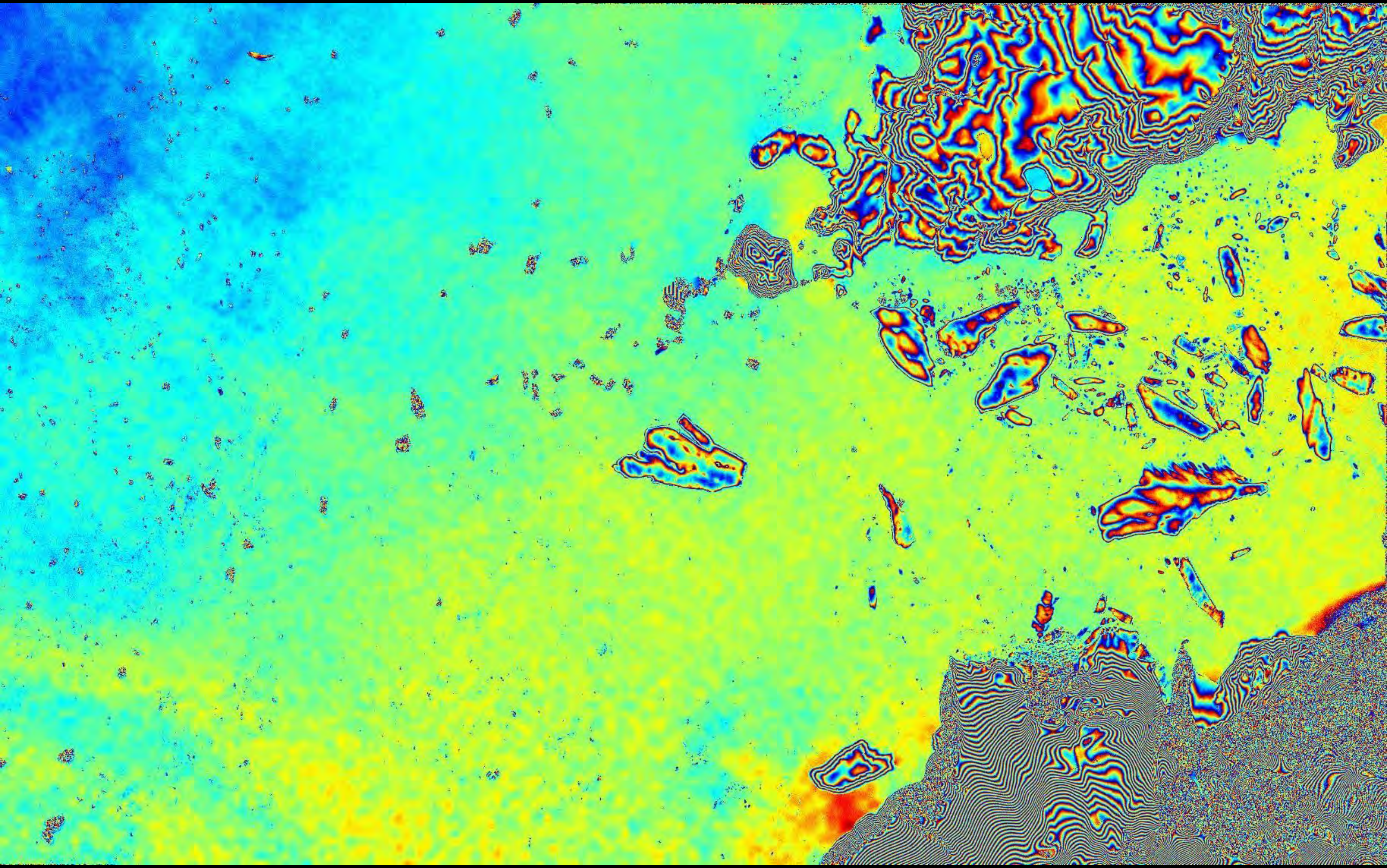

TanDEM-X first DEM

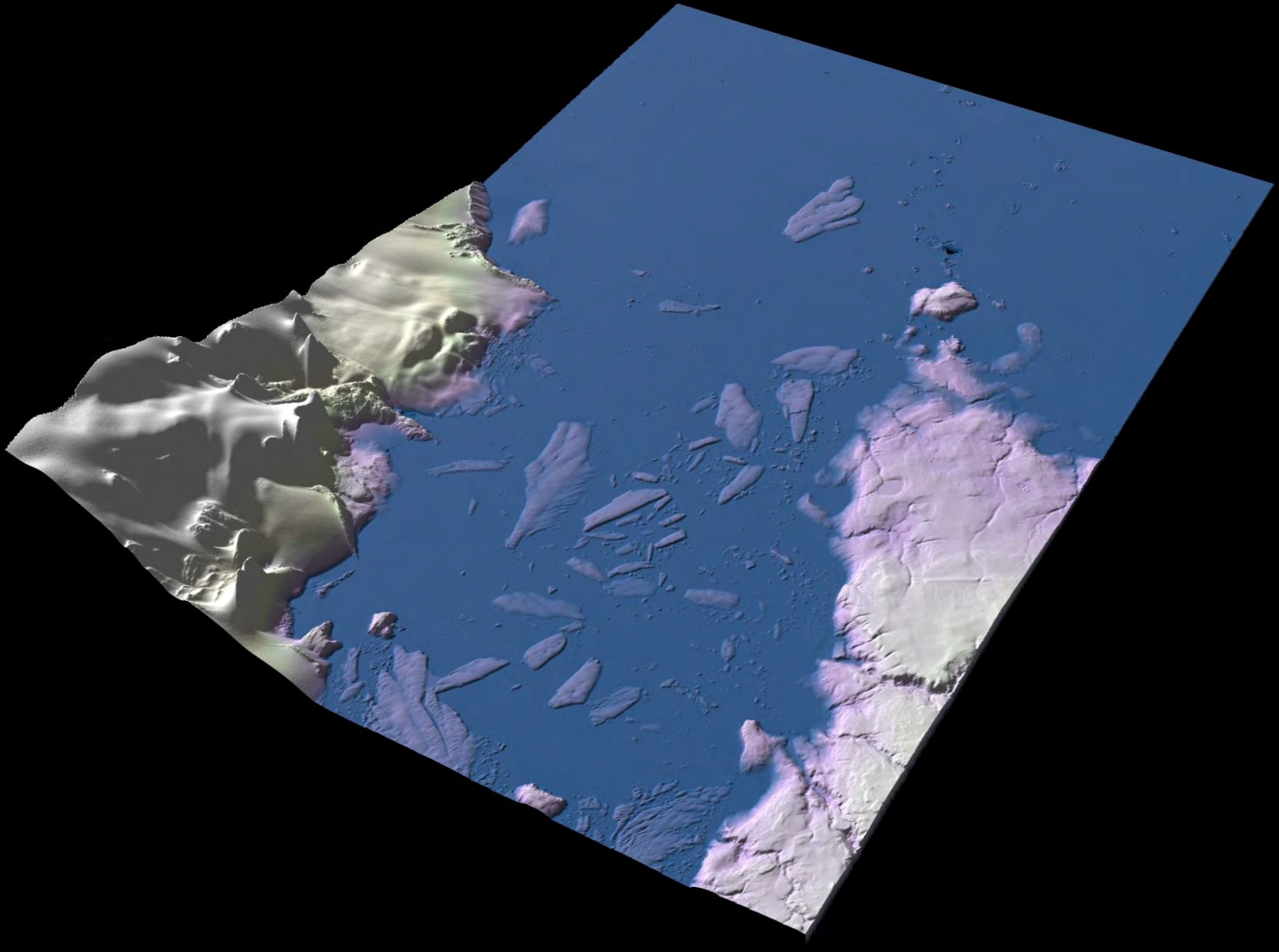

DEM Error/Performance

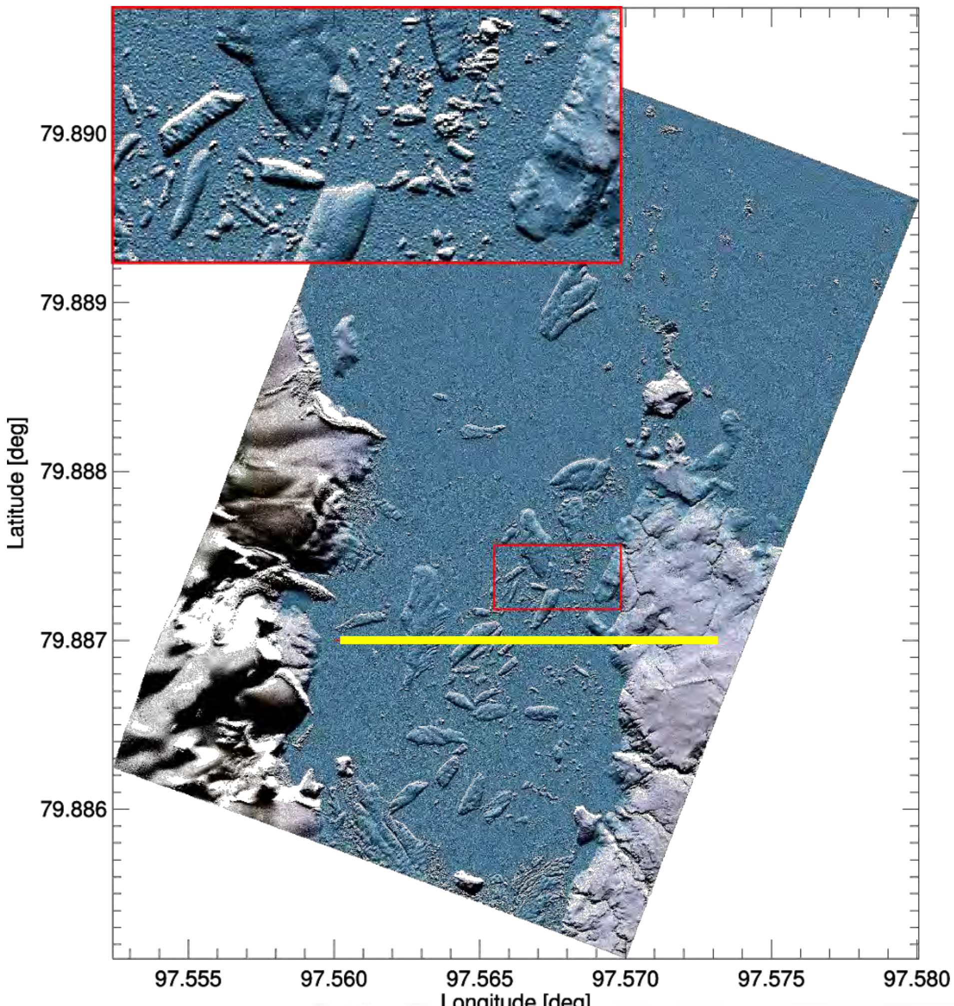

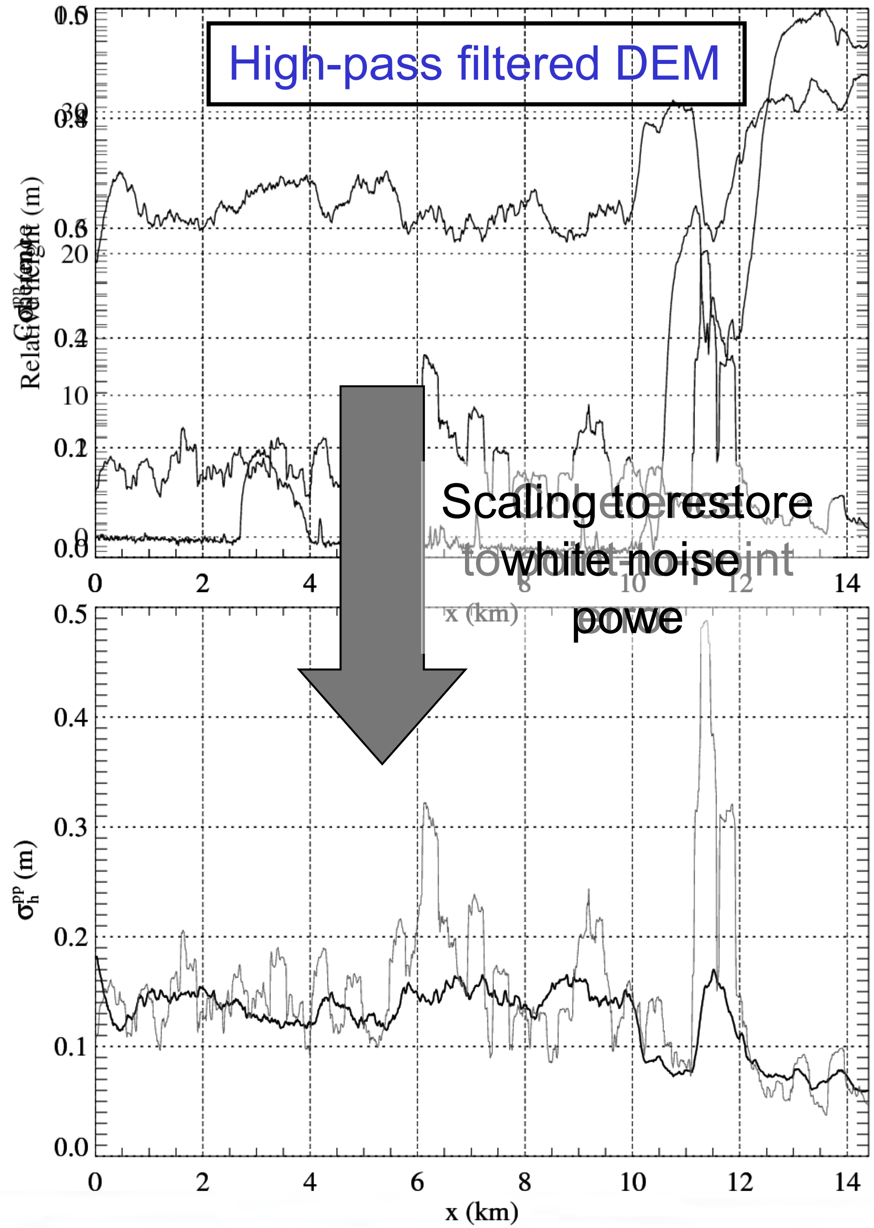

Height of ambiguity and cross-track baseline

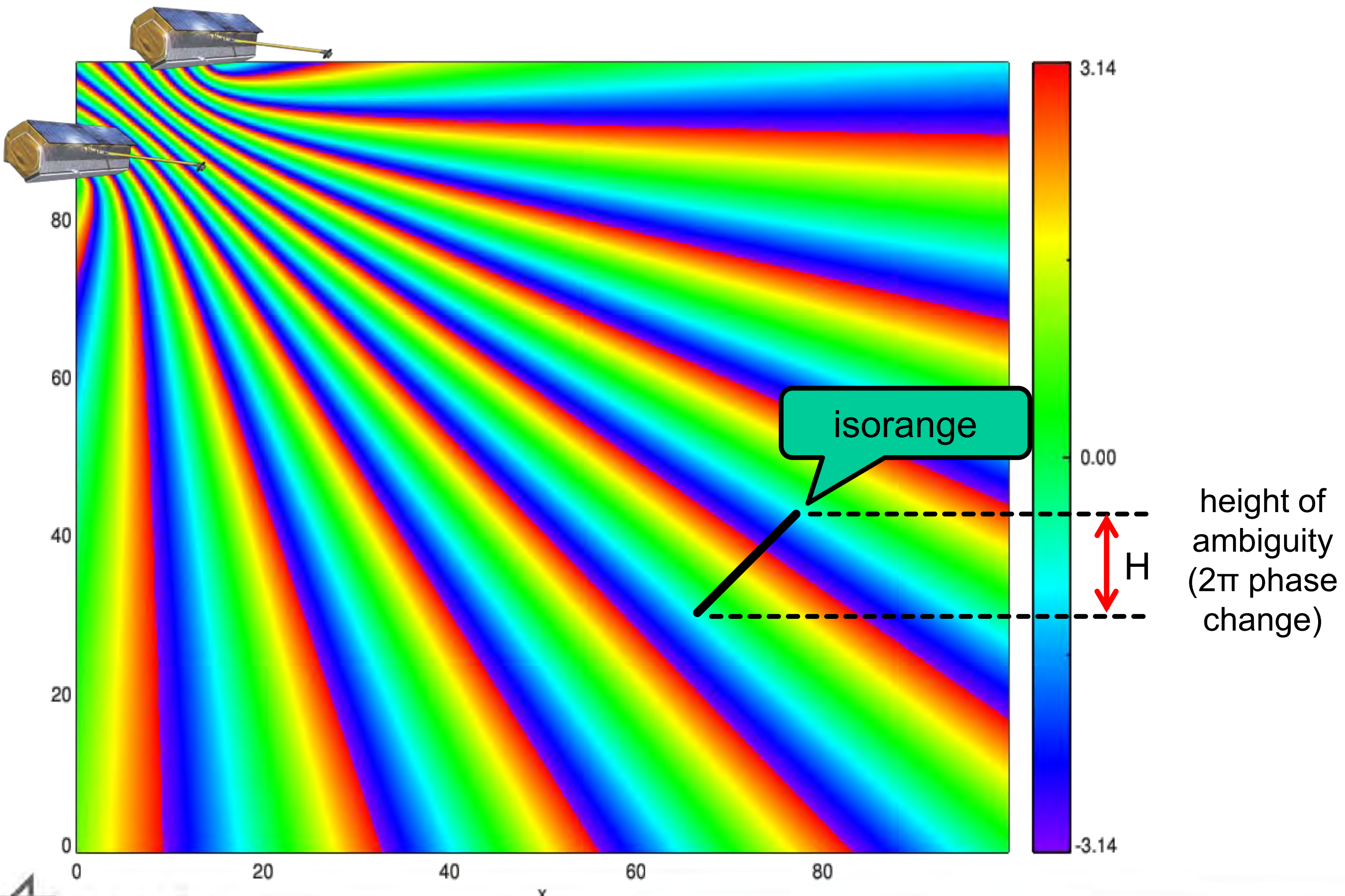

Height of ambiguity and cross-track baseline

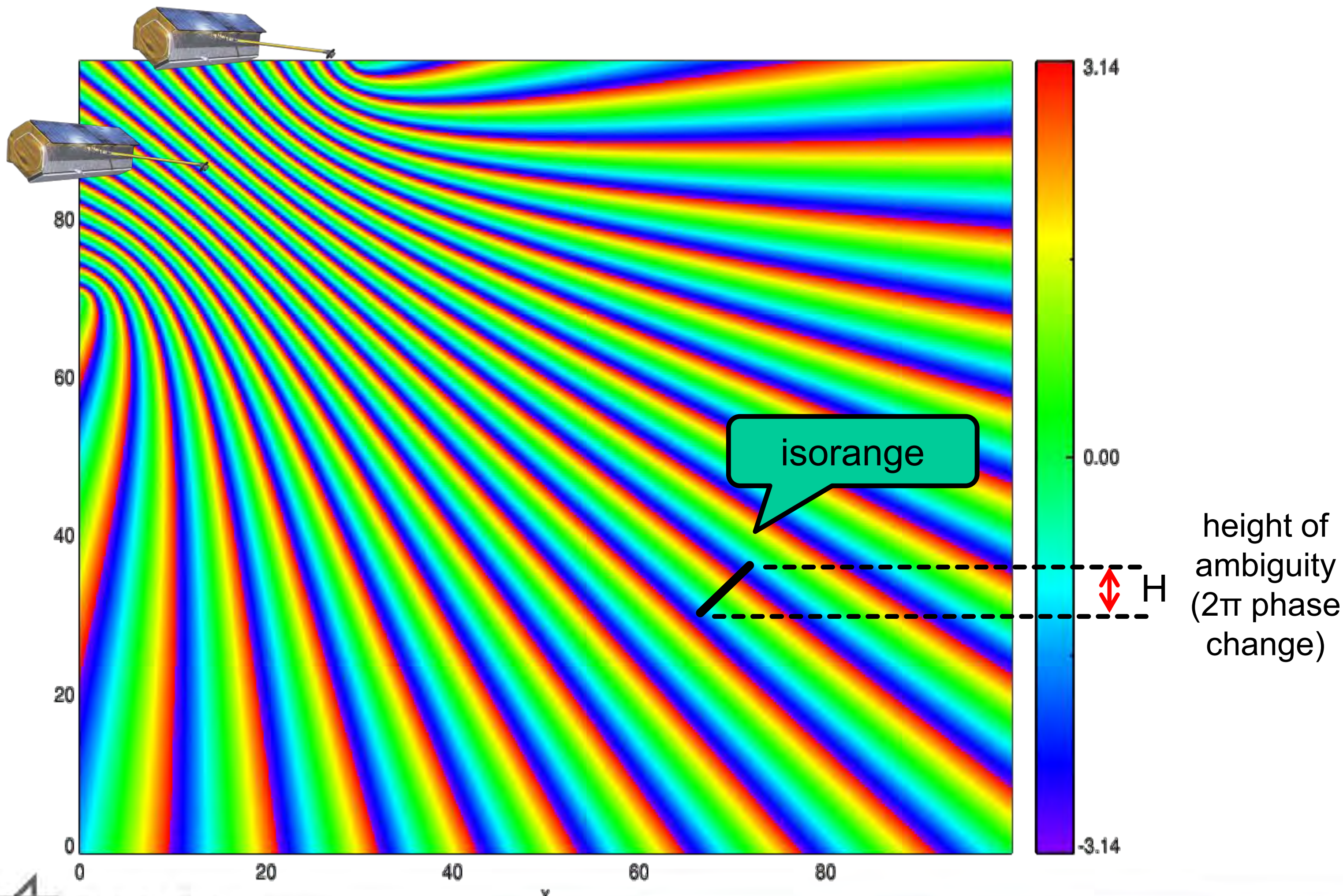

Height of ambiguity

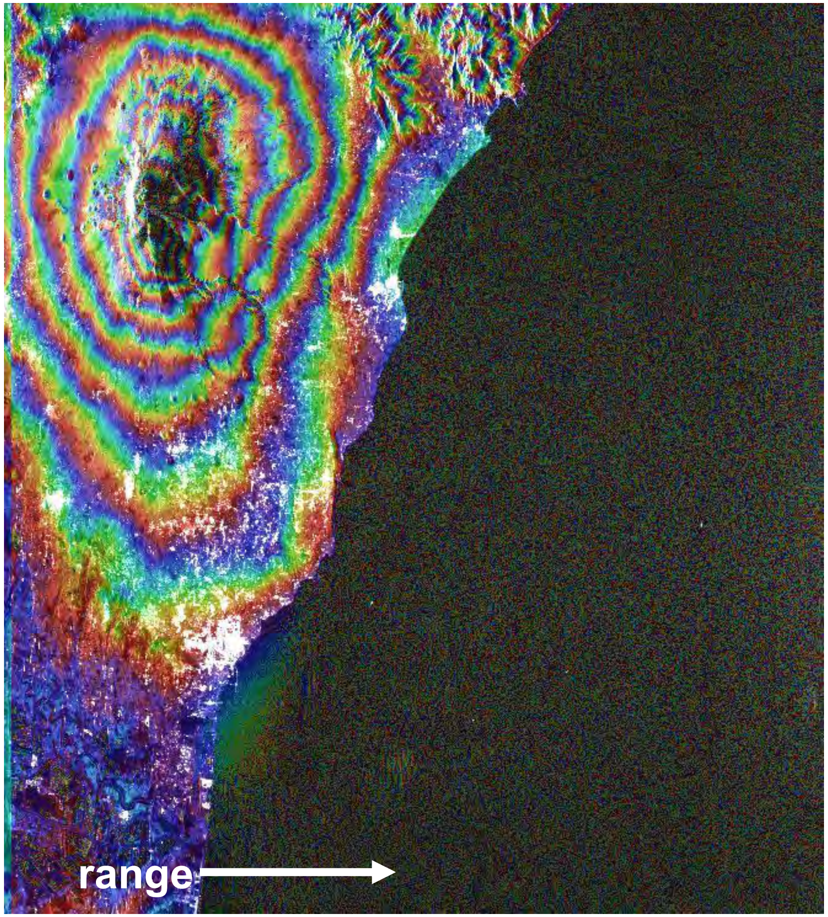

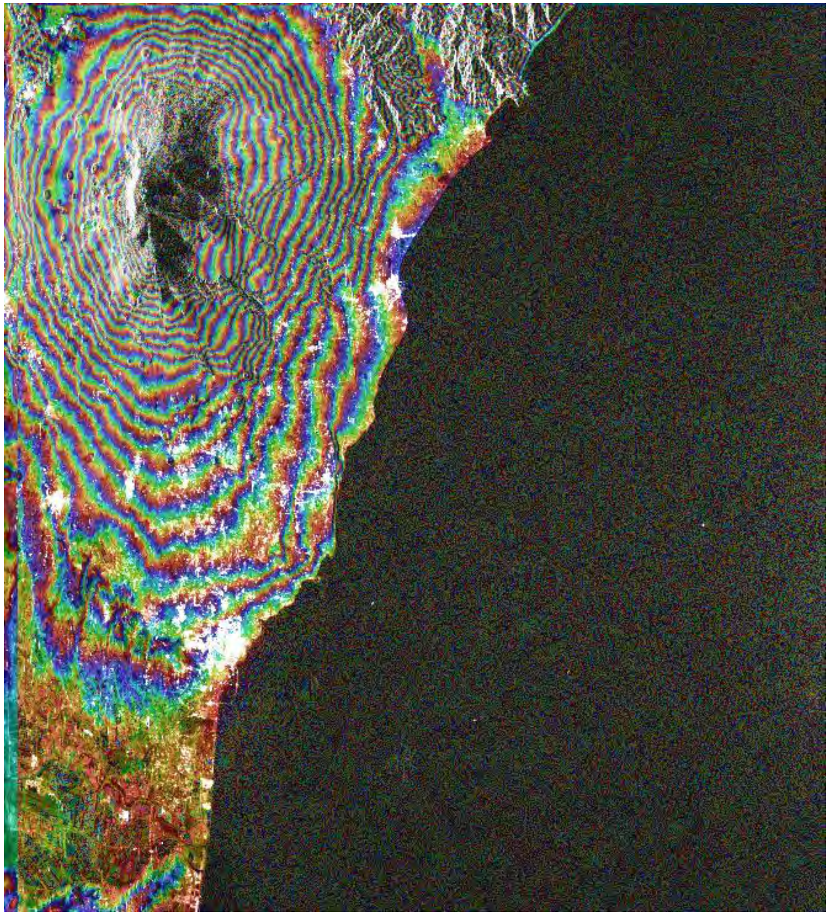

JAXA (PALSAR)

Height of ambiguity: vertical baseline

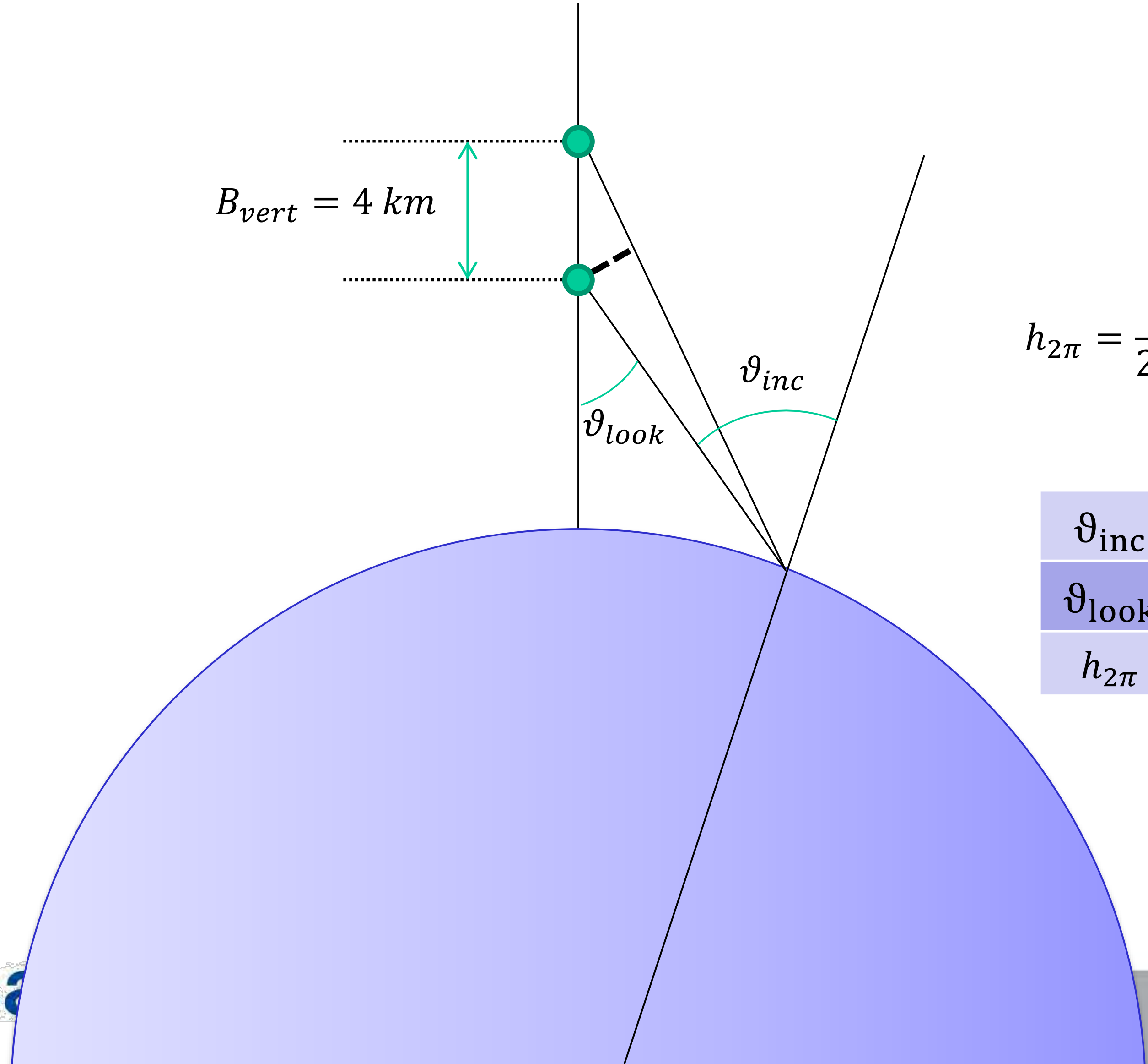

$$h_{2\pi} = \frac{R\ \sin(\vartheta_{inc})\lambda}{2B_{vert}\sin(\vartheta_{look})}$$

ϑ_{inc}	24.8 deg	44.8 deg
$\vartheta_{\mathrm{look}}$	22.0 deg	39.0 deg
$h_{2\pi}$	27.8 m	34.2 m

Height of ambiguity: horizontal baseline

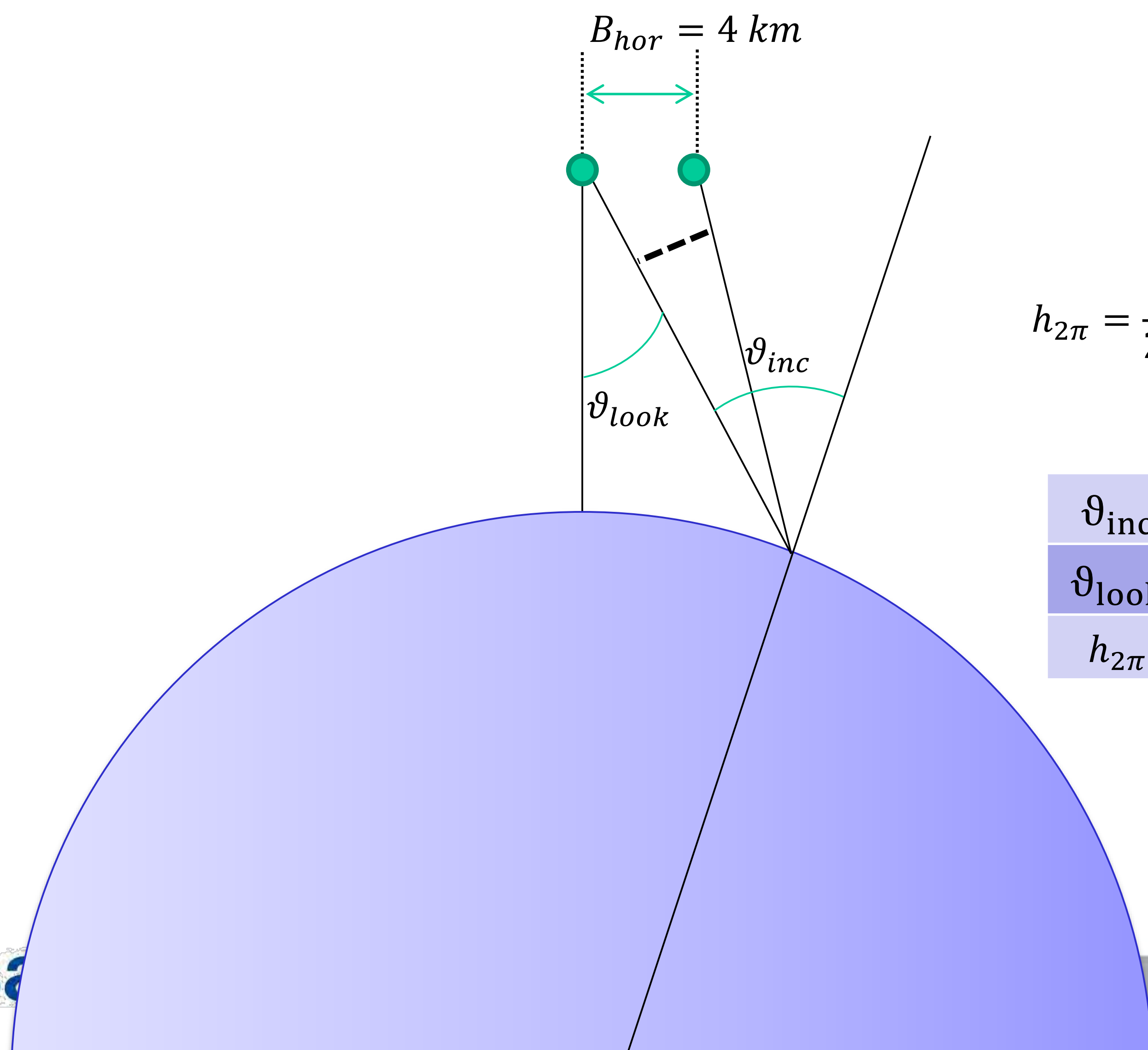

$$h_{2\pi} = \frac{R\ \sin(\vartheta_{inc})\lambda}{2B_{hor}\cos(\vartheta_{look})}$$

ϑ_{inc}	24.8 deg	44.8 deg
$\vartheta_{\mathrm{look}}$	22.0 deg	39.0 deg
$h_{2\pi}$	11.2 m	27.7 m

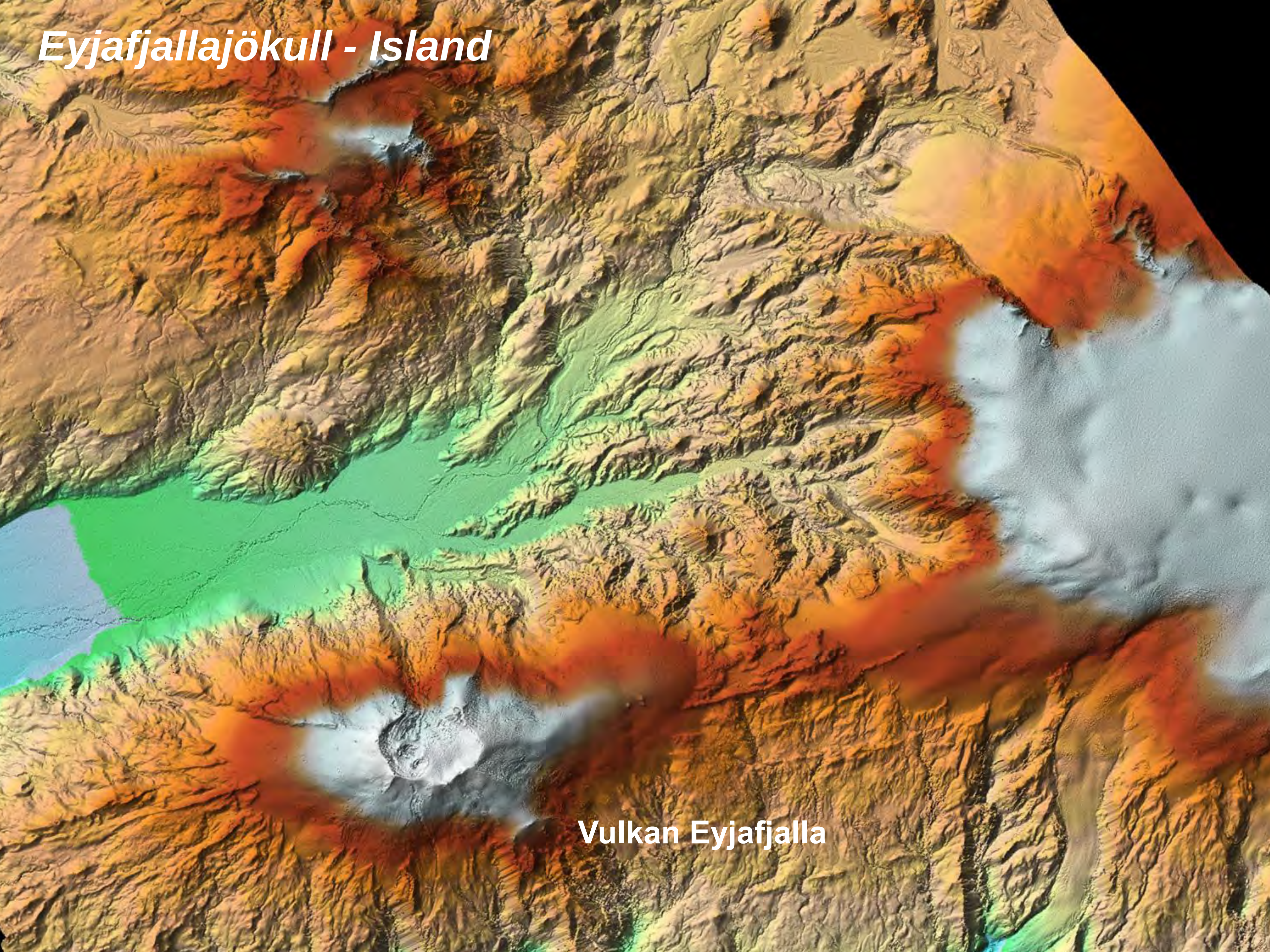
Eyjafjallajökull - Island
Vulkan Eyjafjalla

Further Across-Track Interferometry Applications

Topography

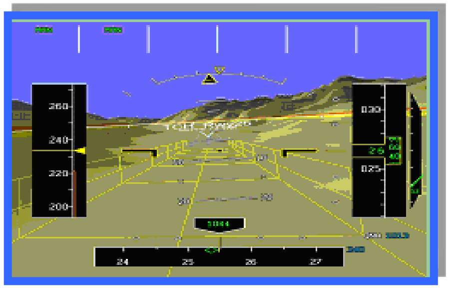

Navigation

Urban areas

Crisis management

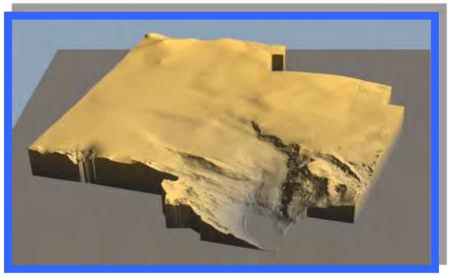

Glaciology

Oceanography

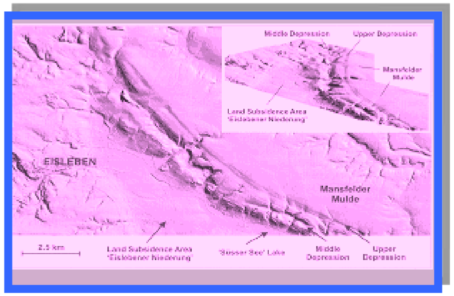

Geology

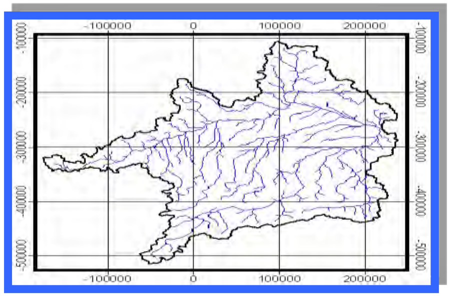

Hydrology

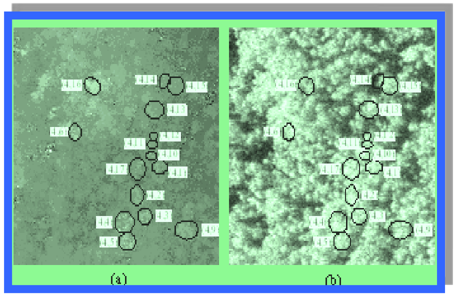

Land cover

Applications:

Along-Track Interferometry (ATI)

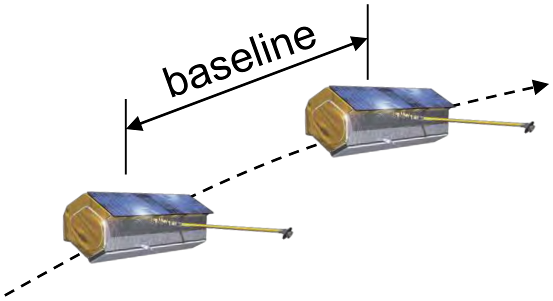

Along-Track Interferometry Principle

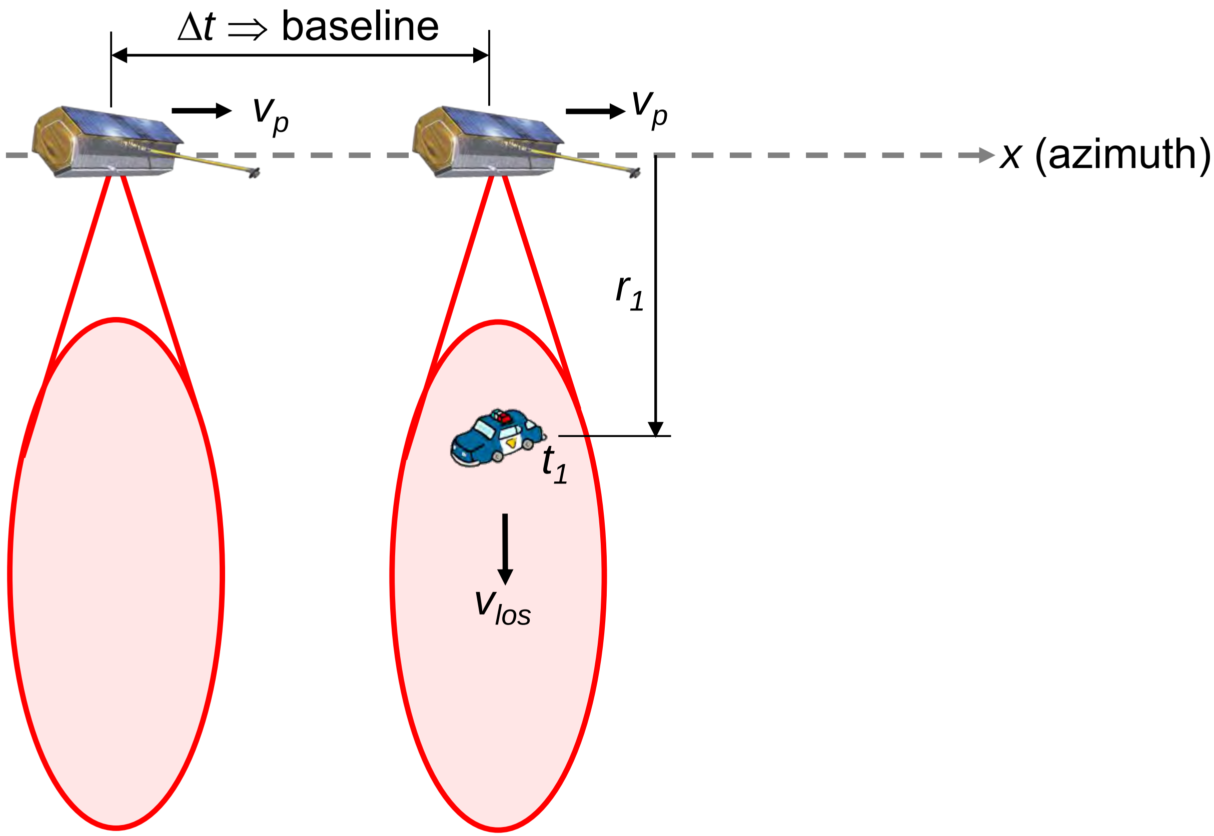

Δt … temporal baseline
v_{los} … line-of-sight velocity

Along-Track Interferometry Principle

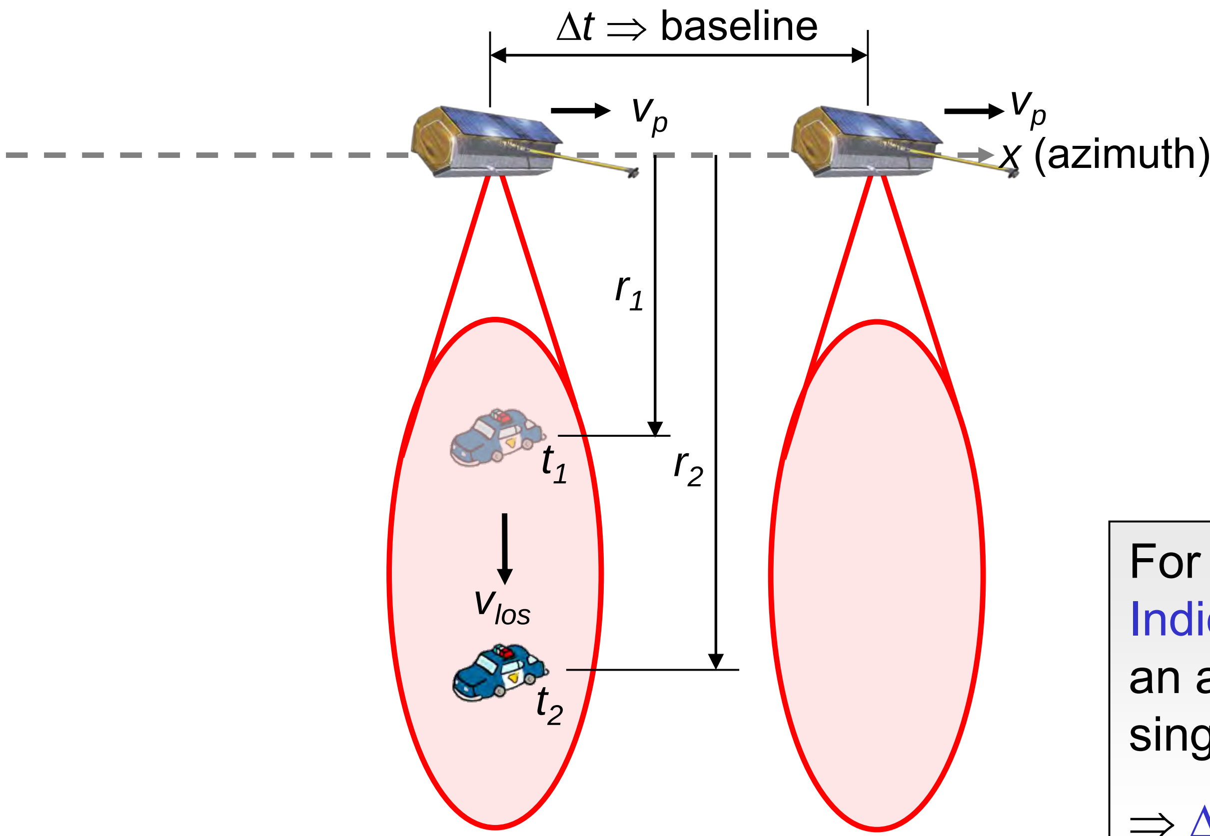

Range Difference

$$\Delta r = r_1 - r_2 = v_{los}\Delta t$$

Interferometric Phase:

$$\Delta\phi = \frac{4\pi}{\lambda}\Delta r = \frac{4\pi}{\lambda} v_{los}\Delta t$$

For "Ground Moving Target Indication" (GMTI) in general an antenna array mounted on a single platform is used!

$\Rightarrow \Delta t$ = ms

Δt … temporal baseline

v_{los} … line-of-sight velocity

Along-Track Interferometry for GMTI

Along-Track Interferometry (ATI)

- ✓ ATI phase ~ line-of-sight velocity
- ✗ No clutter suppression ⇒ erroneous velocity and position estimation

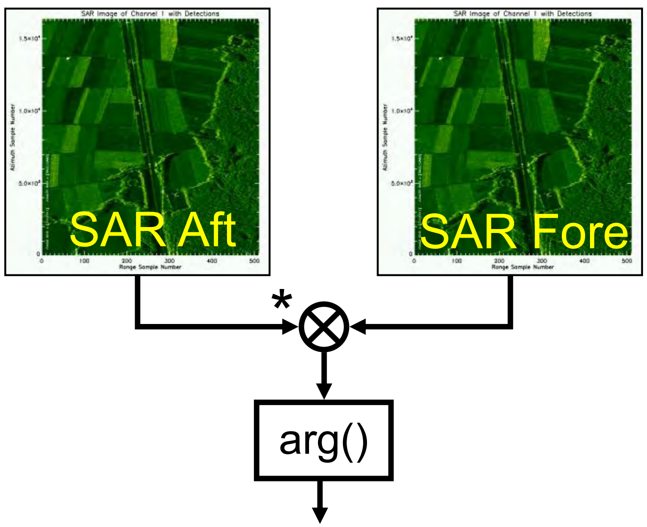

$$\Delta\phi = \frac{4\pi}{\lambda} v_{rad} \Delta t$$

Displaced Phase Center Antenna (DPCA)

- ✓ Real clutter suppression
- ✗ Only two channels: No remaining ATI phase information for parameter estimation ⇒ additional channels required !

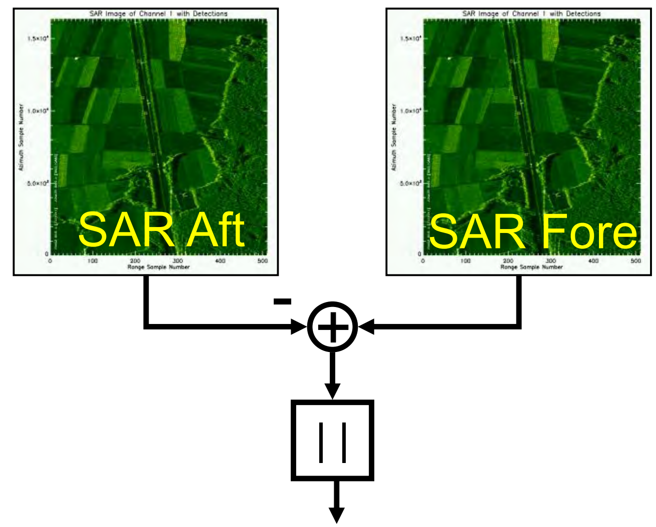

Amplitude proportional to v_{rad}

Along-Track Interferometry for GMTI

Along-Track Interferometry (ATI)

- ✓ ATI phase ~ line-of-sight velocity
- ✗ No clutter suppression ⇒ erroneous velocity and position estimation

Polar Plot of ATI Phases

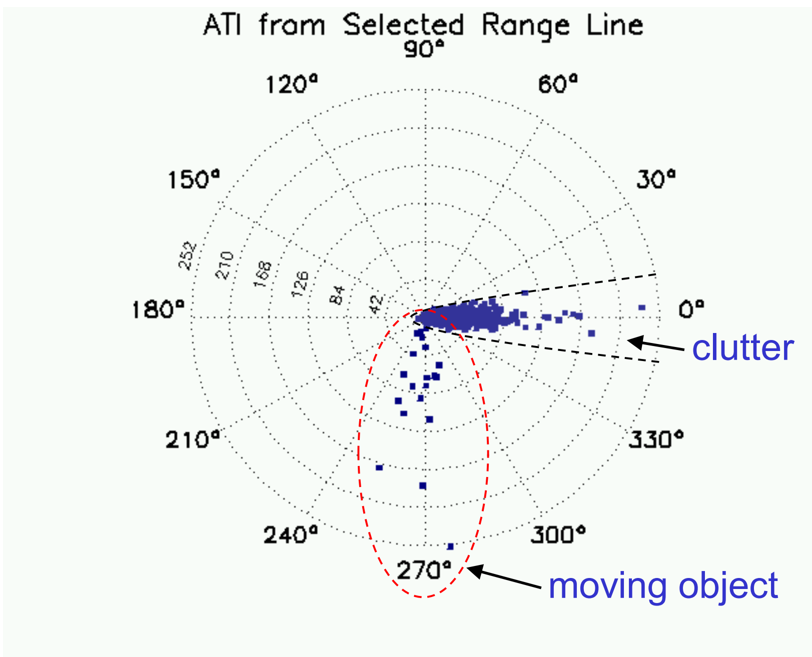

Displaced Phase Center Antenna (DPCA)

- ✓ Real clutter suppression
- ✗ Only two channels: No remaining ATI phase information for parameter

1,2,3 … moving targets

Additional Effects Caused by a Moving Vehicle

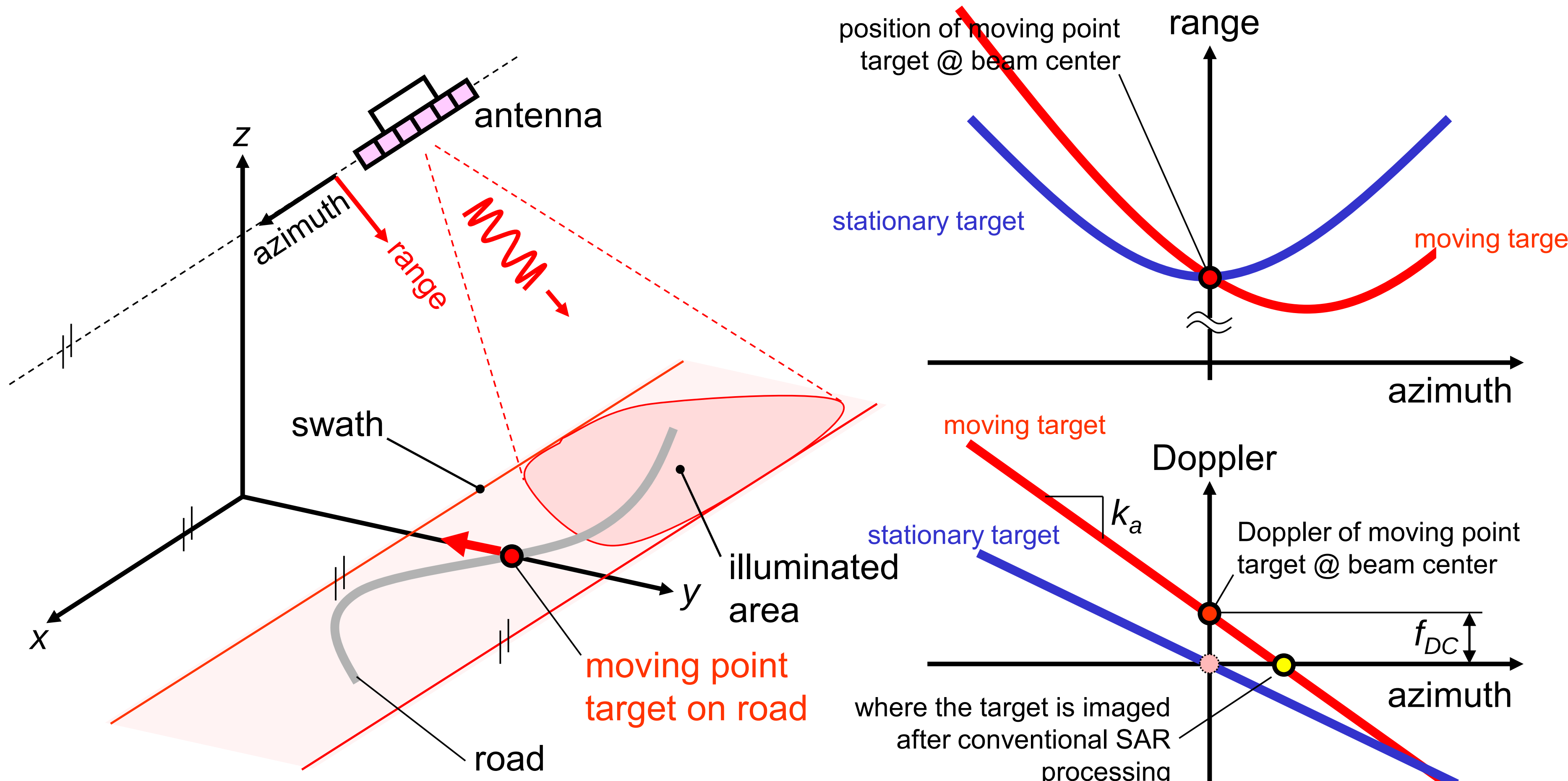

- Moving vehicle ↔ stationary target
  - Doppler shift (caused by across-track velocity)
  - Change of Doppler slope (← along-track velocity + across-track acceleration)

Rotation fringes (20 km ATI, 3 seconds, +- 0.005 deg)

Processing: Rolf Scheiber, DLR

Observation of Sea Ice Drift & Rotation: East Greenland

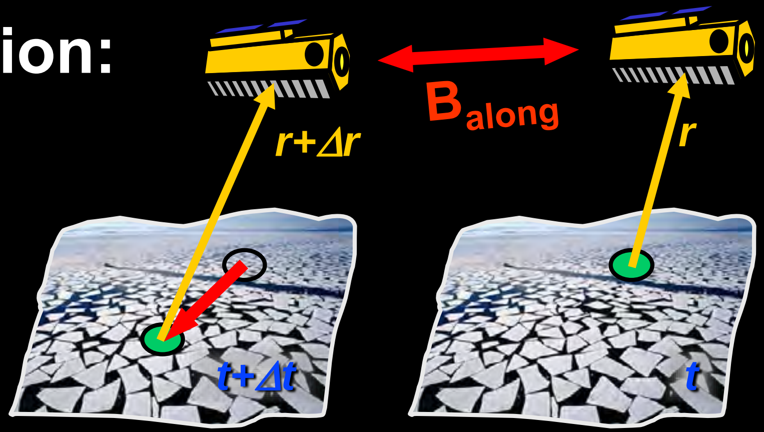

TanDEM-X interferogram (20 km formation):

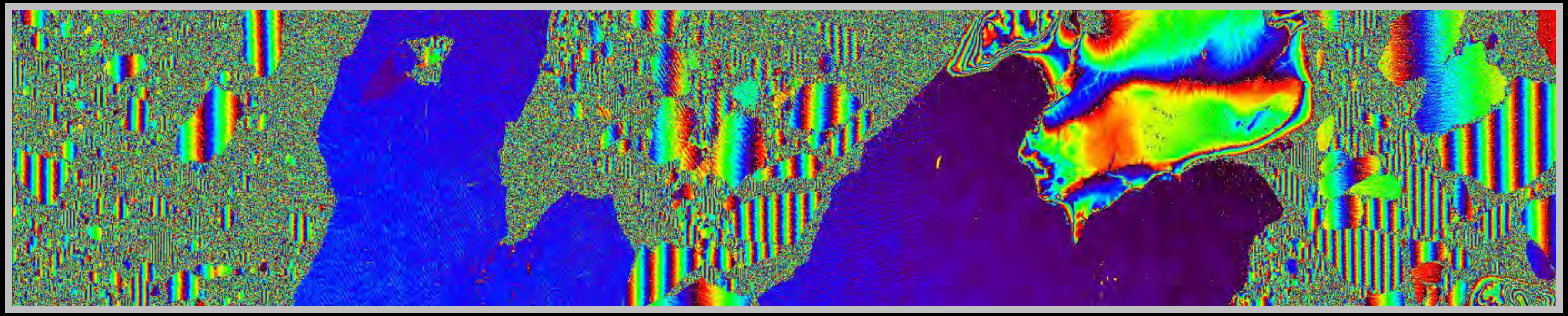

Estimated ice rotation in 3 seconds:

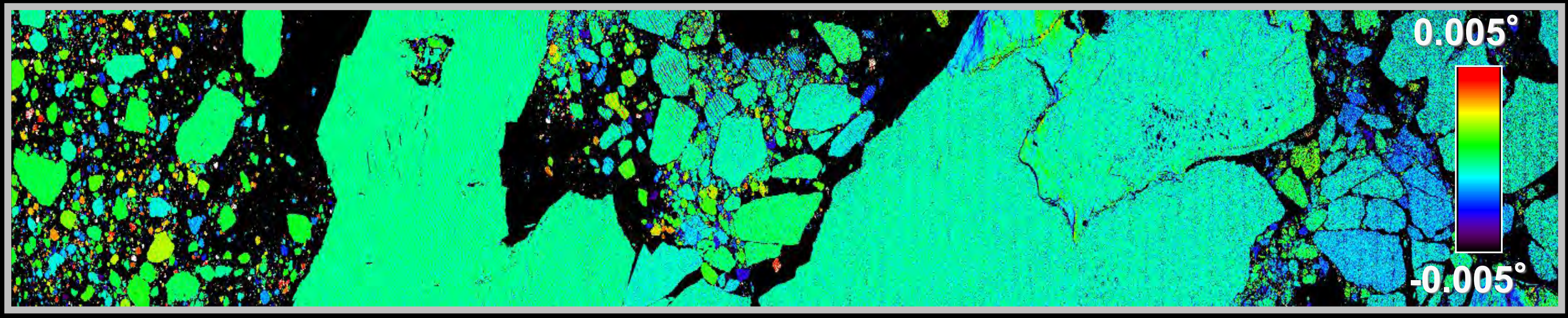

Accuracy better than 10^{-5} deg/s !

DLR TanDEM

Water Currents Measured With E-SAR

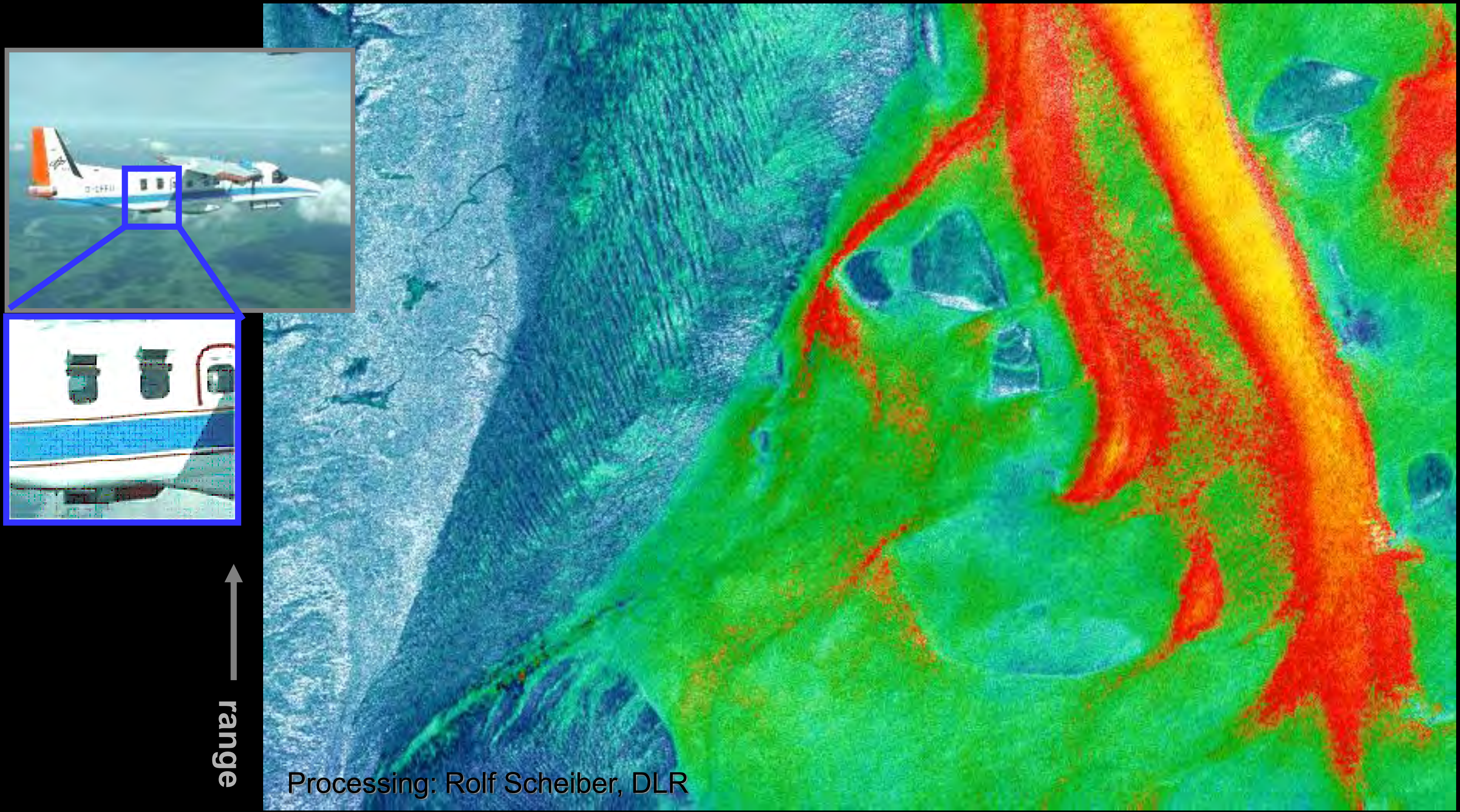

0 m/s   2 m/s

Overlay of SAR image and velocity of water currents
Wadden Sea, Ameland, NL

Further Along-Track Interferometry Applications

Ocean Currents

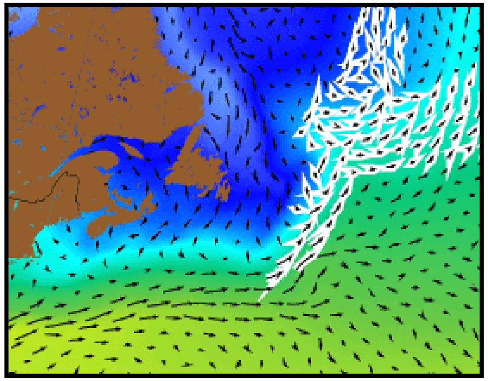

Coastline Surveillance

Drift of Sea Ice

Traffic Monitoring

Dual Beam Interferometry (DBI) concept

- ATI provides direct estimation of **radial velocity** component
  - Thus 1 component out of 3 possible
  - Assumption that targets have $\boldsymbol{v_z = 0}$ is usually more or less valid
  - But at least 2 components are needed
  - DBI:

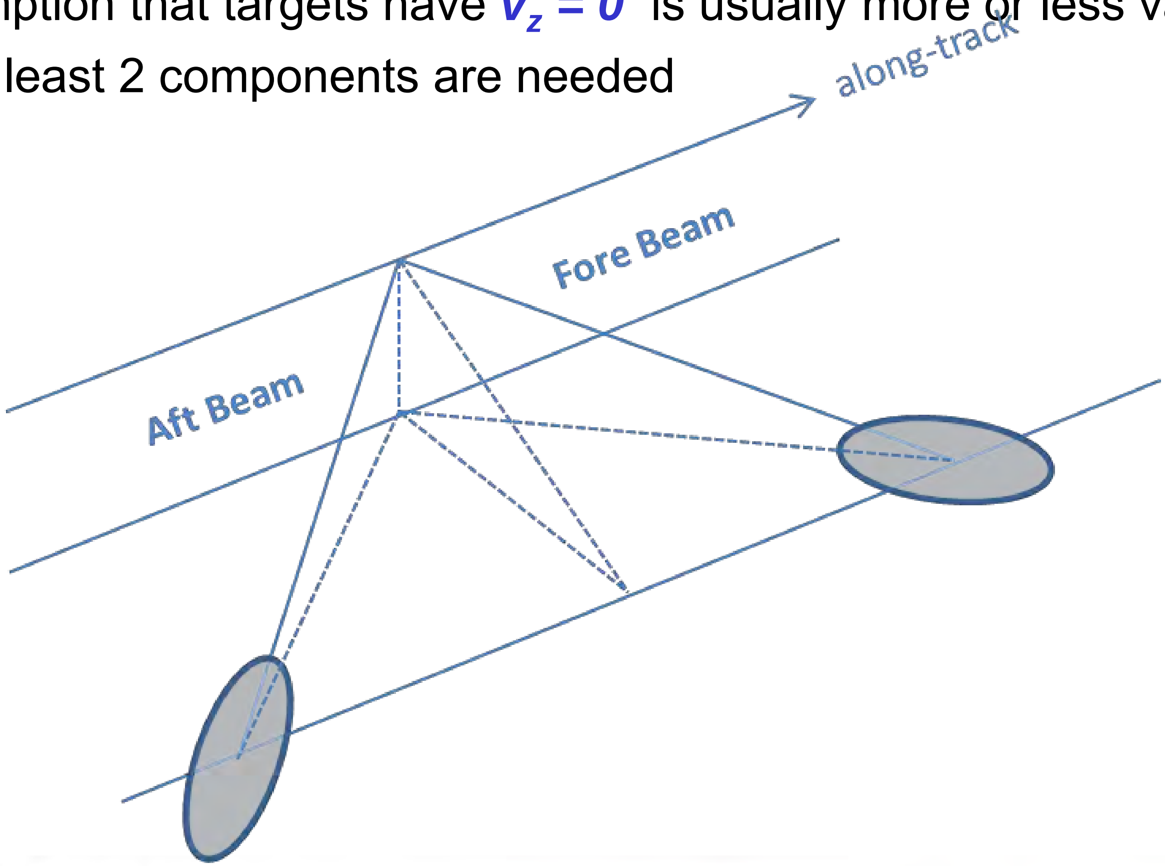

Dual Beam Interferometry (DBI) concept

- ATI provides direct estimation of **radial velocity** component
  - Thus 1 component out of 3 possible
  - ~~Assumption that targets have $v_z = 0$ is usually more or less valid~~
  - But at least 2 components are needed???
  - DBI:

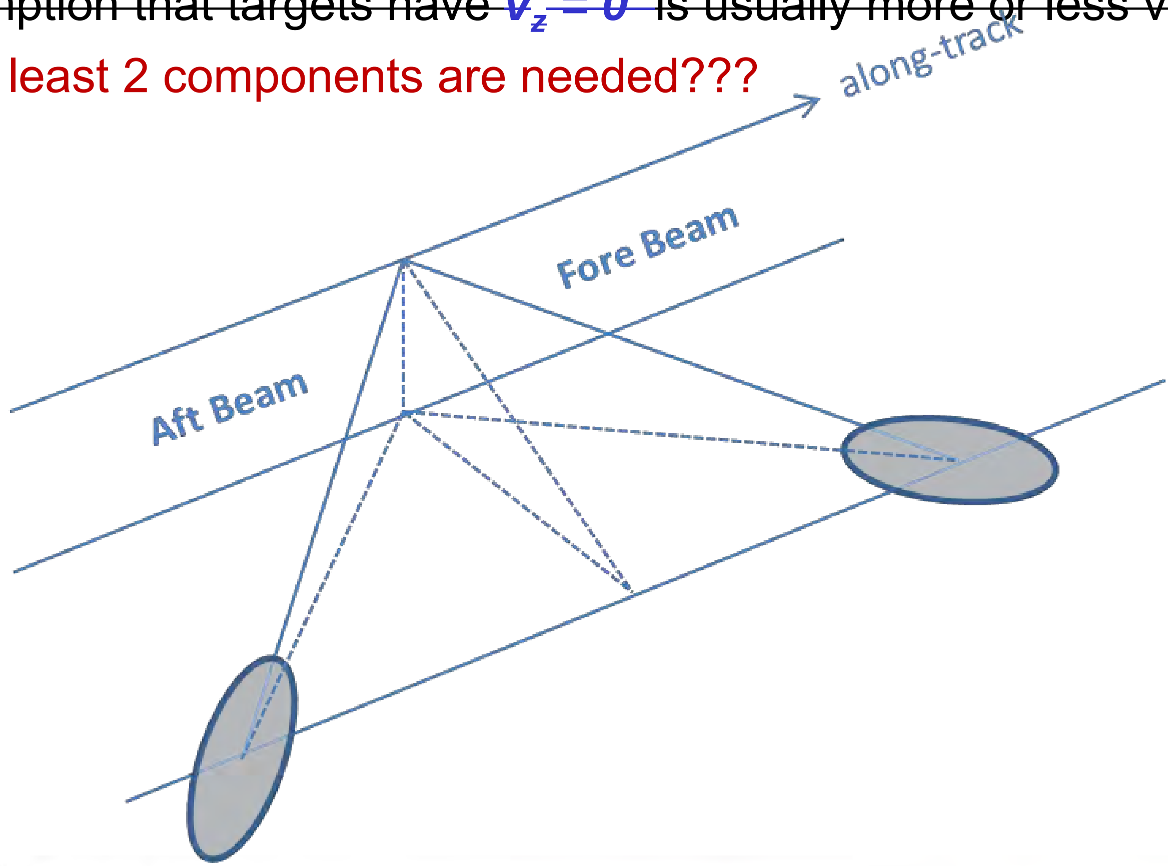

Dual Beam Interferometry (DBI) concept

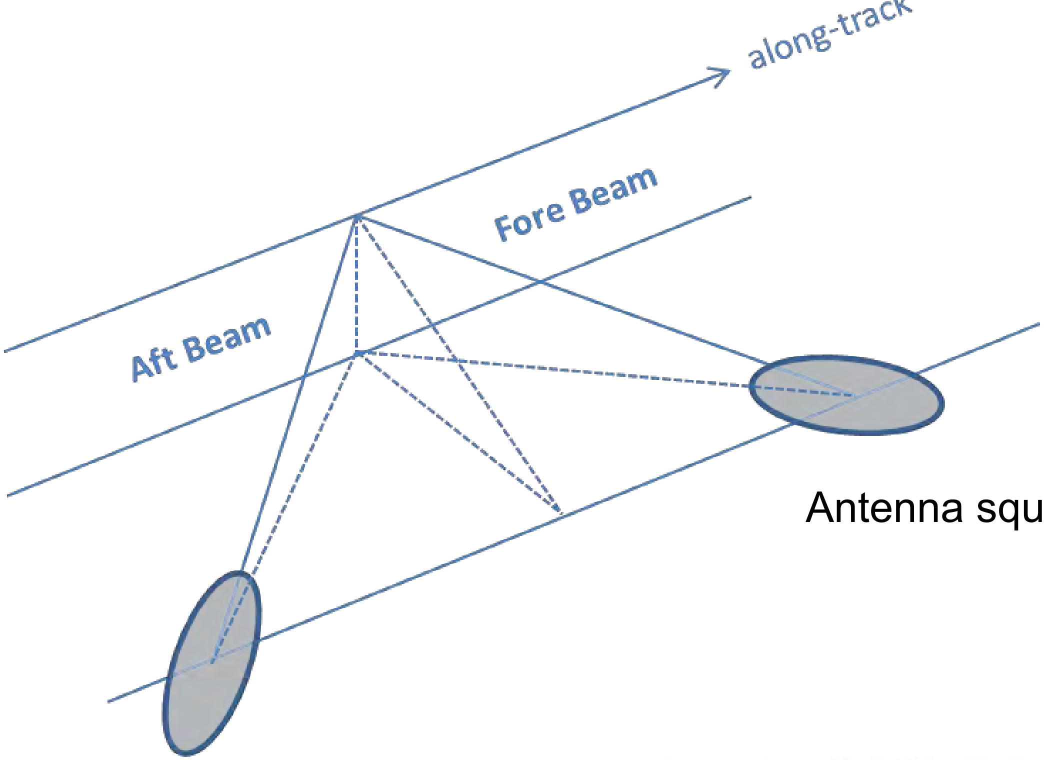

$$\sigma_{v_x}^2 = \frac{\sigma_{v_r^+}^2 + \sigma_{v_r^-}^2}{(2\sin\theta_s \sin\theta_i)^2},$$

$$\sigma_{v_y}^2 = \frac{\sigma_{v_r^+}^2 + \sigma_{v_r^-}^2}{(2\cos\theta_s \sin\theta_i)^2},$$

Antenna squint → Projected squint

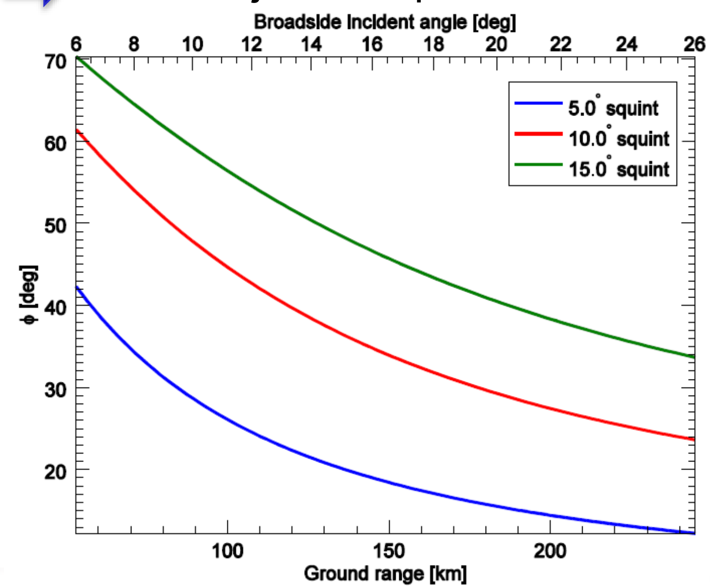

$$\theta_{\text{sq, ground}} = \arctan\frac{\tan\theta_{\text{sq, ant}}}{\sin\theta_{\text{inc}}}$$

OSCM (AKA Wavemill)

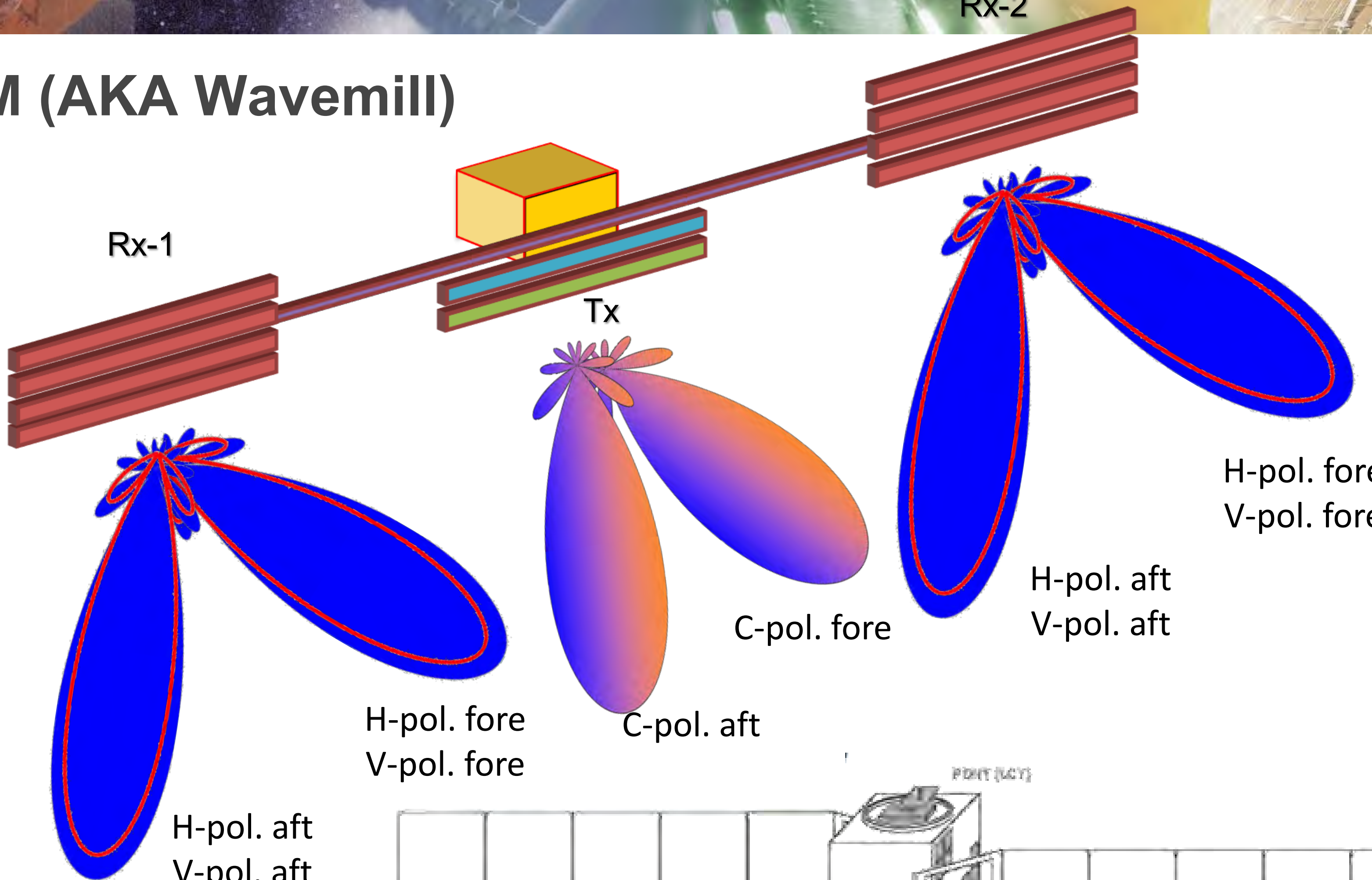

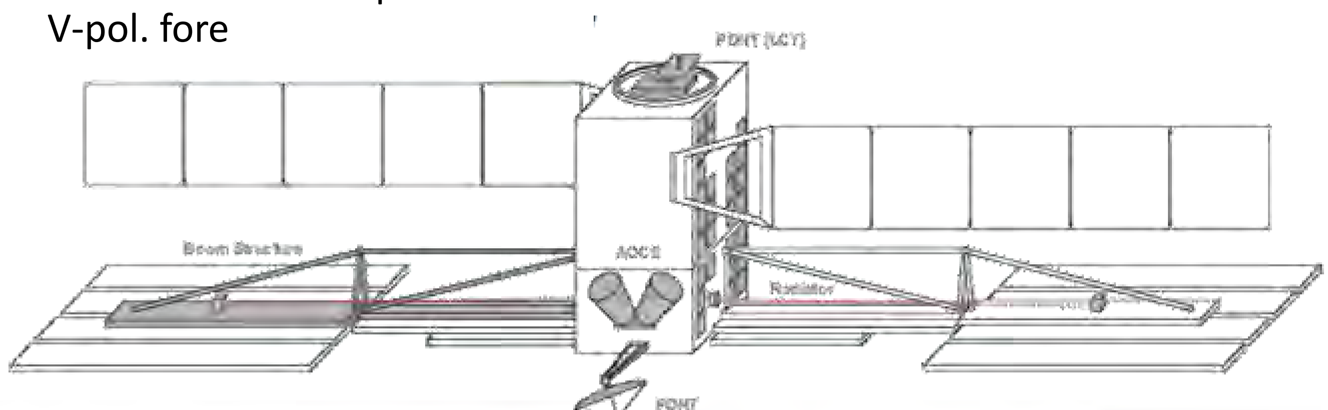

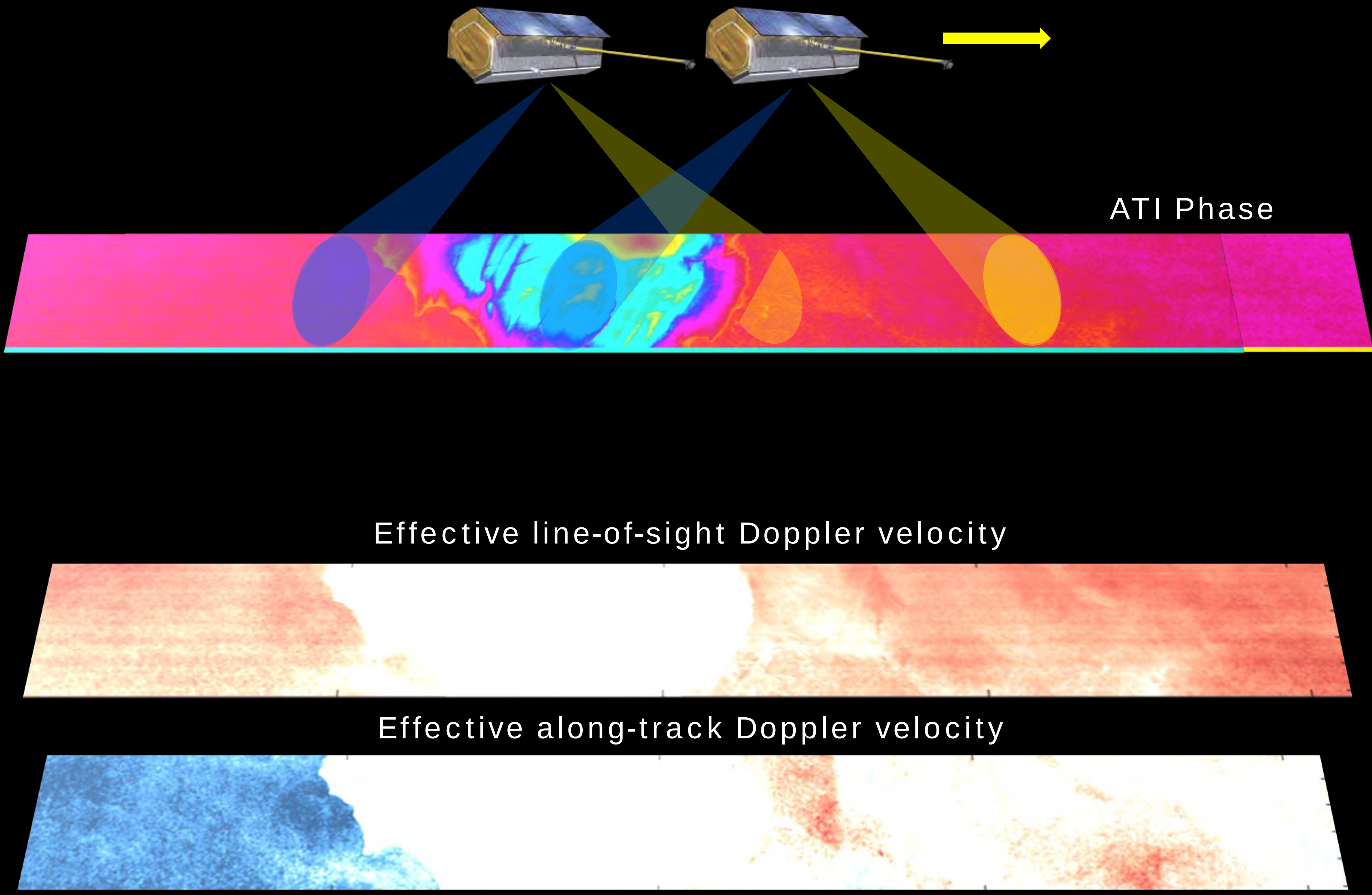
ATI Phase
Effective line-of-sight Doppler velocity
Effective along-track Doppler velocity


US Dept of State Geographer
© 2014 Google
Image Landsat
Data SIO, NOAA, U.S. Navy, NGA, GEBCO
e: 4/10/2013
77°08'39.02" N 76°02'50.49" E elev -803 ft

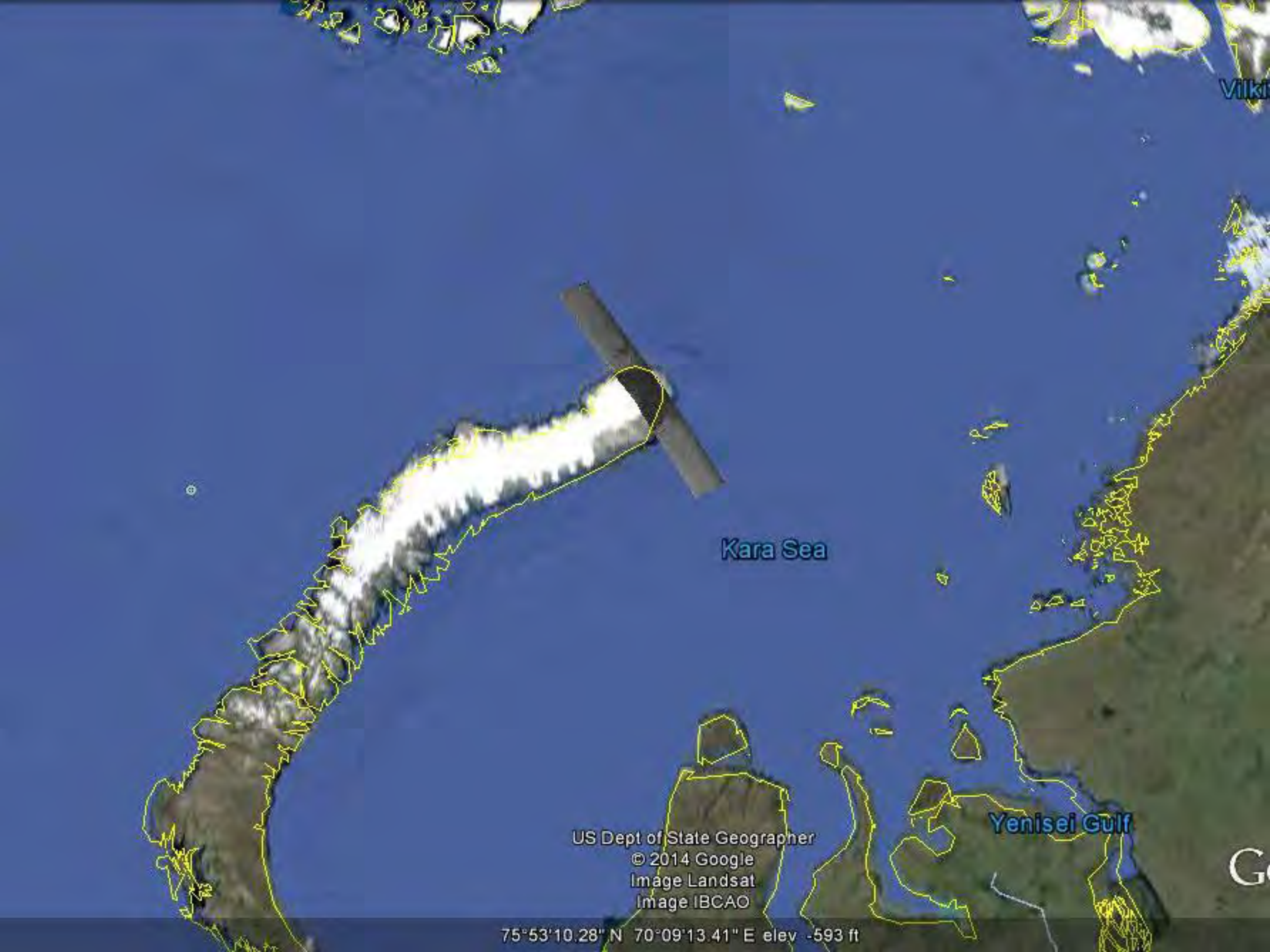
Vilki
Kara Sea
Yenisei Gulf
US Dept of State Geographer
© 2014 Google
Image Landsat
Image IBCAO
75°53'10.28" N 70°09'13.41" E elev -593 ft

Date	Sep. 13th, 2013
AT physical baseline	53 m → 73 m
AT lag	~ 4 ms
Height of ambiguity	> 300 m

L2 Product

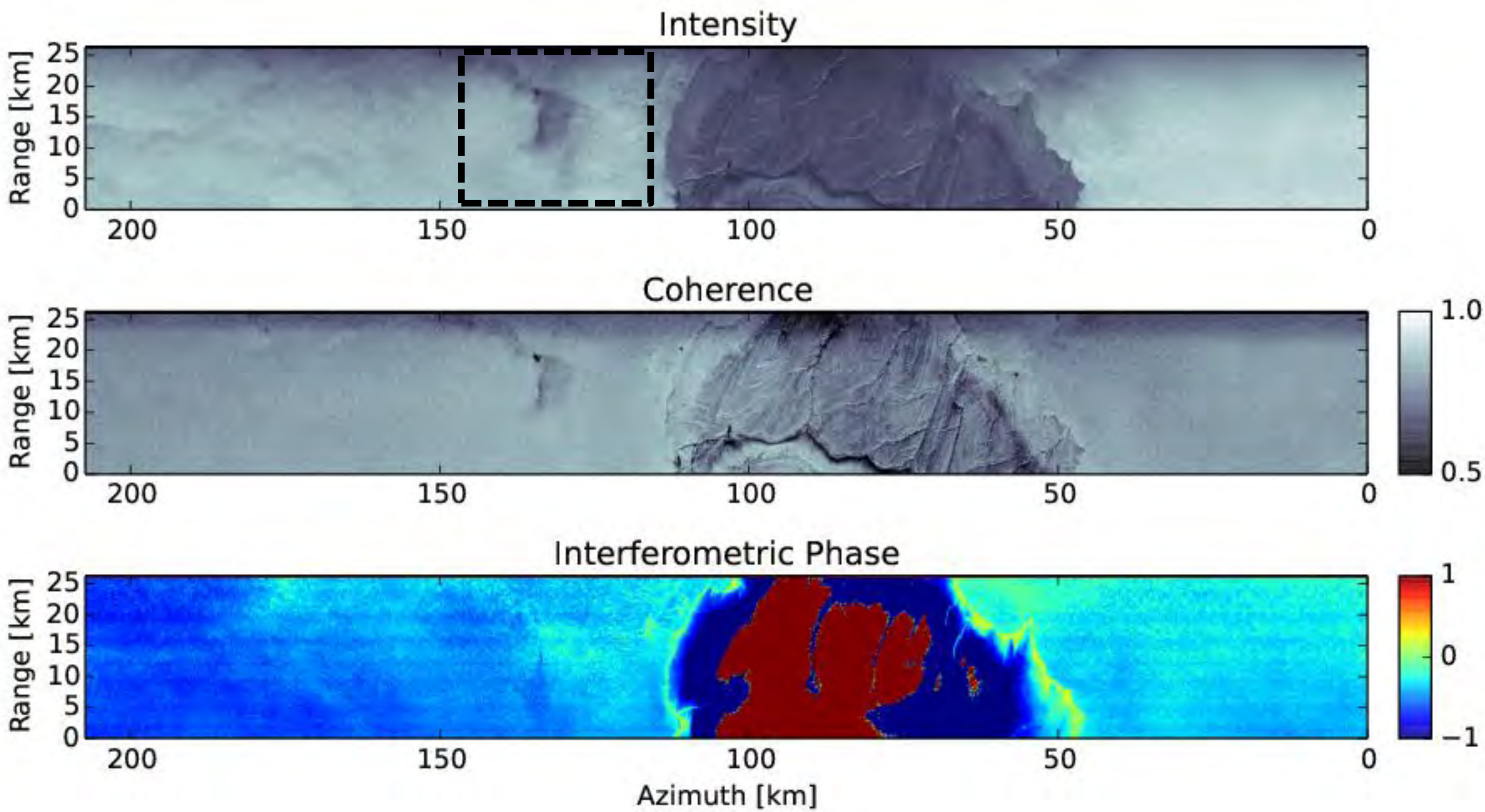

Intensity
Coherence
Interferometric Phase
Range [km]
25
20
15
10
5
0
200
150
100
50
0
Azimuth [km]
1.0
0.5
1
0
−1


Amplitude

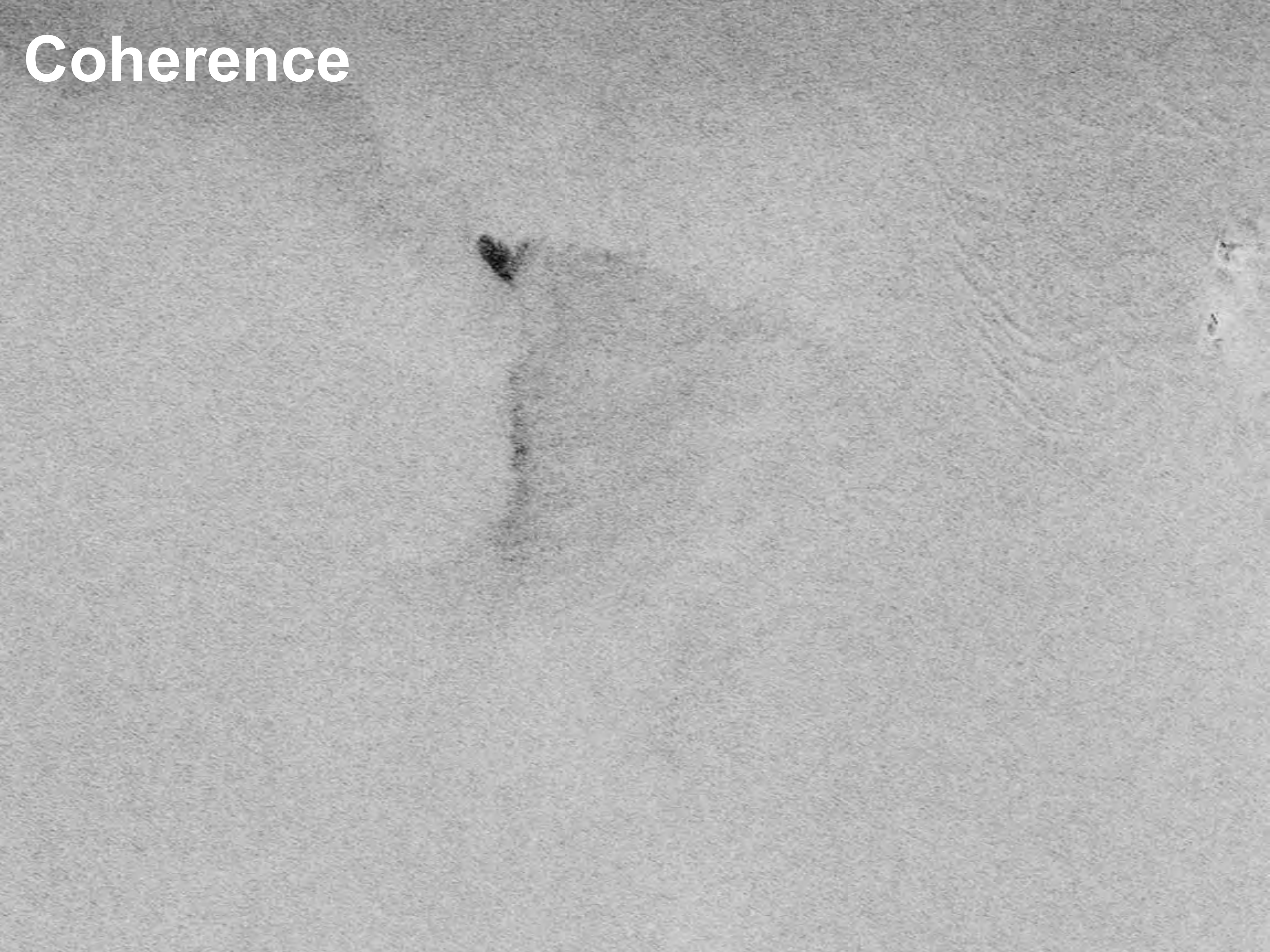
Coherence

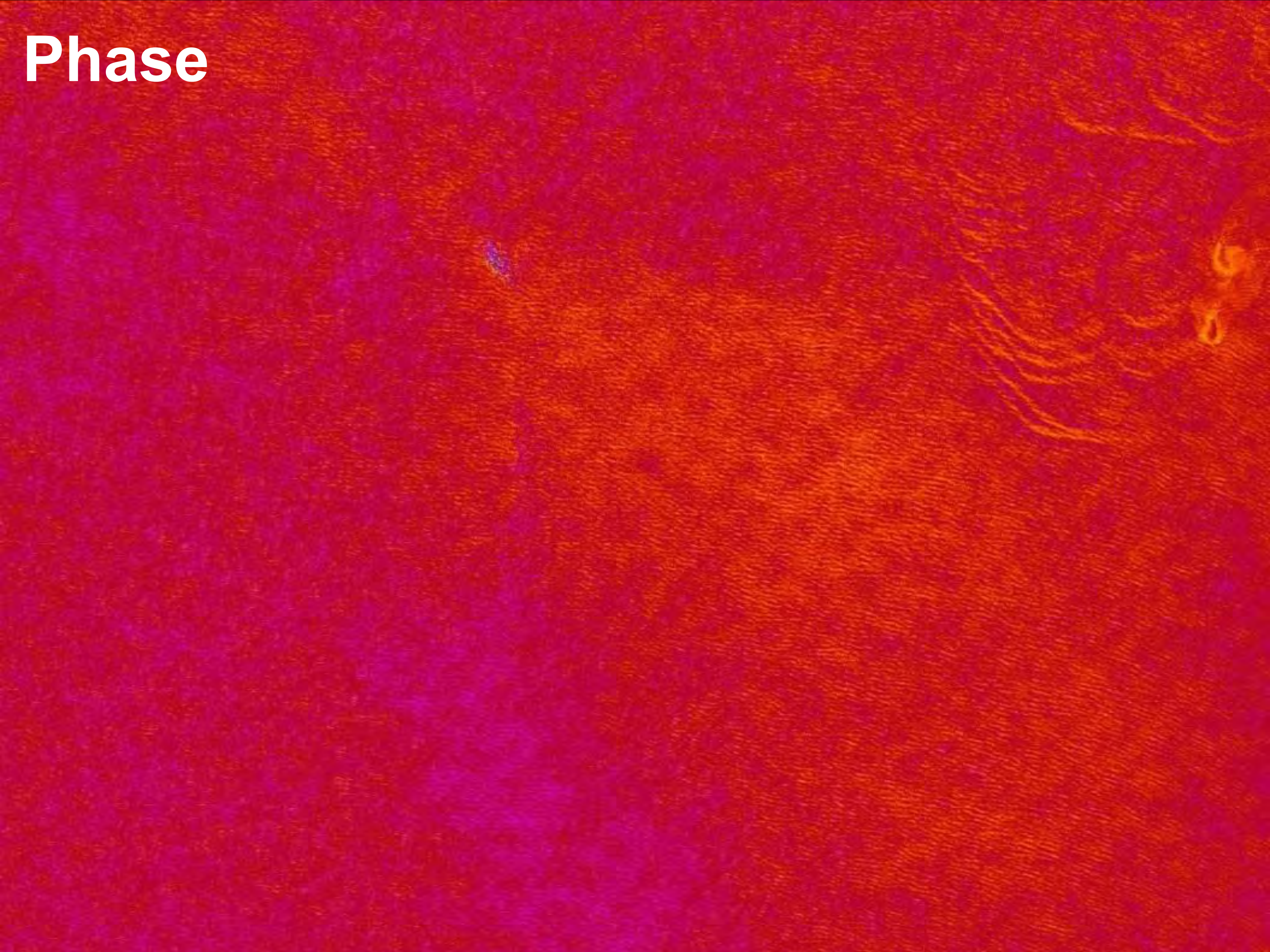
Phase

Effective Doppler velocities

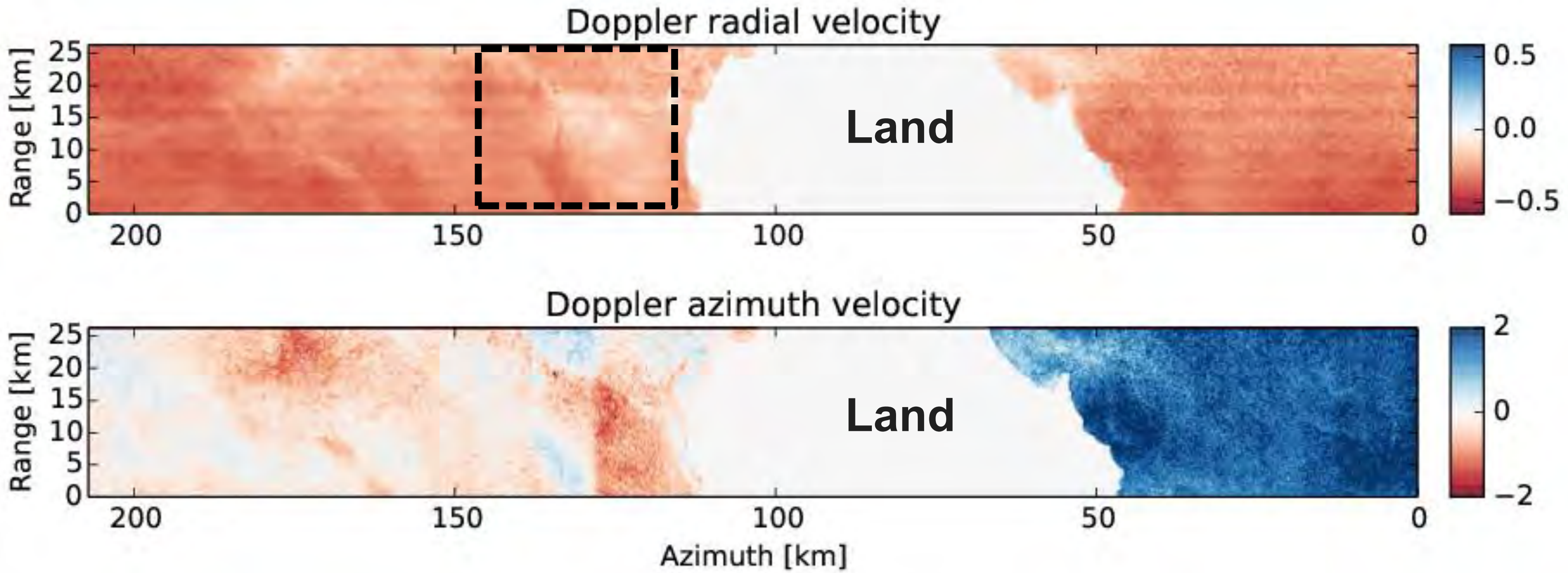

Interpretation

Wrong hypothesis 1: we are seeing only real horizontal surface velocities

„Current“ field

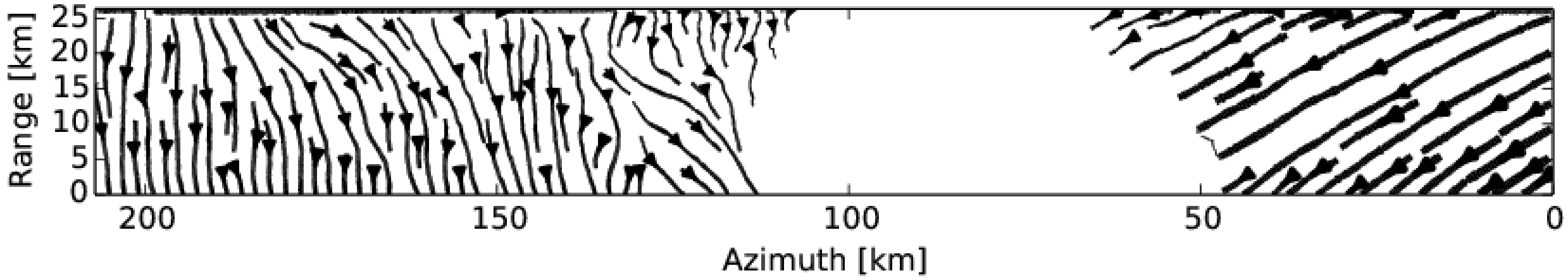

„Wind“ field

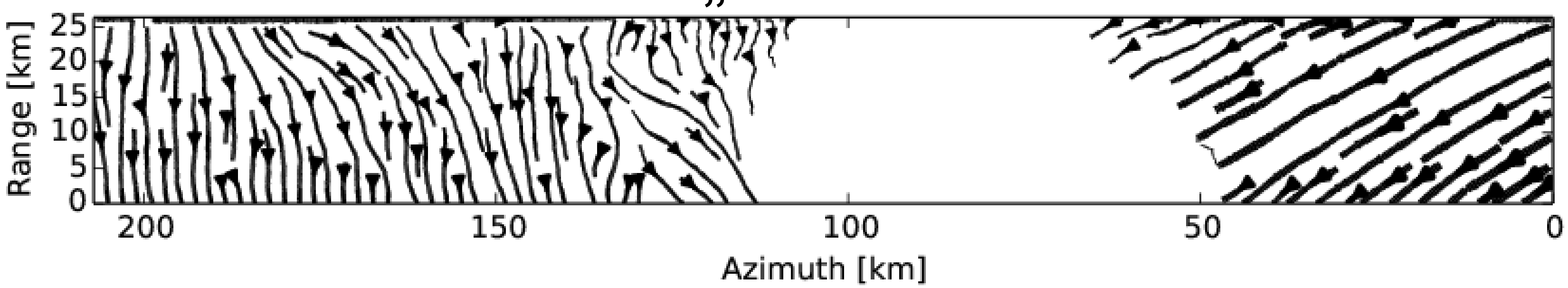

$$\mathrm{GM}F(sea\ state, \theta_{inc}, \phi_s - \phi_0) = A \cdot \cos(\phi_a - \phi_0)$$

Effective Doppler velocities

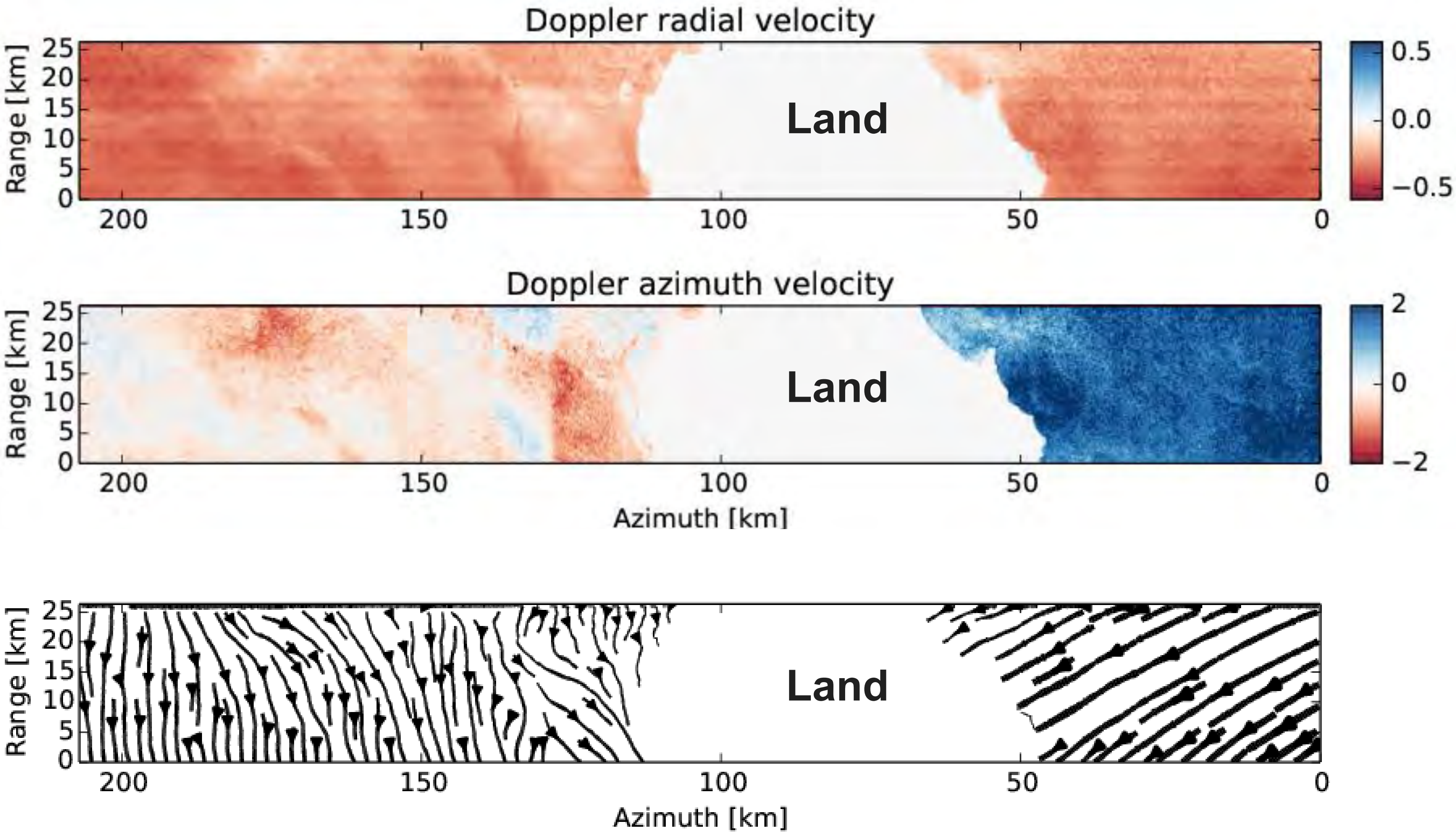

Orkney Island Currents (TSX & TDX)

- Temporal baselines
  - February (20120226): +6.6 ms
  - March (20120319): -10.7 ms

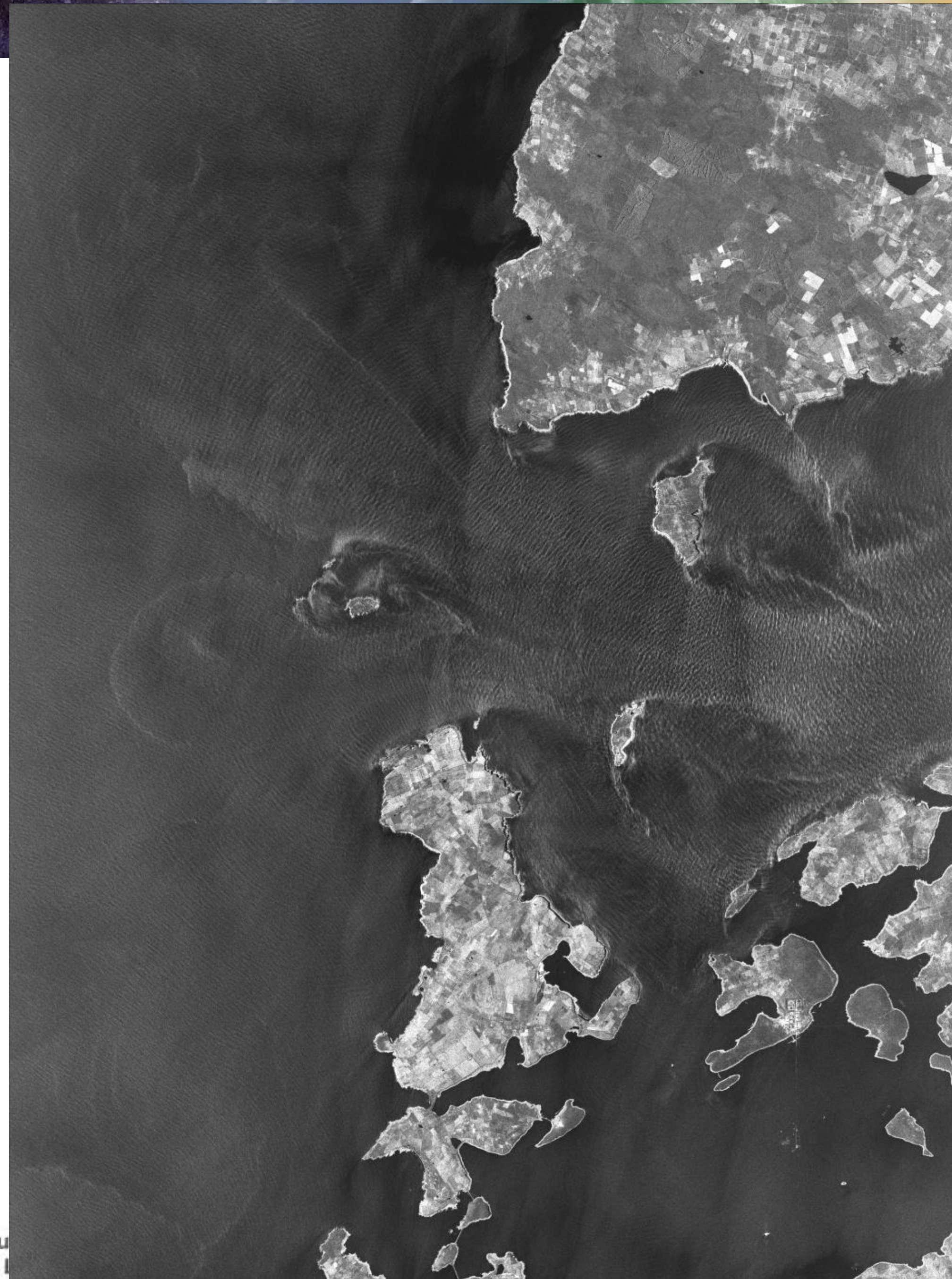

Applications:

Differential SAR Interferometry (D-InSAR)

$$\Delta\phi = \phi_{topo} + \phi_{diff}$$

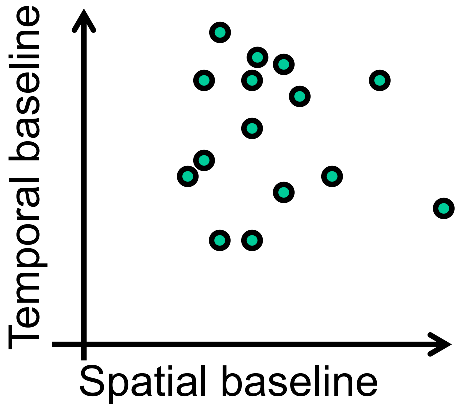

Differential SAR Interferometry Principle (→ Repeat Pass)

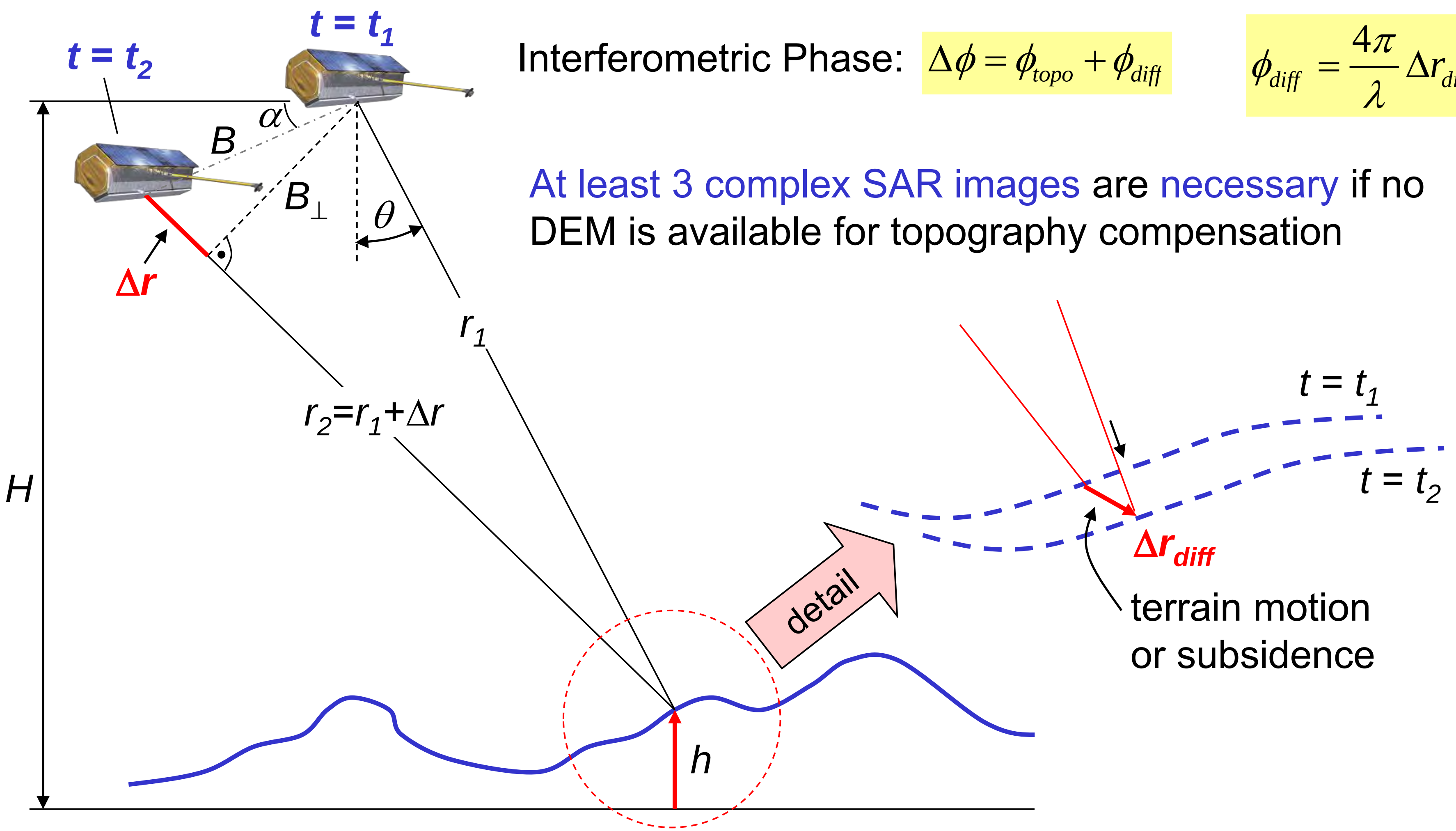

Interferometric Phase: $\Delta\phi = \phi_{topo} + \phi_{diff}$ $\quad \phi_{diff} = \frac{4\pi}{\lambda}\Delta r_{diff}$

At least 3 complex SAR images are necessary if no DEM is available for topography compensation

DInSAR

Main Errors

- Residual topography. Small baselines are therefore better.
- Atmospheric Phase Screen (APS).
  - Spatially smooth
  - Random in time
- Phase unwrapping
- Decorrelation

Stacks

- DInSAR processing chains use long time series (stacks) of images.
- Linear motion models allow estimation of deformation rates down to mm/year (in some cases, sub-millimetric precisions).
- In cities thermal dilation effects become visible.
- Non-linear / fast motions are still a challenge.

Interferometric phase

Proportional to temporal baseline

SNR dependent

$$\Delta\phi_{\text{int}} = \Delta\phi_{topo} + \Delta\phi_{diff} + \Delta\phi_{atm} + \Delta\phi_{noise}$$

Proportional to cross-track baseline

Phase due to atmospheric phase screen (variations). Can only be avoided in single-pass

Interferometric phase suffers from 2π ambiguity and (usually) from random offset.

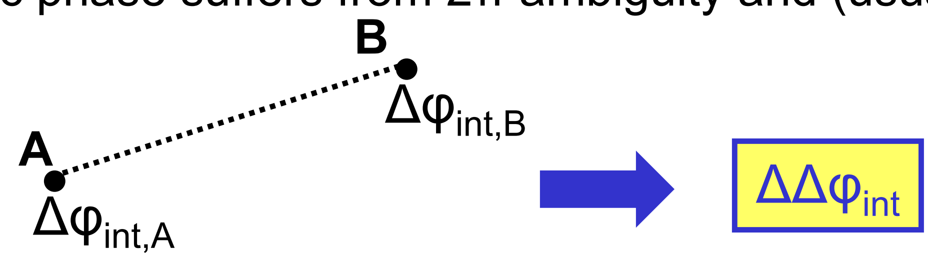

Differential SAR Interferometry With TerraSAR-X

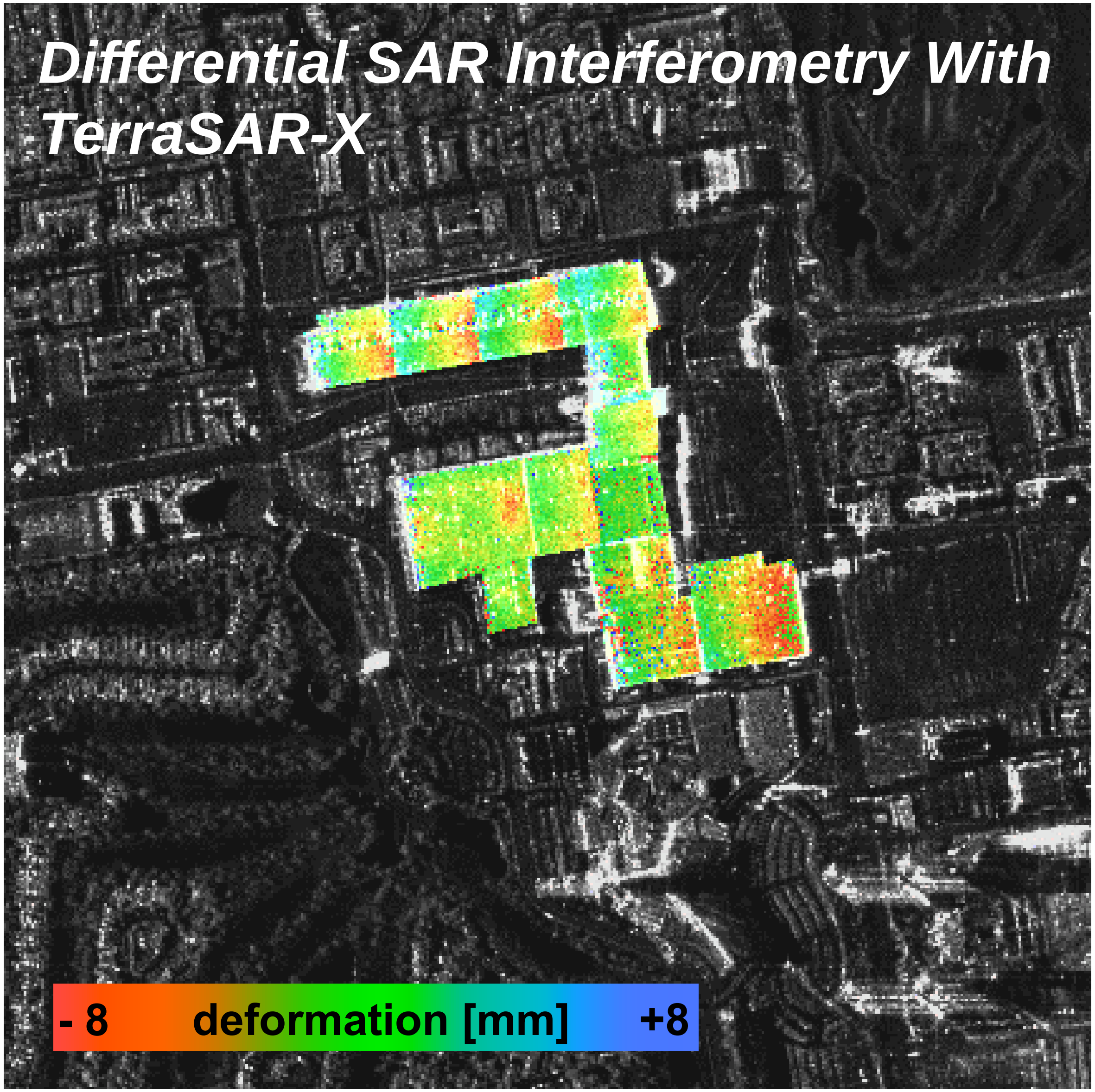

Las Vegas Convention Center

by Remote Sensing Technology Institute

Persistent scatterers (PS-Interferometry, PSI)

- Accurate deformation measurements rely on the identification of “stable” targets.
  - Targets with no temporal decorrelation so that phase variations can be attributed to position changes.
  - Many features in urban environment result in **persistent scatterers.**
    - Typically identified in time-series by their constant amplitude (good calibration required).
    - PS density increases rapidly with improved spatial resolution.
  - PS are much less frequent in natural environment.
    - We can use coherent pixels (for example due to areas with rocks).
- Good PS density required to avoid phase unwrapping problems.
- We should be seeing improvement now with Sentinel-1

Subsidence Monitoring over Urban Areas

Berlin,

63 Images

(1991 – 2000)

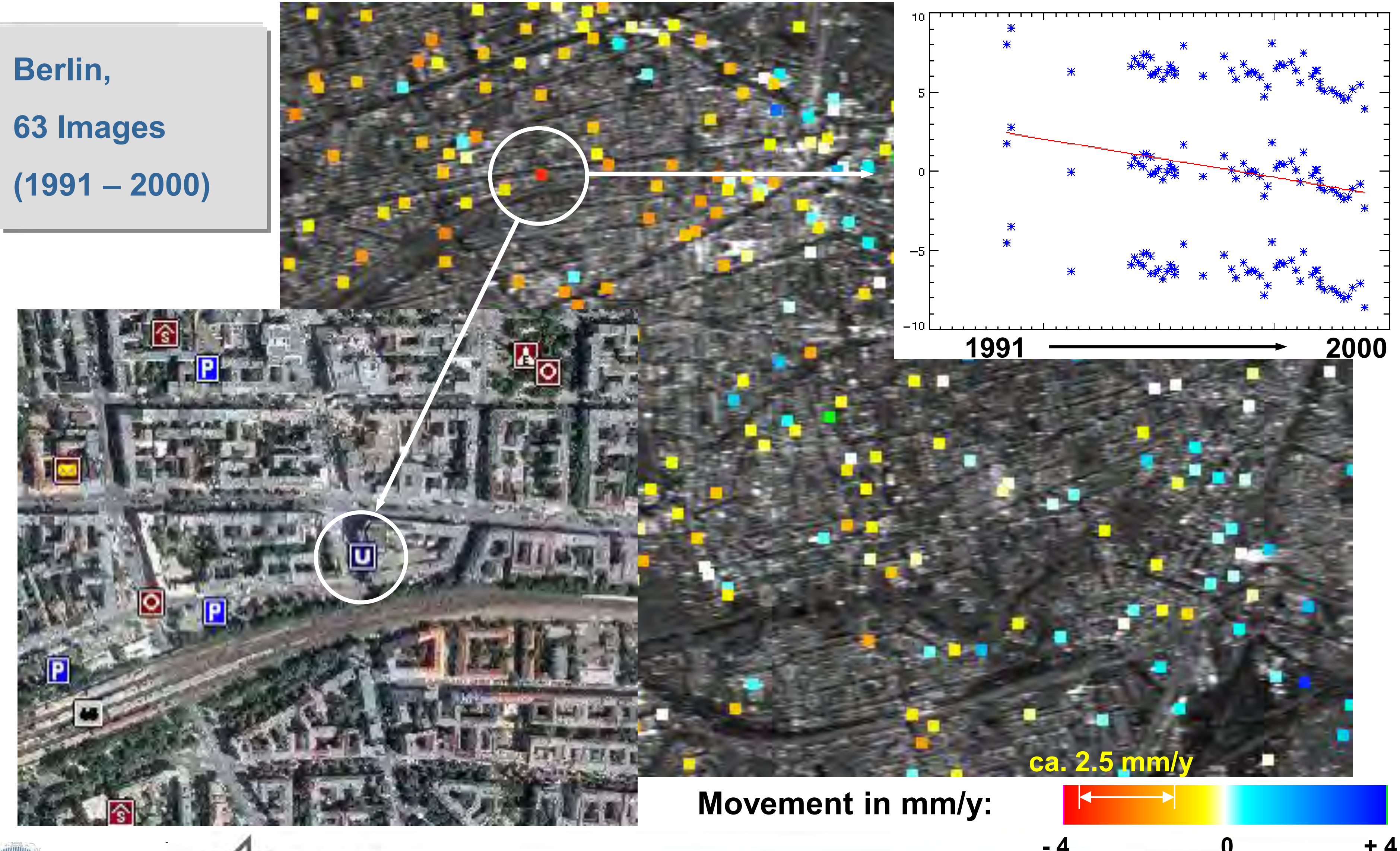

Glacier Movements

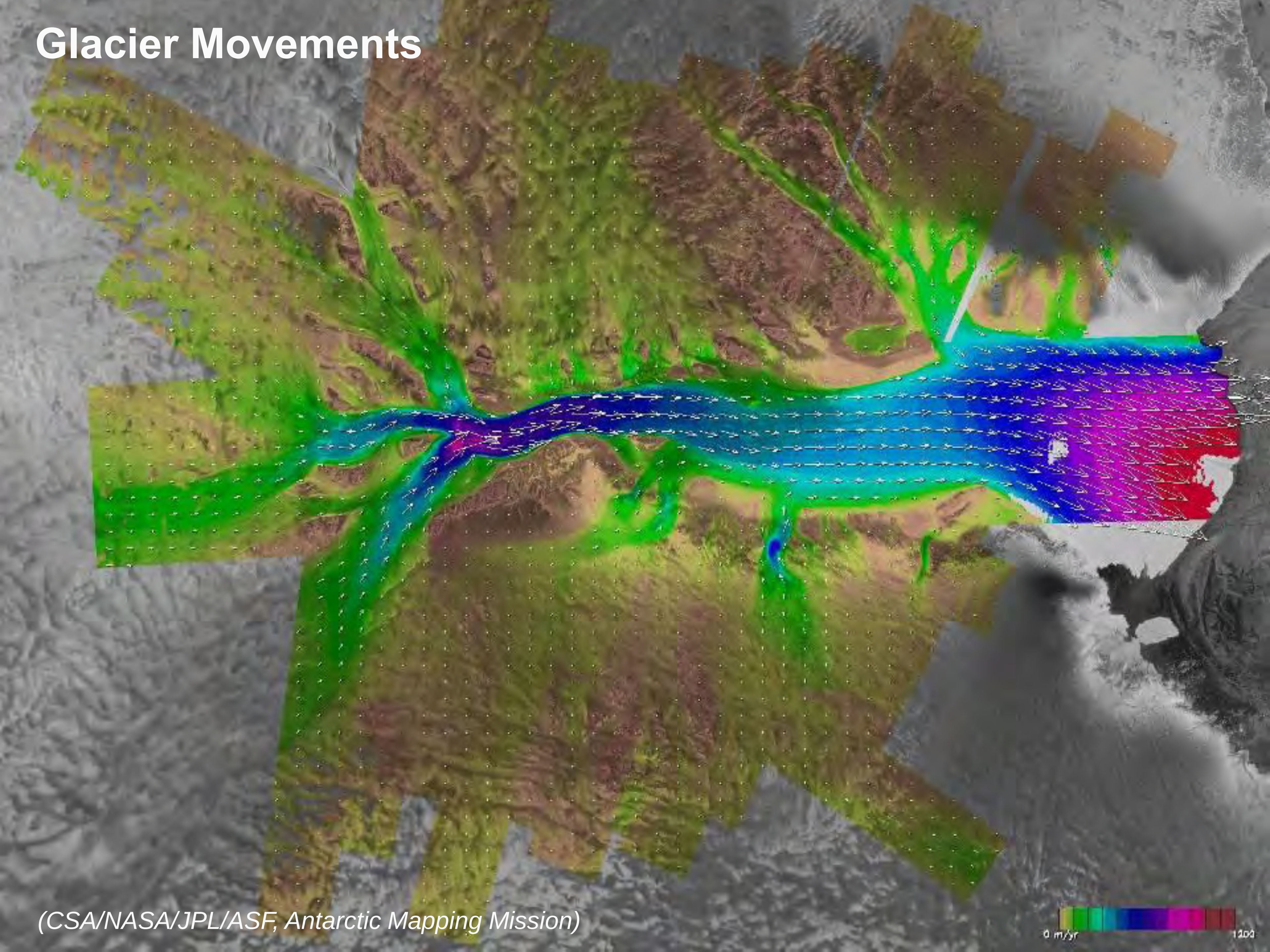

(CSA/NASA/JPL/ASF, Antarctic Mapping Mission)

Subsidence ERS-1/2

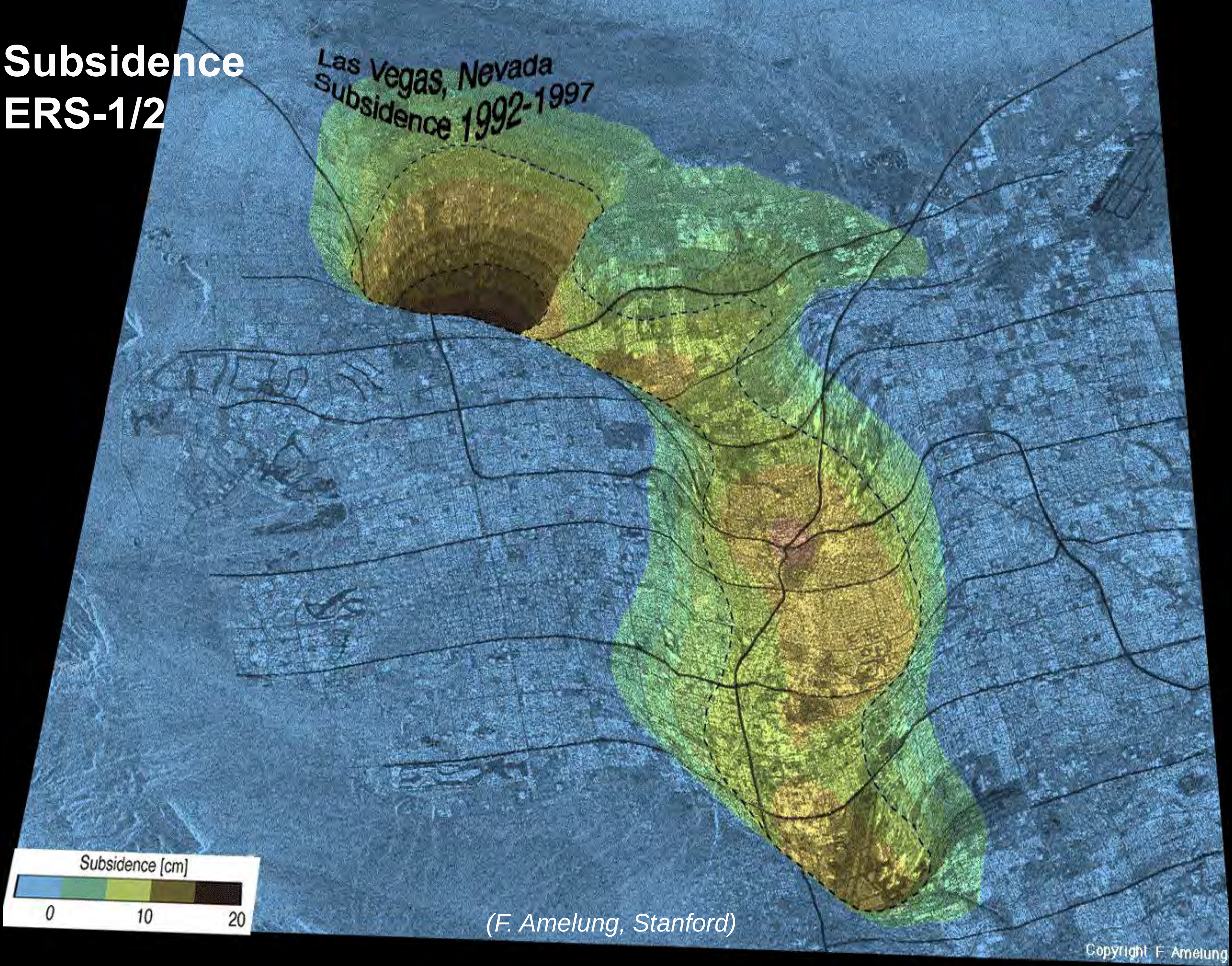

(F. Amelung, Stanford)

BAM Earthquake (Envisat/ASAR)

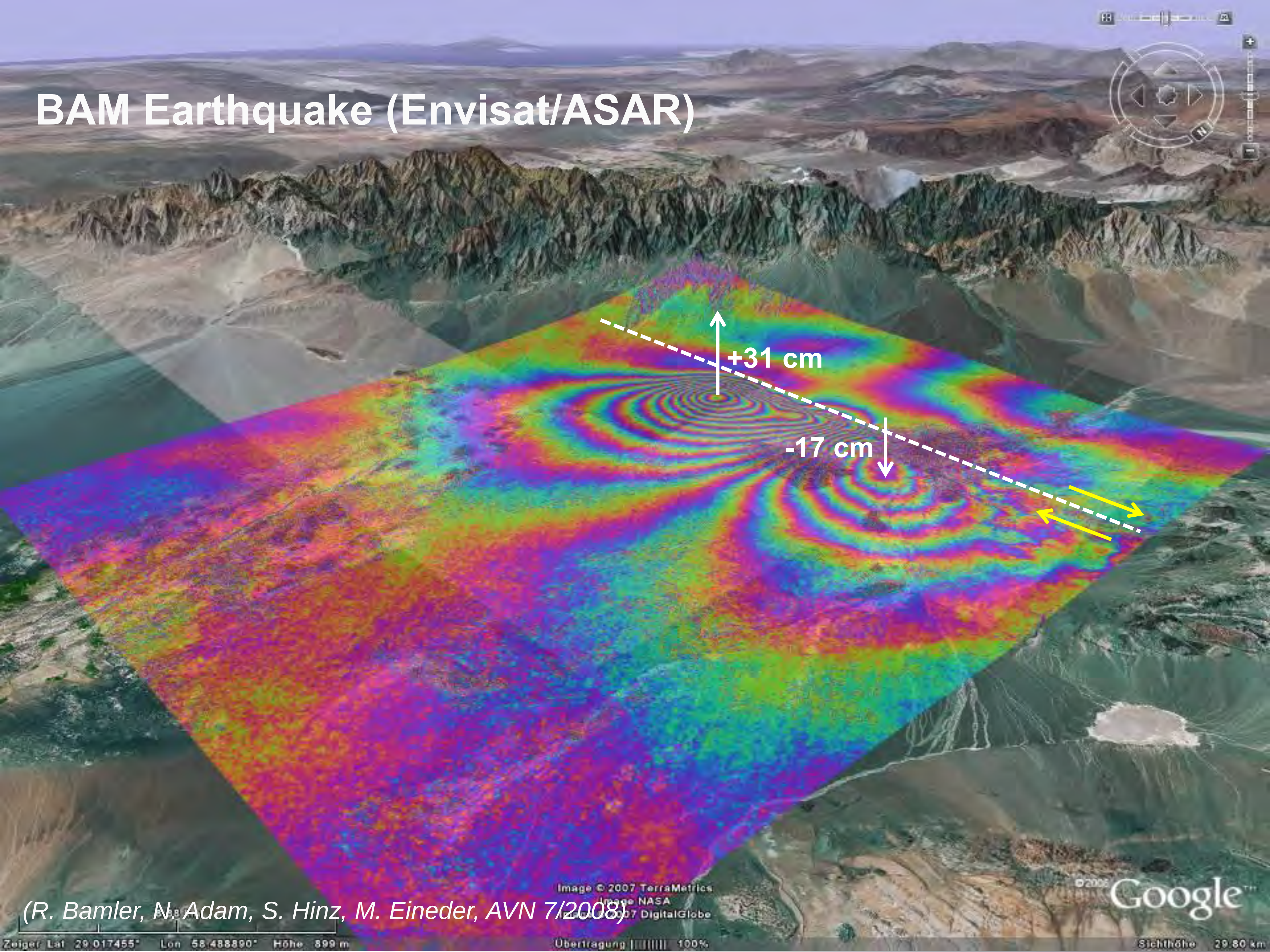

(R. Bamler, N. Adam, S. Hinz, M. Eineder, AVN 7/2008)

Acquisition Geometry of a TerraSAR-X cross-orbit experiment

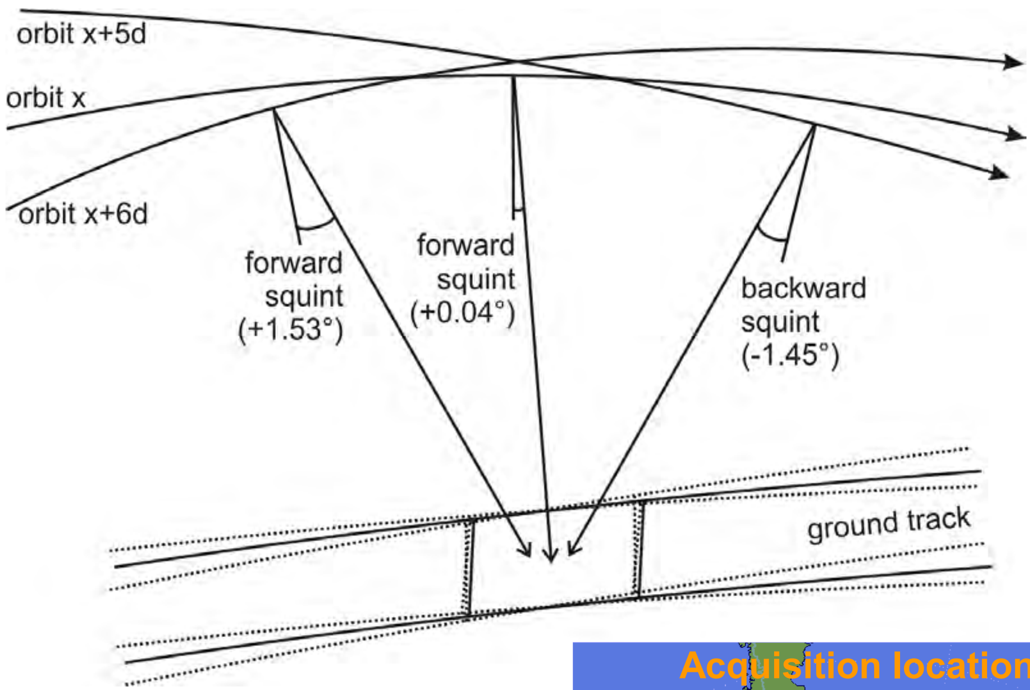

- Shorter revisit times than the repeat pass cycle of 11 days
- Close orbit constellation possible after 1 and 5(6) days at high and low latitudes:

  → North: 84.5° to 88°, South: -75° to -80°
- Squinted azimuth beams necessary to compensate crossing angles

  → Crossing angles: 2.1° (5d/6d) and 4.2° (1d)

Note: Orbits are crossing only in earth fixed coordinates!

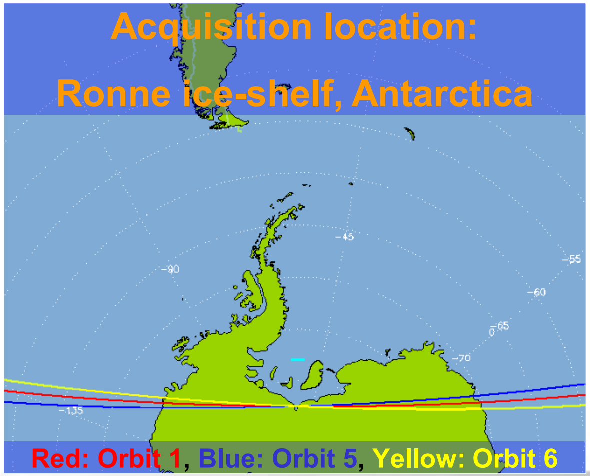

esa

DLR Deutsches Zentrum für Luft- und Raumfahrt e.V. in der Helmholtz-Gemeinschaft

Courtesy of Steffen Wollstadt

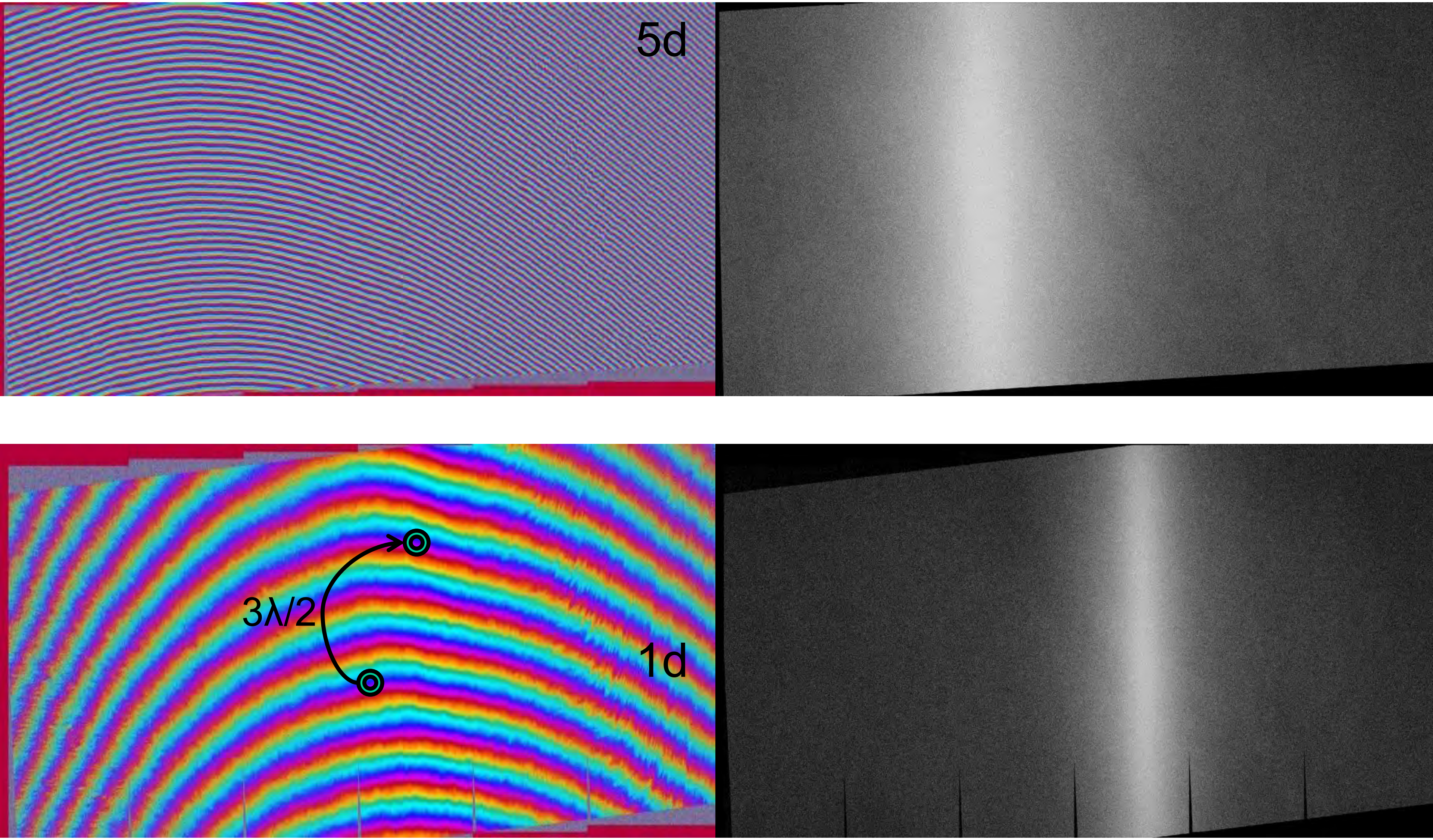

Courtesy of Steffen Wollstadt

Multi-angle geometries

- Projection of motion along LoS
- 2 LoS -> 2D motion (e.g. Ascending/Descending)
- 3 LoS -> 3D motion (Ascending/Descending/Squinted or Left/Right)
- Geological models (subsidence, etc.)
- Along-track displacements with reduced sensitivity

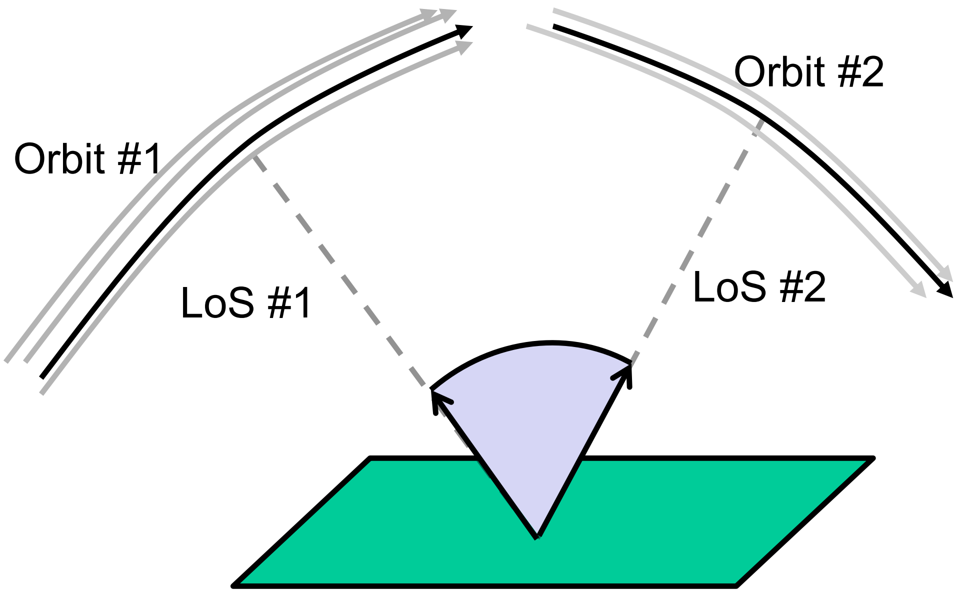

Interferometric processing

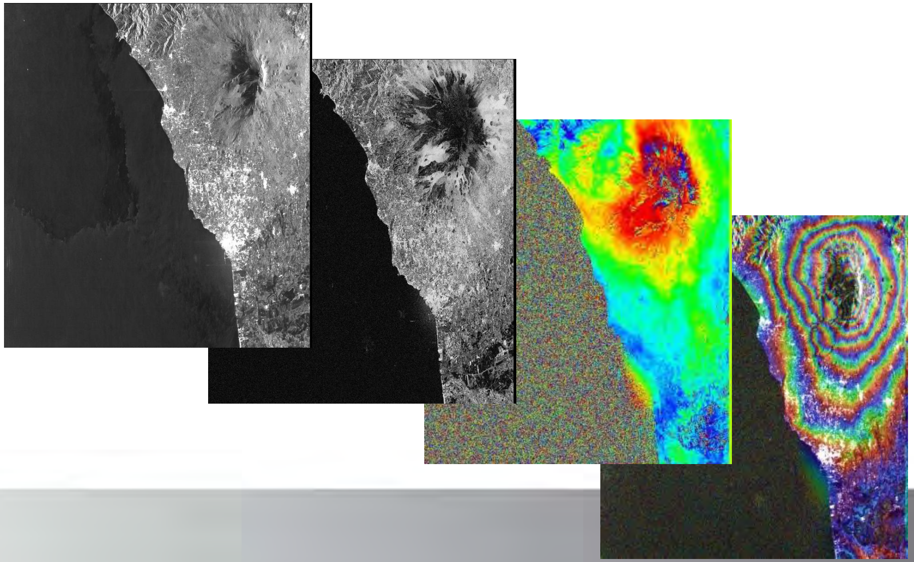

Interferometric processing

- (Acquisition)
- (Focusing)
- Coregistration (phase robustness to mis-registration)
- Filtering (Spectral shift)
- Interferogram generation
- Flattening (to simplify the next steps)
- Multilooking (Averaging, Filtering)
  - Output: Phase and Coherence
- Phase unwrapping
- Specific processing
- Geocoding (a change of coordinates)

Co-registration: master and slave have different geometries

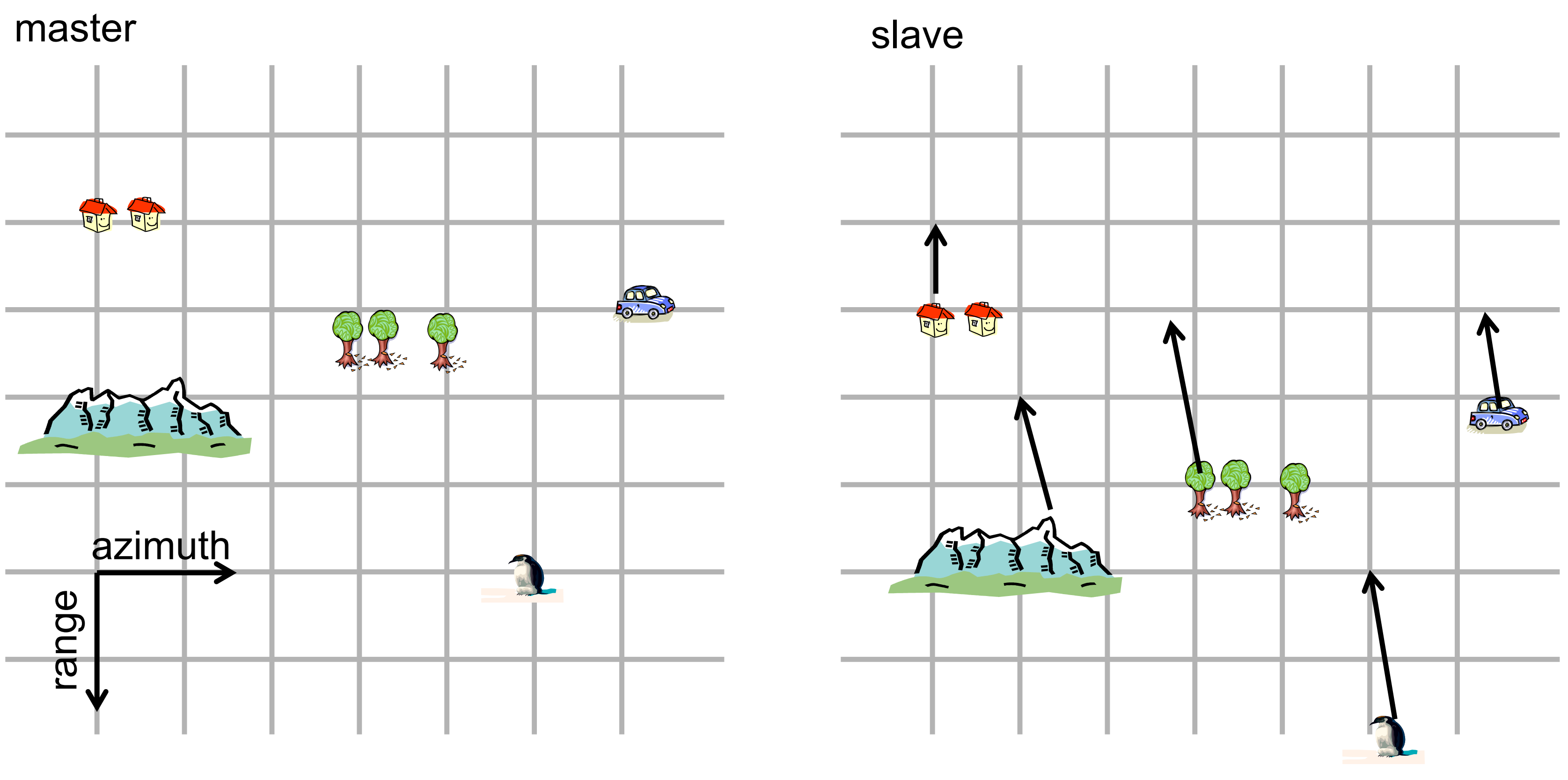

Interferogram generation (pixel by pixel)

$$u_1 = x_1 + jy_1 = |G_1| \cdot \exp(j\varphi_1)$$

$$u_2 = x_2 + jy_2 = |G_2| \cdot \exp(j\varphi_2)$$

$$u_1 \cdot u_2^* = (x_1 + jy_1) \cdot (x_2 - jy_2) = \overbrace{(x_1 x_2 + y_1 y_2)}^{\text{real part}} + j\overbrace{(x_2 y_1 - x_1 y_2)}^{\text{imaginary part}}$$

$$= |G_1| \cdot |G_2| \cdot \exp[j(\varphi_1 - \varphi_2)]$$

SAR Image 1

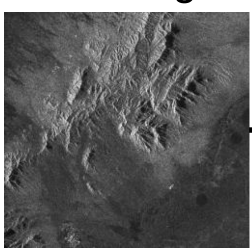

$u_1 = |G_1| \exp\left(j\varphi_1\right)$

SAR Image 2

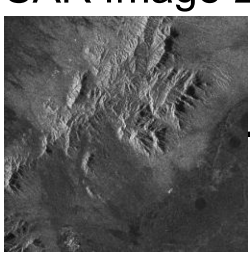

$u_2 = |G_2| \exp\left(j\varphi_2\right)$

$*$

$v = |G_1||G_2| \exp\left[j\left(\varphi_1 - \varphi_2\right)\right]$

arg()

$\Delta\phi = \varphi_1 - \varphi_2$

Interferogram

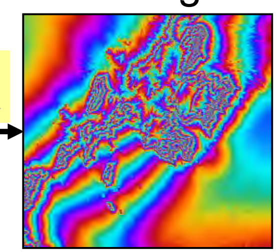

* … means complex conjugated

Deutsches Zentrum für Luft- und Raumfahrt e.V. in der Helmholtz-Gemeinschaft

Slopes correspond to frequencies in the interferogram

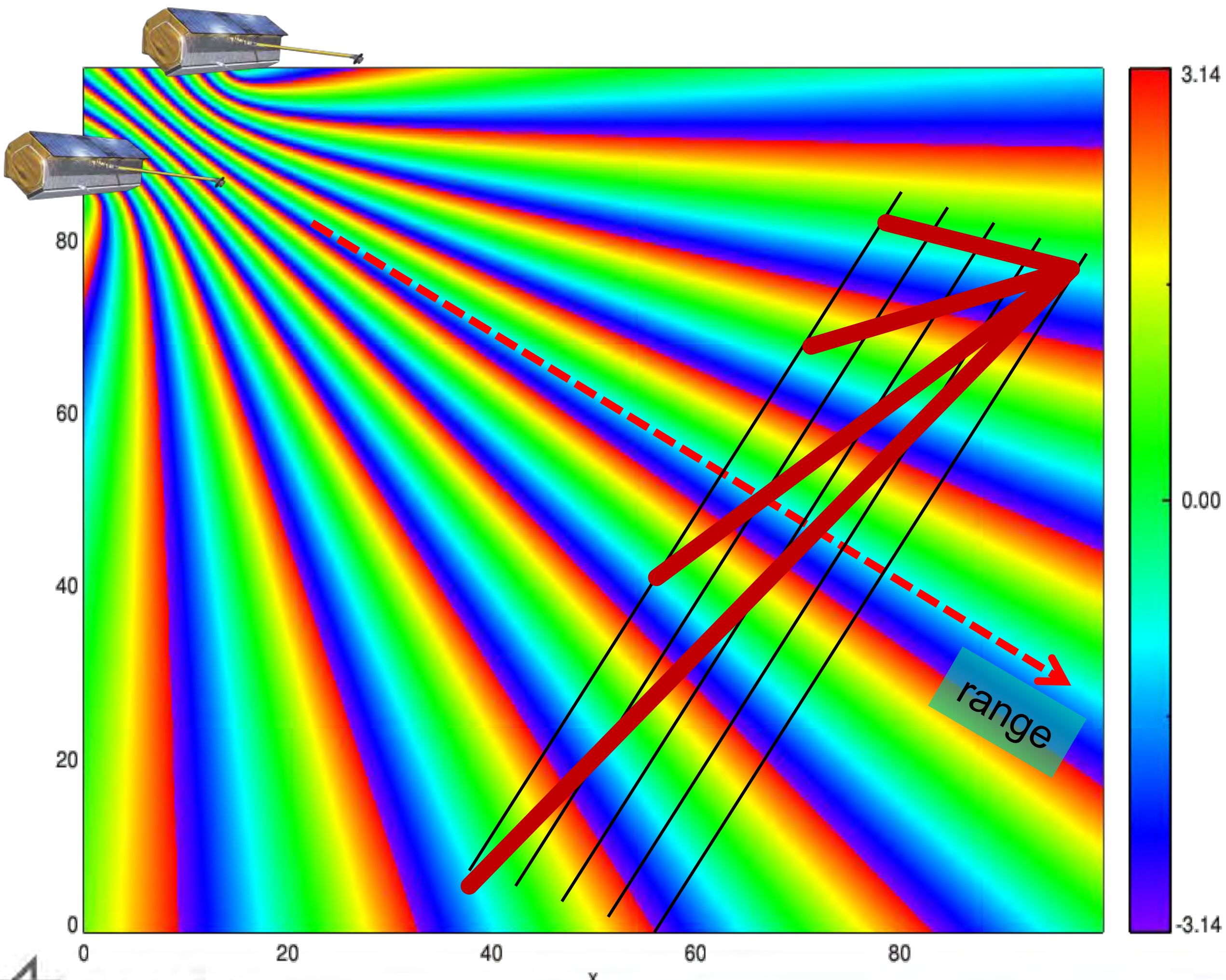

Flath-Earth phase

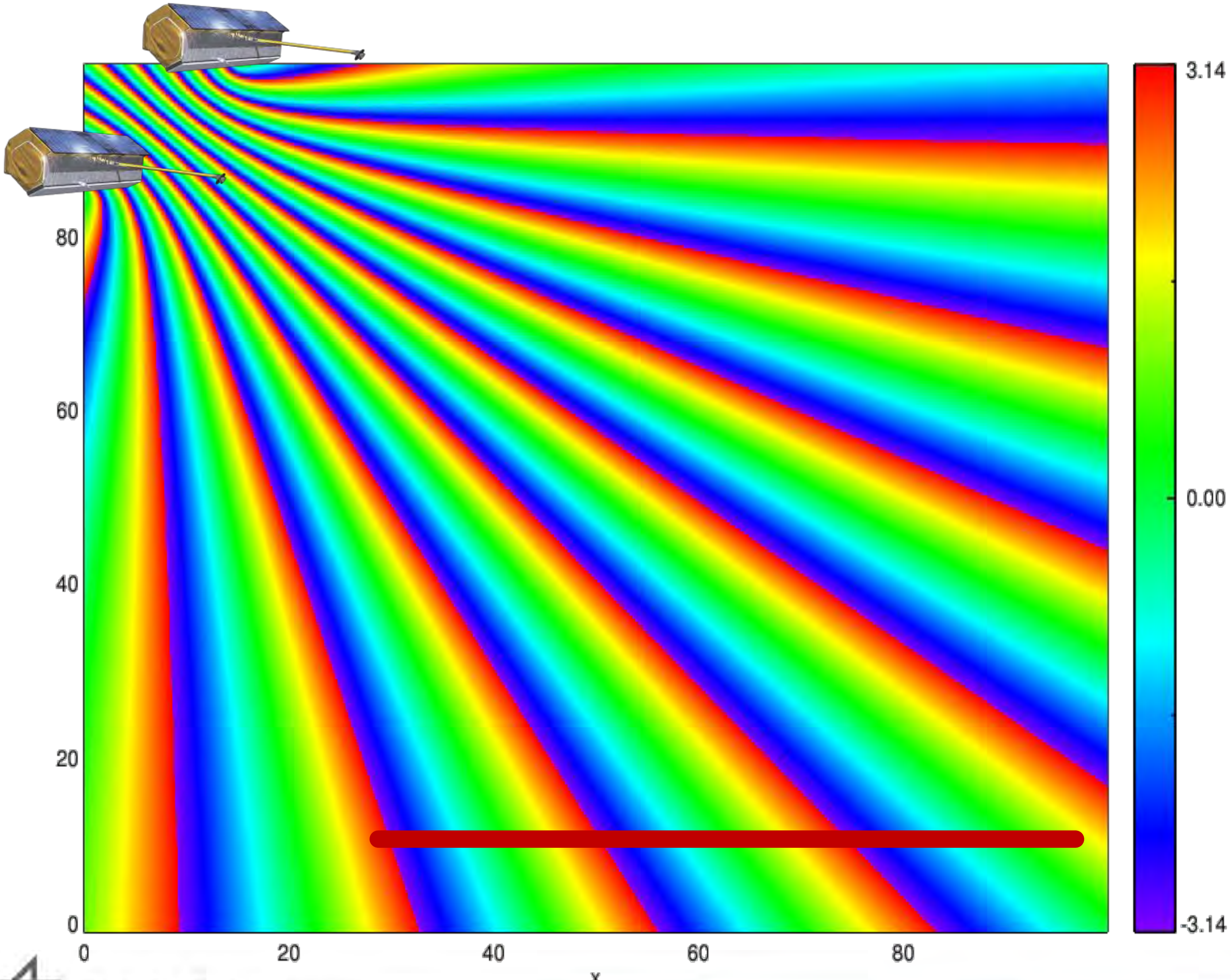

Interferogram flattening (ellipsoid)

$$\mathrm{int}(r,a) \quad * \quad \exp(-j\varphi_{\mathrm{predicted}}(r,a)) \quad = \quad \mathrm{int}_{\mathrm{flattened}}(r,a)$$

$$\varphi_{\mathrm{interf}} \quad - \quad \varphi_{\mathrm{predicted}} \quad = \quad \varphi_{\mathrm{residual}} \quad \mathrm{mod}\, 2\pi$$

Original interferogram — Flattening phase (ellipsoid) — Residual phase

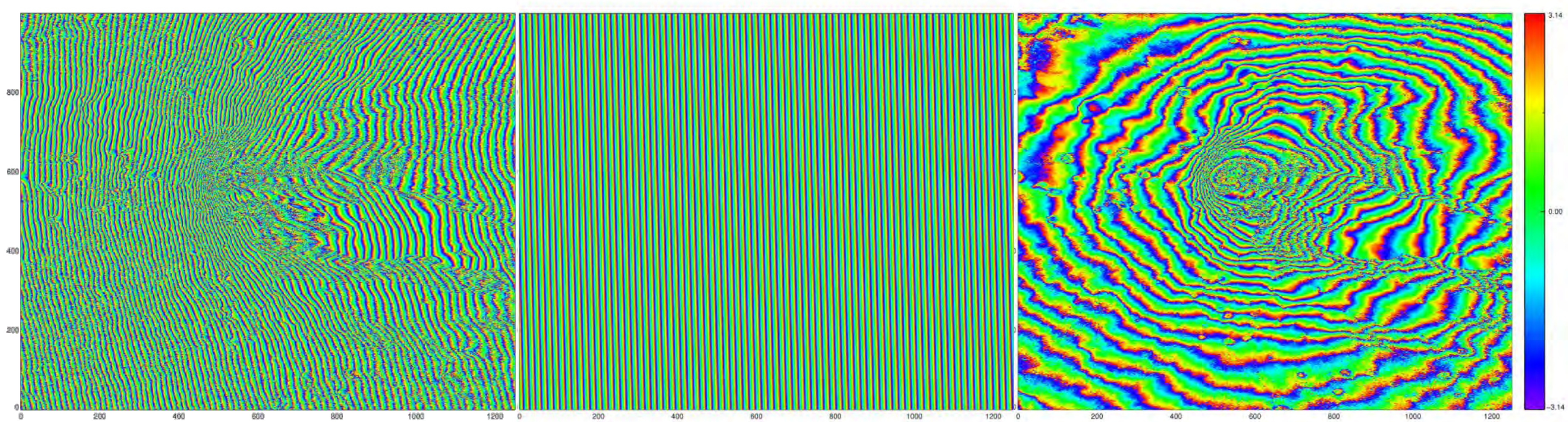

Interferogram flattening (ellipsoid)

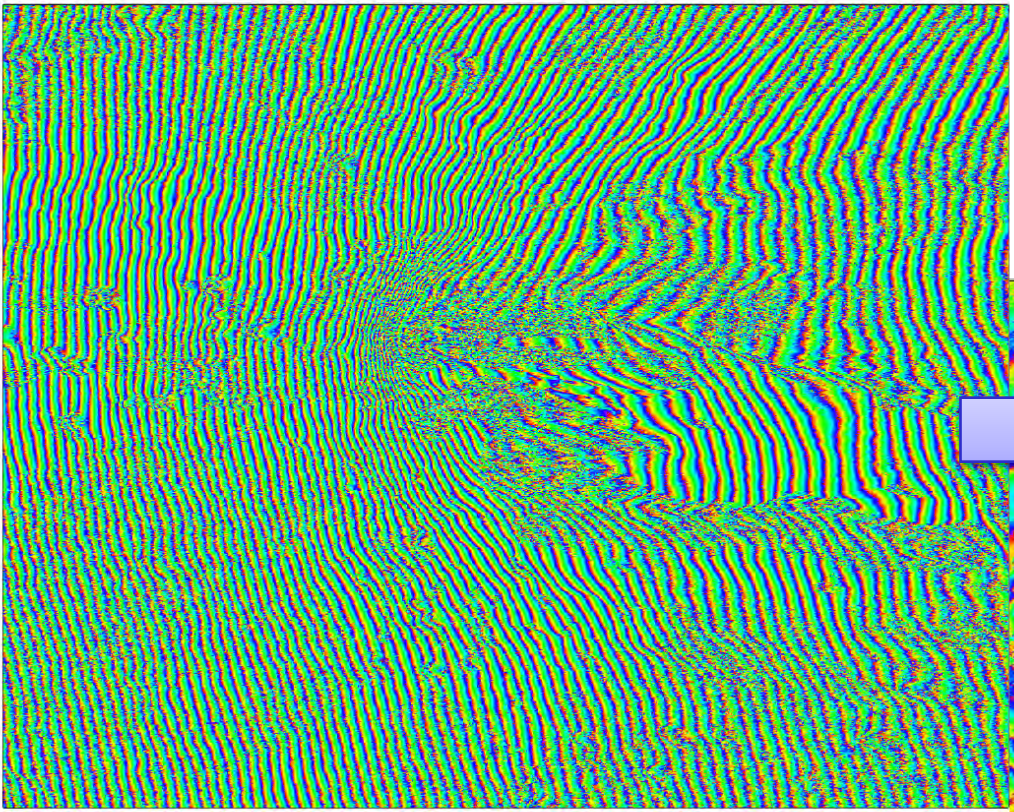

range

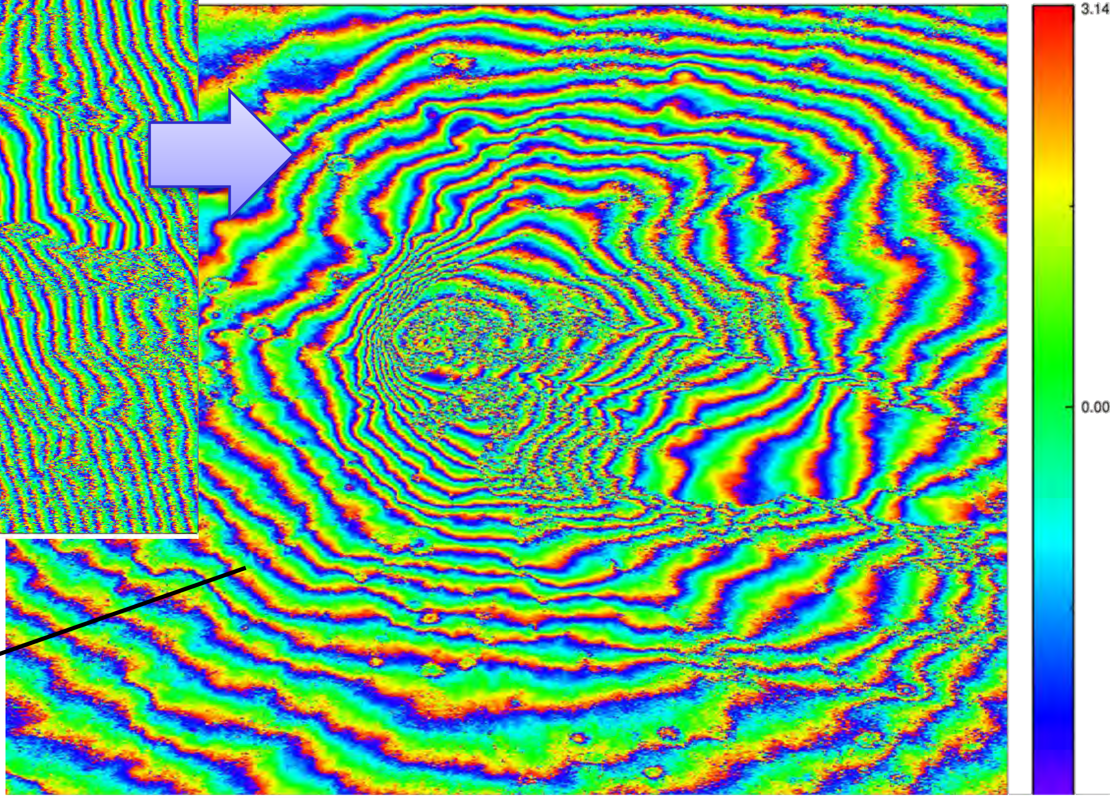

Similar to contour lines:

Constant phase = constant height

Mt. Etna, JAXA (PALSAR)

Interferogram flattening: ellipsoid + available DEM (e.g. SRTM)

$$\mathrm{int}(r,a) \quad * \quad \exp(-j\varphi_{\mathrm{predicted}}(r,a)) \quad = \quad \mathrm{int}_{\mathrm{flattened}}(r,a)$$

$$\varphi_{\mathrm{interf}} \quad - \quad \varphi_{\mathrm{predicted}} \quad = \quad \varphi_{\mathrm{residual}} \quad \mathrm{mod}\, 2\pi$$

Original interferogram | Flattening phase (with SRTM) | Residual phase

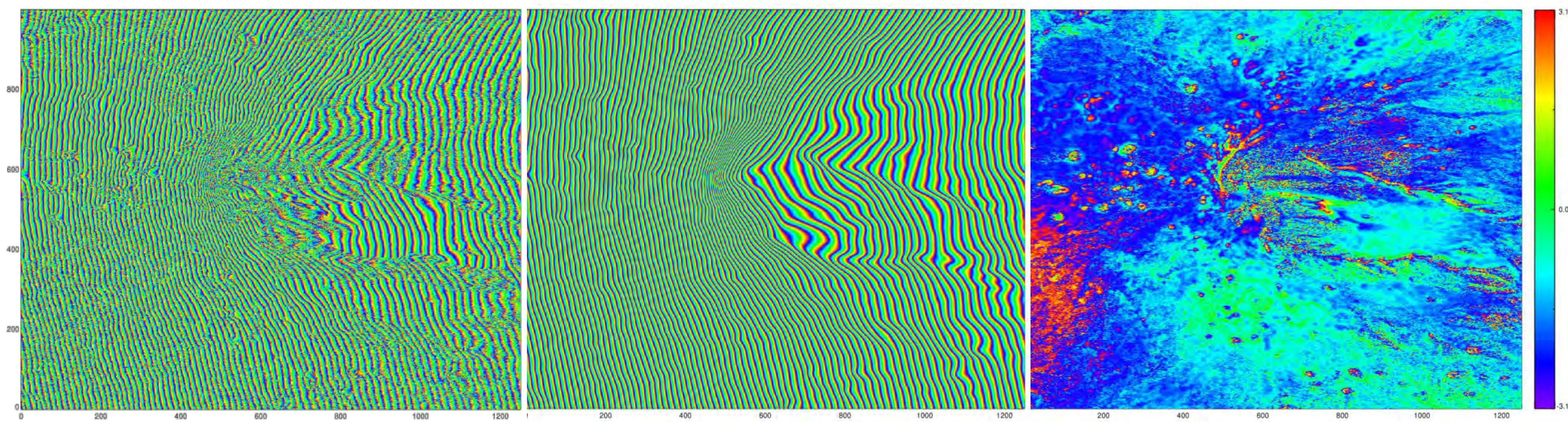

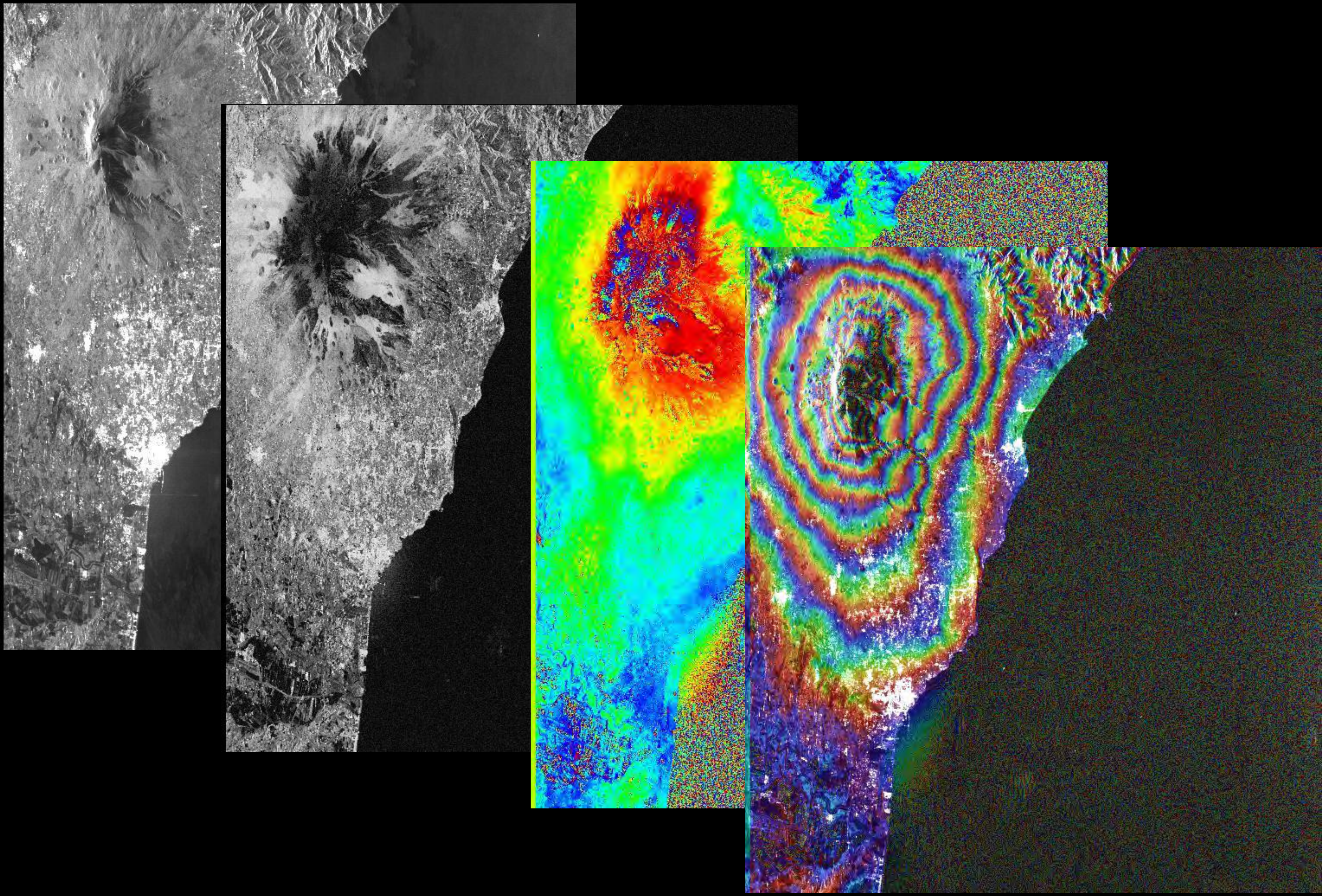

JAXA (PALSAR)

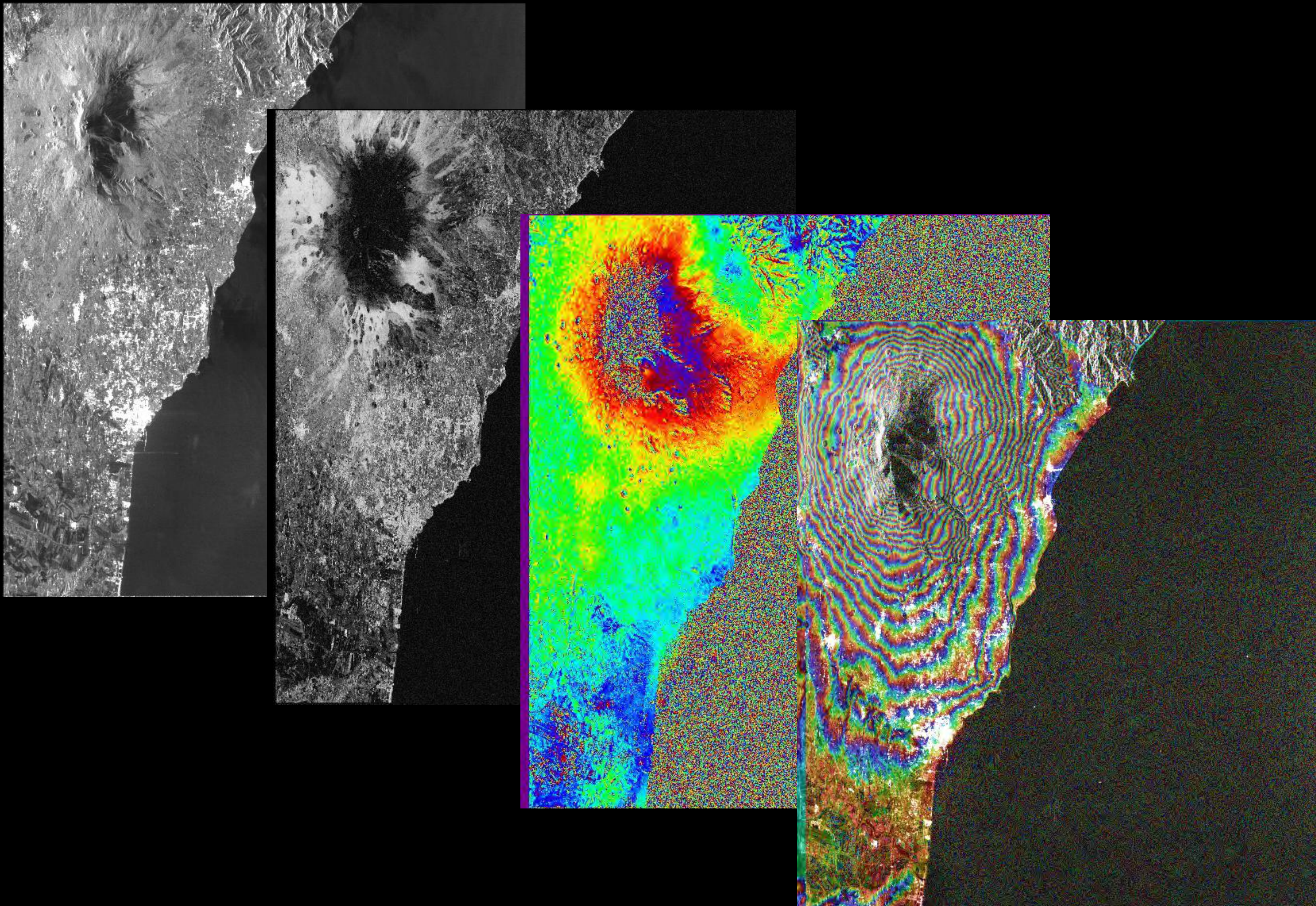

JAXA (PALSAR)

Averaging or Filtering or Multilooking

- Complex numbers are averaged before extracting the phase

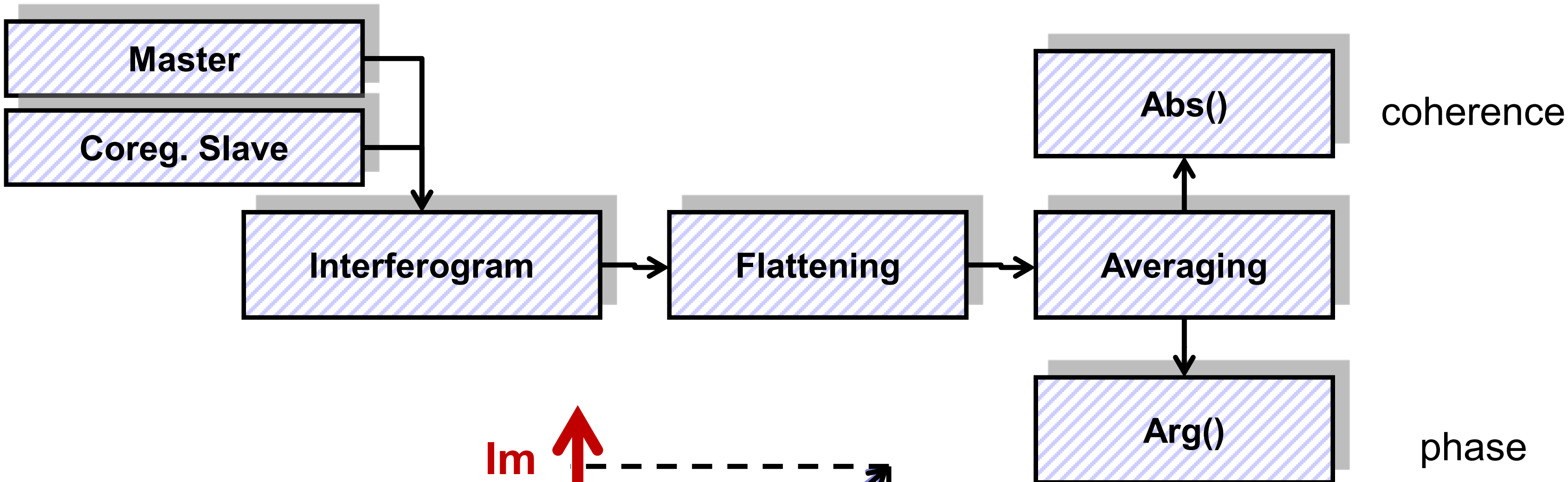

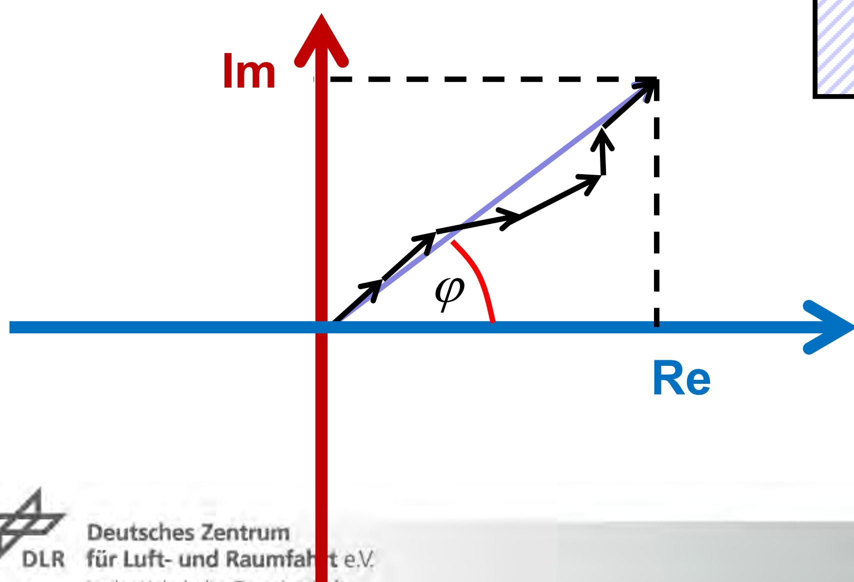

$$\varphi = \arctan\left(\frac{\mathrm{Im}[\sum_{k=1}^{L} z_m(k)\bar{z}_s(k)]}{\mathrm{Re}[\sum_{k=1}^{L} z_m(k)\bar{z}_s(k)]}\right)$$

Phase unwrapping

- Assigning each phase the correct number of “missing” 2 π

$$\varphi_{\text{unwrapped}} = \varphi_{\text{wrapped}} + k \cdot 2\pi$$

- 1-D phase unwrapping

wrapped

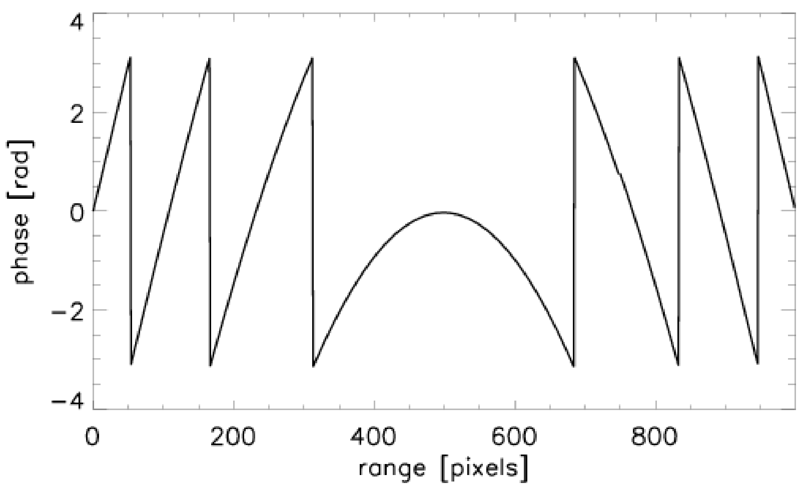

unwrapped

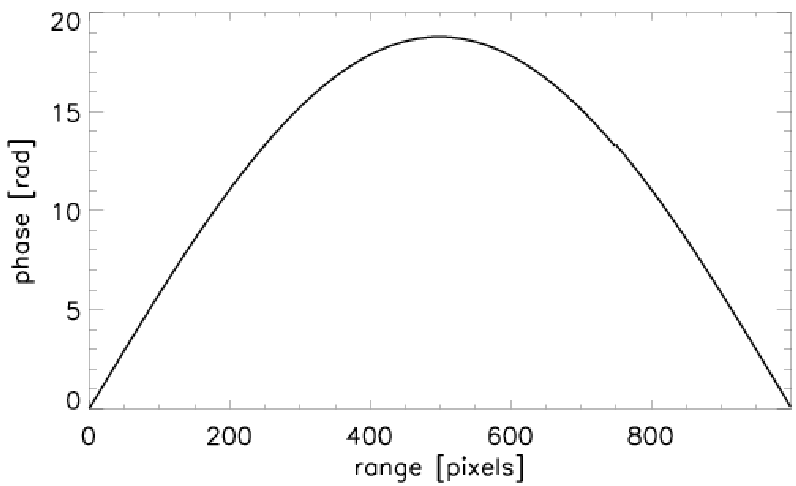

Phase Unwrapping

- Interferometric phase values belong to the interval $\varphi_{int} \in [0, 2\pi[$
- The range differences Δr will be mapped to this interrval

$$\varphi_{int} = (2\pi/\lambda) \cdot \Delta r \mod 2\pi$$

- The information on the distance is thus ambiguous

$$\Delta r = (\lambda/2\pi) \cdot \varphi_{int} + k \cdot \lambda/2 \qquad k \in \mathbb{Z}$$

- If the sampling is fine enough and there are enough well behaved regions, the ambiguities can be solved

→ „*phase unwrapping*“

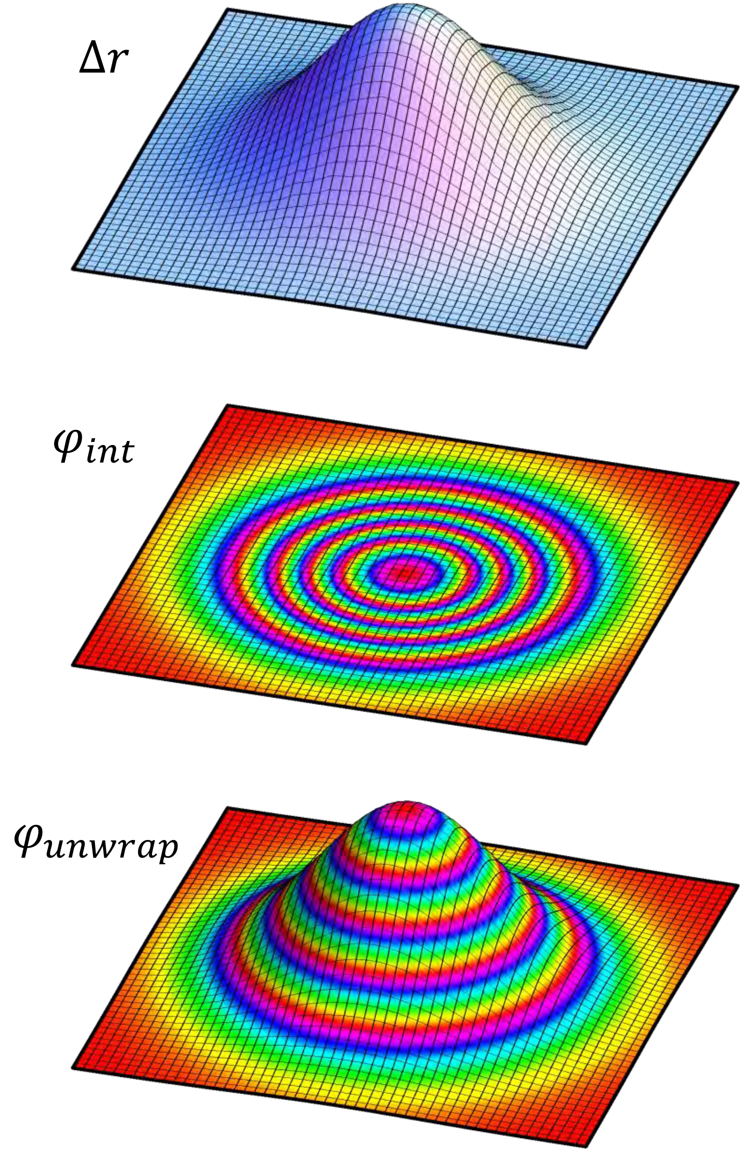

Geocoding

- From SAR coordinates to "usual" coordinates (UTM or Lat/Lon)

SAR coordinates

Geodetic coordinates

$$(r, a, \varphi) \leftrightarrow (x, y, z) \leftrightarrow (\mathrm{lat}, \mathrm{lon}, \mathrm{height}) \leftrightarrow (\mathrm{E}, \mathrm{N}, \mathrm{height})$$

ECEF coordinates

Local coordinates

- Geocoding is essentially a change of coordinates & resampling

References

- **SAR Basics and Processing:**
  - J. C. Curlander, R. N. McDonough, Synthetic Aperture Radar: Systems and Signal Processing. New York: Jon Wiley & Sons, 1991.
  - I. Cumming, F. Wong, Digital processing of synthetic aperture radar data: signal processing algorithms. Boston: Artech House, 2005.
  - F. Henderson (Ed.), Manual of Remote Sensing: Principles and Applications of Radar Imaging, Wiley, 1999.
- **Interferometry, Tomography**
  - R. Hanssen, Radar interferometry: data interpretation and error analysis, Dordrecht, Kluwer Academic Publishers, 2001.
  - A. Reigber, A. Moreira, “First demonstration of airborne SAR tomography using multibaseline L-band data”, IEEE Trans. Geosc. and Remote Sens., Vol. 38, No. 5, pp. 2142-2152, 2000.
- **SRTM, TerraSAR-X, TanDEM-X**
  - T. Farr et al. "The Shuttle Radar Topography Mission", Reviews of Geophysics, vol. 45, 2007.
  - M. Stangl, R. Werninghaus, B. Schweizer, C. Fischer, M. Brandfass, J. Mittermayer, H. Breit, "TerraSAR-X technologies and first results", IEE Proceedings - Radar, Sonar and Navigation, vol. 153, pp. 86-95, 2006.
  - G. Krieger, A. Moreira, H. Fiedler, I. Hajnsek, M. Younis, C. Werner, and M. Zink, "The TanDEM-X mission: a satellite formation for high resolution SAR interferometry", to appear in IEEE Transactions on Geoscience and Remote Sensing, 2007.